UNIVERSITY OF OKLAHOMA

GRADUATE COLLEGE

FLOODPLAIN ANALYSIS OF THE NEOSHO RIVER ASSOCIATED WITH PROPOSED RULE CURVE MODIFICATIONS FOR GRAND LAKE O' THE CHEROKEES

A THESIS

SUBMITTED TO THE GRADUATE FACULTY

in partial fulfillment of the requirements for the

Degree of

MASTER OF SCIENCE

By

ALAN C. DENNIS
Norman, Oklahoma
2014

FLOODPLAIN ANALYSIS OF THE NEOSHO RIVER
ASSOCIATED WITH PROPOSED RULE CURVE MODIFICATIONS
FOR GRAND LAKE O' THE CHEROKEES

A THESIS APPROVED FOR THE
SCHOOL OF CIVIL ENGINEERING AND ENVIRONMENTAL SCIENCE

BY

Dr. Randall L. Kolar, Chair

Dr. Kendra Dresback

Dr. Robert Nairn

Dr. Robert Knox

© Copyright by ALAN C. DENNIS 2014
All Rights Reserved.

For Melinda, my love

Acknowledgements

The research summarized in the pages that follow was only possible as a result of the contributions and support of many people. I would like to take this opportunity to express my heartfelt gratitude to as many of those people as possible.

First, I must thank my advisor, Dr. Randall Kolar, for allowing me the opportunity to join his excellent group of researchers, and for his patience as I made the transition back into the academic world here at the University of Oklahoma. Dr. Kolar's approach to teaching has taught me engineering concepts that cannot be quantified on a test or in a paper, even one as long as this. His focus on teaching his students information that will be more beneficial to real world problems than any idealized test case helped me to keep my head above water in this very real-world research application, and will benefit me for years to come.

I thank Dr. Kendra Dresback for the time she devoted to answering my endless, and often times ridiculous, questions. Dr. Dresback helped maintain my sanity numerous times by answering all my trivial questions from how to get HEC-RAS to run, to how to get the computer to boot up using Windows. This often required much of her time on short notice, and her door was always open.

I am grateful to Dr. Robert Nairn for his willingness to share all of the information he knows about the Grand Lake and Miami area with me. Dr. Nairn was always encouraging when he noticed that this research was starting to seem like more than what I signed up for. I am also grateful to Dr. Robert Knox for his thoughtful input on the subject of the Miami area, as well as his expertise in technical formatting.

Among all those who contributed to this thesis on an academic level, I am especially grateful to my friends Kevin Geoghegan, Dr. Evan Tromble, Amanda Oehlert,

Sam Bush, and Russ Dutnell. The weekly research meetings with Kevin, Amanda, Sam, and I were crucial in reminding me that I was not in this alone, and that we were all struggling together. While serving as a teaching assistant to Dr. Tromble and a student in his class, he was always able to provide a perspective on what all of this research was leading toward: work outside of academia. Russ and I spent many days struggling through data collection on Little River in Norman. This experience hanging out with Russ and tugging extremely heavy "torpedoes" up and down the bridge taught me much about what research is all about once you step away from the computer screen. Most of all, I am grateful to Kevin for teaching me essentially everything he learned throughout the one year head start he had on me in grad school. I most certainly would not be typing this thesis in LaTeX right now if it weren't for Kevin, and that is one of many skills that he shared to make my life easier throughout this process.

I gratefully acknowledge the following institutions that provided funding and other resources that made this research possible: The United States Army Corps of Engineers (USACE), The Grand River Dam Authority (GRDA), The Oklahoma Water Resources Board (OWRB). I am specifically grateful for the patient attentiveness of David Adams and Jerrod Smith at the United States Geological Survey (USGS) office in Oklahoma City. Mr. Adams and Mr. Smith were extremely eager to help and answer all of the questions I had about the hydrologic data provided by the USGS. Particularly during the brief government shutdown of 2013, I came to truly appreciate living in a country where agencies such as these generously contribute to advancing our knowledge of the world so that we can continue to enjoy the resources with which we have been blessed.

The most wonderful blessing in my life is unquestionably my tirelessly supportive and loving wife Melinda. I owe her all of my deepest thanks for helping to accomplish this task. Even while being exhausted by her own graduate studies, she selflessly

served me and kept me feeling loved throughout the time and work involved with this thesis. Her confidence in my ability to endure and keep my focus on a higher purpose was my sustenance throughout this process. She is the most wonderful wife for which a man could ask. I am grateful to Al and Lynette Gore for their loving upbringing of Melinda, and for loving me as their own son over the past few years.

My family is the reason I am in this position of being a Master's candidate at the University of Oklahoma. My mother and father's years of love and kind upbringing was too often thankless work, but it truly is the foundation of the man I am today. My mother taught me endless faith, and my father taught me that no one can have too much patience. I have never once felt the burden that so many feel, that of having to live up to my parents expectations. They supported me through every moment of my life, and had faith in the Lord that the wrong ways I took would turn out for good. Their patient, loving upbringing molded me into a man with a patience of my own, and a faith that all will be made well. That faith and patience was especially crucial in the process of editing this thesis. My little brother Kevin is an example of strength and discipline of which I will always look up to. My father's mother and father have both left a memory of loving patience and endurance for me to follow. My mother's father and mother continue to share their beautiful stories of faith that are a wonderful foretaste of heaven.

The Lord always will be that which he always has been. That knowledge sustains my every breath.

"Come to earth to taste our sadness,

he whose glories knew no end;

by his life he brings us gladness,

our Redeemer, Shepherd, Friend."

Contents

List of Tables

List of Figures

Abstract

A hydraulic model of the Grand Lake O' The Cherokees hydrologic system was developed for the purpose of analyzing the backwater effect of a proposed rule curve adjustment at Pensacola Dam in Langley, OK. The HEC-RAS and HEC-GeoRAS software developed by the U.S. Army Corps of Engineers were used to develop the hydraulic model.

Statistical analyses of four streams (Neosho, Spring, and Elk Rivers and Tar Creek) were conducted in order to estimate extreme flood events. Two methods of data extraction for statistical analysis were compared, namely annual maxima and partial duration, or peaks-over-threshold. The partial duration method was found to be a better fit of the data based on root mean squared error comparison, and the annual maxima method was found to be more conservative. The more conservative annual maxima method was chosen for the final flood-frequency analysis. The flood frequency estimation guidelines included in Bulletin 17B were employed to calculate the final flood frequency streamflows for the hydraulic model.

Model calibration and validation were conducted using the unsteady flow routing capability of HEC-RAS, and sensitivity analyses and model application were conducted using the steady-state capability of the program. The flood frequency streamflows were applied to the hydraulic model with two downstream conditions representing the existing and proposed rule curves. The upstream effect of the change in downstream conditions was recorded and analyzed to understand the effect of the proposed rule curve adjustment. According to the model, upstream water surface elevations are influenced much more by streamflow magnitude than downstream dam conditions.

The conclusions of the study found that the proposed rule curve adjustment would cause a minimal increase in water surface elevations for upstream locations near Mi-

ami, OK. Several sensitivity analyses were performed, testing various phenomena in the model to ensure that the conclusions are not sensitive to changes in the different parameters. These sensitivity analyses provide insight into the physics governing the behavior of the hydraulic system, which in turn provides more confidence that the model results faithfully represent that system.

CHAPTER 1

Introduction and Problem Statement

1.1 Introduction

The Lake O' The Cherokees watershed, upstream of Pensacola Dam in Langley, Oklahoma, is a vital resource for the state of Oklahoma. The watershed is important for the economy of the region, thus the ecological, environmental, and hydrologic health of the region must be maintained. The Grand River Dam Authority (GRDA) is responsible for ecosystems management of the area [GRDA, 2008]. The body of water retained by Pensacola Dam, Grand Lake O' The Cherokees (Grand Lake), is a hydrologic concern in the case of a major rainfall event, as downstream lake levels may exacerbate upstream flooding in low-lying areas. Four major watersheds feed into Grand Lake, namely the Neosho River, Elk River, Spring River, and the Lake O' The Cherokees watersheds, as shown in Figure 1.1.

The City of Miami, OK lies in the Lake O' The Cherokees watershed on the banks of the Neosho River, upstream of the confluence of the Neosho and Spring rivers. The confluence of these rivers occurs at Twin Bridges State Park, near Fairland, OK, and this location is considered the upstream boundary of Grand Lake [OWRB, 2009]. Floodwaters from extreme rain events in the Neosho watershed in Kansas and Oklahoma contribute to a flooding threat for locations upstream of Twin Bridges, including Miami.

Significant flooding has occurred at least 14 times in Miami since 1986 [Manders, 2009]. Many of these floods have produced serious economic hardships for Miami residents. For example, a flood event in July 2007 forced 1,500-2,000 people to evacuate

and affected about 500 homes and 30 businesses. The photo in Figure 1.2 shows the extent of flooding in Miami during the 2007 flood.

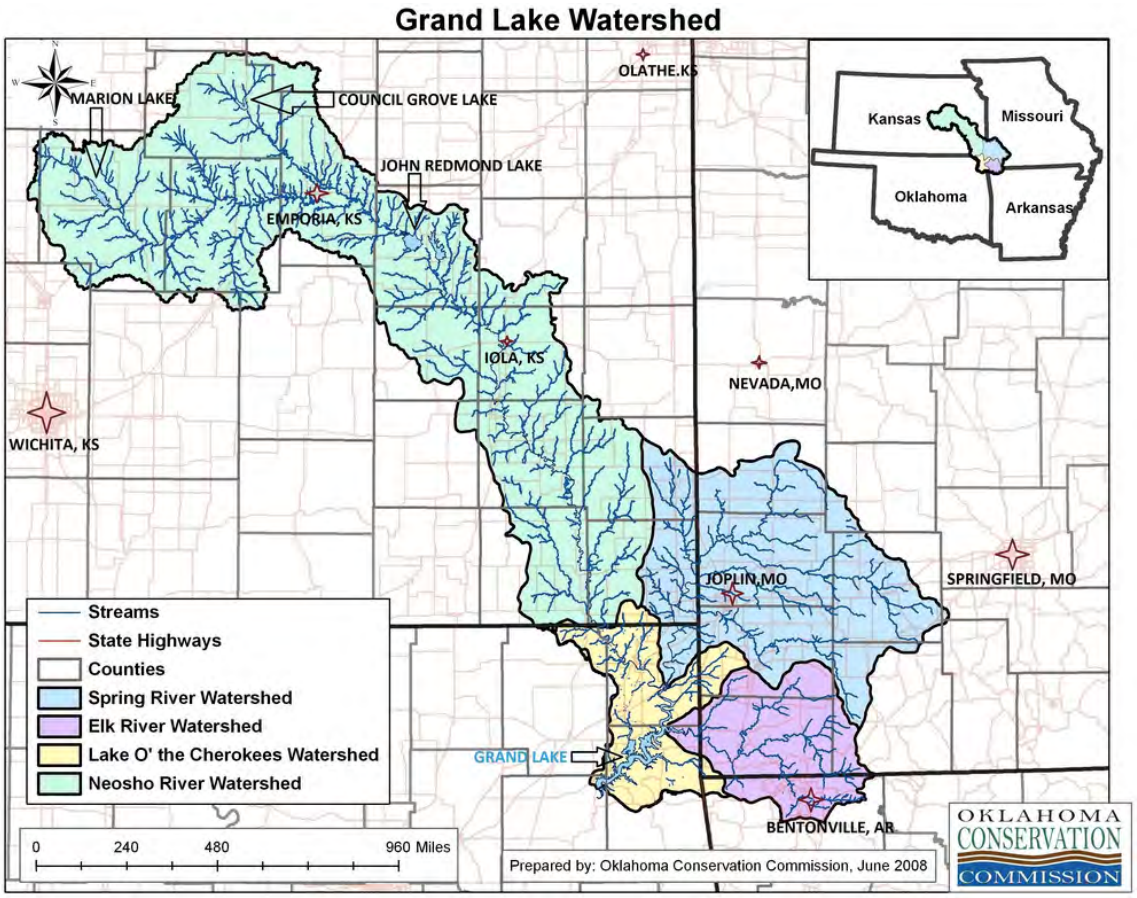

Figure 1.1. Watersheds that feed into Grand Lake [GLWAF, 2008].

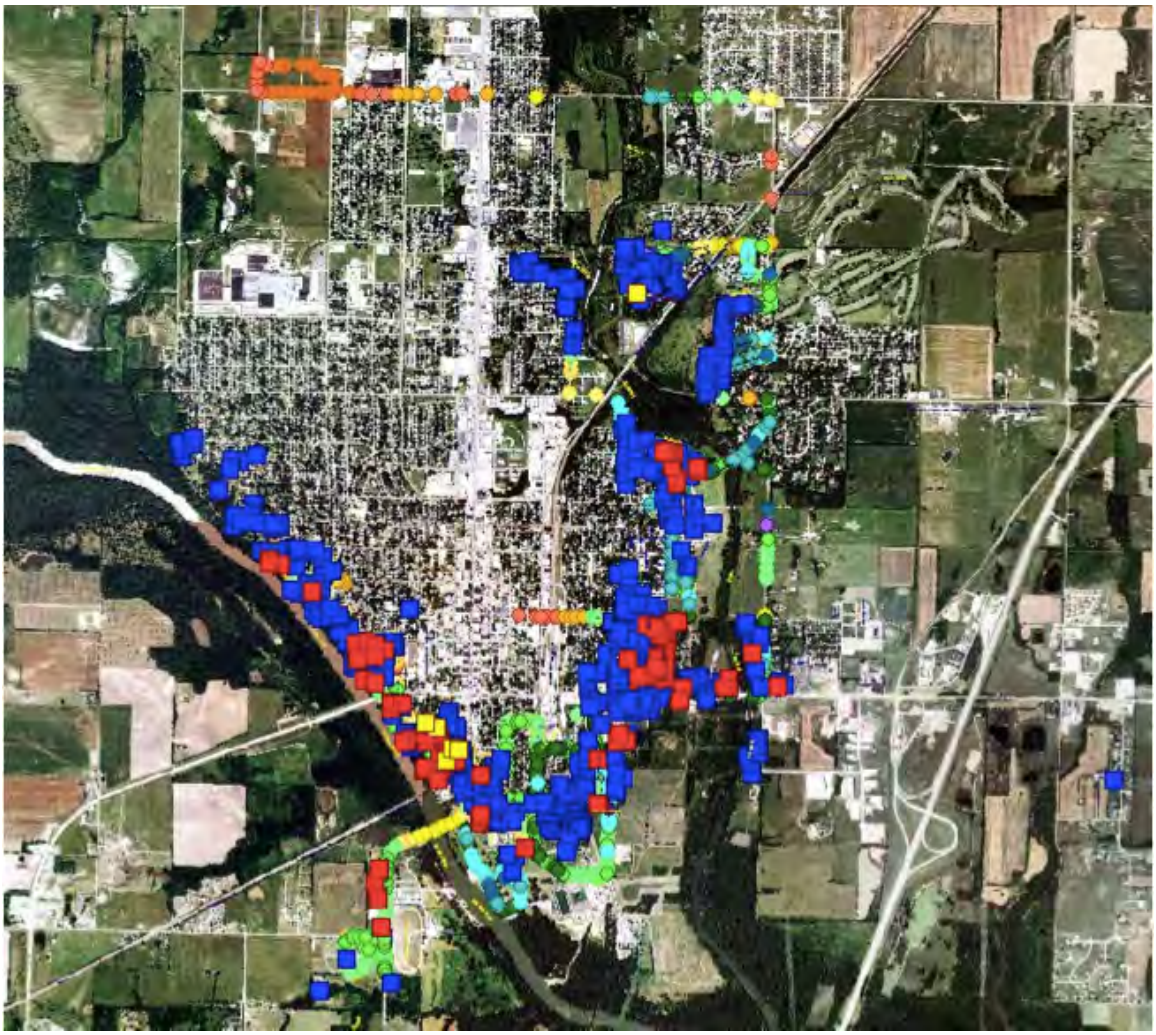

Figure 1.2. Photo from Manders (2009), indicating buildings damaged (blue squares), and destroyed (red squares) in the 2007 Miami flood. The Neosho River runs from the left to the bottom of the picture, and Tar Creek runs from top to bottom in the center of the picture.

1.2 Problem Statement

This research will examine whether the flooding threat upstream of Twin Bridges is significantly affected by water surface levels maintained on the Grand Lake reservoir at Pensacola Dam during the time period from August 15 to September 15 in any given year. This time period was chosen in order to compare the effect of the lake levels under the existing rule curve to proposed changes in the lake levels for the period under a proposed rule curve adjustment (Figure 1.3). The 2007 flood illustrated in Figure 1.2 is a well-documented example of why flooding is a major concern for the City of Miami. This event is used to illustrate the major flooding concern for Miami, but the event itself is not directly applicable to this research because it occurred in July, a time frame that is not affected by the proposed rule curve adjustments.

The rule curve is used by GRDA to regulate lake levels at Pensacola Dam during a normal water year. The Federal Energy Regulatory Commission (FERC) authorizes this rule curve and any adjustments made to it. GRDA has proposed an adjustment to the rule curve that would involve maintaining the lake level at 743 ft Pensacola Datum (PD) from August 15 to September 15, as shown in Figure 1.3 [GRDA, 2013].

Currently, in the event of extreme rainfall scenarios, both GRDA and the United States Army Corps of Engineers (USACE) control lake levels and discharge at Pensacola Dam. GRDA controls outflow from the Dam until the lake stage reaches the top of the "power pool" at 745.0 ft Pensacola Datum (PD elevations are equal to North American Vertical Datum 1988 (NAVD88) elevations minus 1.40 ft [USGS, 2014]). When the lake stage reaches 745.1 ft PD, the USACE takes control of outflow in order to manage floodwater upstream and downstream throughout the region [GRDA, 2013].

The research contained in this thesis addresses the question: "Do the changes in water surface elevations due to the proposed rule curve adjustment for the August

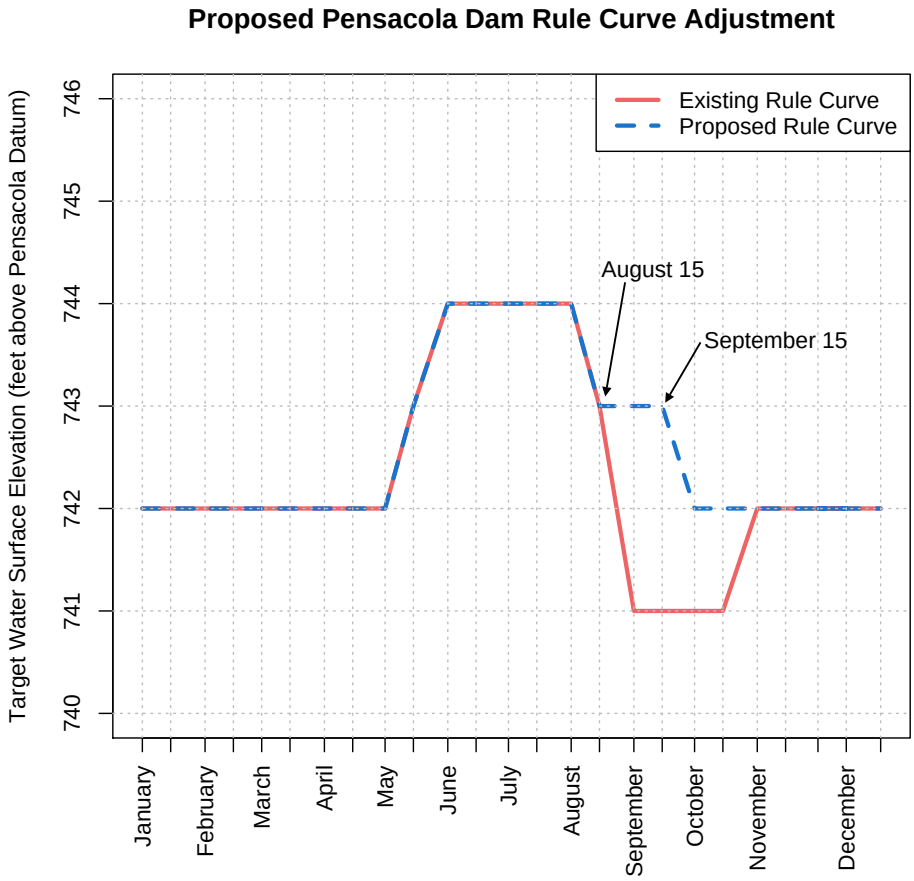

Figure 1.3. Proposed target water surface elevations at Pensacola Dam [GRDA, 2013].

15-September 15 time period have an effect on major flooding levels upstream of Twin Bridges and, primarily, the City of Miami, OK?" Three components of this problem are specifically addressed:

I. The first problem is to determine a reasonable and conservative statistical estimation for an extreme streamflow event for the major streams in the area. The four streams addressed in detail are the Neosho River, Tar Creek, Spring River, and Elk River. Historical streamflow data from the August 15 to September 15 time period are used for the streamflow analysis.

II. The second problem is to create a detailed hydraulic model that represents the study area with the best available datasets. These datasets include topograph-

ical data representing the landscape surrounding the water bodies as well as bathymetric data representing the ground elevations underneath the surface of the water. The hydraulic model also takes into account hydraulic roughness conditions of the floodplain areas for the August 15 to September 15 time period.

III. The final problem is to apply the hydraulic model to the research question in order to determine the effect of a difference in water surface elevations (WSEs) from 741 ft PD to 743 ft PD at the location of Pensacola Dam for the August 15 to September 15 time period.

This thesis is divided into five chapters: an introduction, a literature review, a methods chapter, a results/analysis chapter, and conclusions. Each chapter is divided into sections that discuss the individual problems mentioned above.

CHAPTER 2

Literature Review

A review of previously-published literature is helpful in order to both learn from others' research, and to compare the results of this research to previously-published studies in this context. The literature review is divided into four sections:

1. Previous studies investigating the specific research context of Grand Lake and the Neosho River near Miami, OK;
2. Studies involving statistical streamflow analysis;
3. Studies involving building a hydraulic model with modern technology; and,
4. Studies related to executing a hydraulic computer model.

2.1 Studies Investigating Grand Lake and the Neosho River Near Miami, OK

Previous studies have investigated Neosho River flooding, but the available literature is not adequate to answer the questions that will be addressed in this thesis. The *Chronicles of Oklahoma* gives the historical account of the flood studies that were conducted on the river prior to Pensacola Dam being built [Holway, 1948]. The USACE published a report in 1998 investigating easement elevations in the Grand Lake area [USACE, 1998]. A judicial report filed in 1999 by Holly contains an investigation into the 1992-1995 floods in Miami [Holly Jr., 1999]. Holly also published an article investigating the effects of a previously proposed power-pool change in 2004

[Holly Jr., 2004]. Manders (2009) investigated the effects and mapped locations of the 2007 major flood on the Neosho River at Miami. The existing literature does not specifically investigate the effect of the current proposed rule curve adjustment, and it does not incorporate the most recent geometric and hydrologic data for the river system.

2.1.1 Chronicles of Oklahoma

A periodical titled *Chronicles of Oklahoma* contains a historical account of the building of Pensacola Dam [Holway, 1948]. Holway (1948) states that the "U.S. Army Engineers," prior to the construction of the dam, completed a flood study of the Grand River. This article does not mention the reach of the Neosho River upstream of the confluence of the Neosho and Spring Rivers. There is no documentation available for reference from this flood study, but it is noted that there was a flood study performed prior to construction of the dam.

2.1.2 USACE Hydraulic Analysis of Grand Lake

In 1998, the USACE published a report of their findings from a hydraulic Real Estate Adequacy Study conducted on Grand Lake of the Cherokees [USACE, 1998]. This study investigated the adequacy of the elevations of the flood easements the USACE owns, extending upstream into the tributaries. This report contains useful information about the locations and hydraulic descriptions of the areas included in this thesis. The report includes river mile descriptions, channel and overbank hydraulic roughness conditions for the rivers, and information about the USGS gauge stations located in the study area. This report also includes information about the easement elevations owned by the USACE in the Miami area, which is helpful in determining what levels constitute the designation of a "flood" in this area [USACE, 1998].

The conclusions of this report state that the upstream effect from Grand Lake does not affect flood elevations on the Neosho upstream of USGS gauge 07185000, near Commerce, OK. The conclusions also state that the full-lake elevation of 755 ft PD has less than a 6-inch effect on backwater WSEs upstream of the abandoned bridge in Miami for the 50- and 100-year floods [USACE, 1998]. While this study is extremely helpful as a guide for the model geometry setup portion of this thesis, it does not adequately answer the question of what effect the current proposed rule curve has on backwater flooding.

2.1.3 Holly Reports

Dr. Forrest Holly, Professor Emeritus at the University of Iowa and Adjunct Professor at the University of Arizona, served as a referee for a legal report published in 1999 concerning flooding on the Neosho River in relation to Pensacola Dam. Holly also published an academic research report on the same subject in 2004.

1999 Referee Report, including Amendment

In 1999, Holly was appointed as a professional referee on a legal case in the District Court of Ottawa County [Holly Jr., 1999]. Holly was given the task of determining the difference in floodwater elevations and durations for with- and without-dam conditions for fourteen specified floods that occurred on the Neosho River between 1992 and 1995. Holly was also asked to develop a backwater envelope curve to represent the effect of Pensacola Dam for each of the 14 floods.

The hydraulic model used in this study was a one-dimensional model called CARIMA [Holly Jr. and Benoit-Guyod, 1977]. This model was used because it was capable of modeling unsteady flow. Although HEC-RAS[1] was developed in 1995, the unsteady-flow modeling capabilities of HEC-RAS were not added until version 3.1.1,

[1]See Section 2.3.1 for more information about HEC-RAS

which was publicly released in May 2003 [Brunner, 2010]. It should be noted that the CARIMA model is fundamentally based on the same unsteady-flow equations (see Section 2.3.1) as the unsteady HEC-RAS model [Holly Jr. and Benoit-Guyod, 1977; Brunner, 2010].

Based on the research conducted, Holly (1999) concluded that, when comparing the with-dam conditions to without-dam conditions, Pensacola Dam had a maximum 3 ft flood-exceedance impact on locations along the Neosho River near Miami, OK. These conclusions are based on comparing results from running the CARIMA model with the a) hypothetical scenario of no dam influence, and b) the actual recorded dam stage elevations for the 14 floods.

Because Holly was investigating the effects of Pensacola Dam based on actual historical datasets for the 14 floods included in the report, this research is only partially relevant to the research included in this thesis. The model setup and model geometry are relevant because Holly was modeling the same reach of the Neosho River. However, the results of the report are limited to specific floods for actual Pensacola Dam datasets, and, therefore, not adequate to answer the question this thesis addresses concerning the proposed rule curve change.

2004 Investigation of Proposed Power Pool Change

In 2004, Holly conducted a study investigating the effect of a change in the power pool elevation of Grand Lake from 741 ft PD to 745 ft PD [Holly Jr., 2004]. For this research, Holly used the historical streamflow dataset from one of the 14 floods mentioned in Holly (1999), namely Flood 13 (2 - 22 June 1995), to investigate the differences in WSEs along the Neosho River based on the hypothetical situation of holding the dam WSE at 741 ft PD versus 745 ft PD. A hydraulic model called C1/C2 was used for the hydraulic analysis portion of this report [Holly Jr., 1999].

The C1/C2 model was developed by Holly in the late 1970s and it is a one-dimensional/two-dimensional combination hydraulic model. The model has the capability to treat the flood plain of a stream as a individual cells, while maintaining 1D representation of the river channel. This cell-type rendering of the flood plain was used upstream of Miami for Holly (2004). This location was chosen for the cell-type floodplain rendering because the river channel is very sinuous in this portion of the stream.

The hydraulic transfer between the cell-type floodplain and 1D channel was achieved by assigning a weir-type or fluvial-type designation for each cell along the combination portion of the stream [Holly Jr., 2004]. According to Holly (2004), "The overall purpose of this expanded modeling approach is to capture, as faithfully as possible in a one-dimensional modeling context, the dynamic storage effects of flood plain areas where the highly sinuous channel meanders within the flood plain, in particular upstream of Miami" [Holly Jr., 2004]. Thus, Holly's approach can be considered a pseudo-2D model in that it allows floodplain storage and routing to behave independently of the river channel, but it does not apply the full two-dimensional St. Venant equations to the combined channel/ floodplain system. Holly (2004) maintained a purely 1D representation of the river (similar to the HEC-RAS model used in this thesis) in the section of the Neosho River downstream of Miami where the channel is not as sinuous.

Holly (2004) concluded that the effect of the hypothetical dam WSE change from 741 to 745 ft PD for the historical streamflows recorded for Flood 13 had an effect of about 0.20 ft at "river mile 142.0," which represents the location of Miami, OK. This conclusion is very relevant for the research included in this thesis. The research contained in this thesis is very similar to Holly (2004) with a few exceptions:

- Instead of modeling observed streamflow hydrographs with hypothetical dam WSEs, this research will be using flood-frequency streamflows, which were de-

termined from the historical streamflow information, as the upstream boundary conditions for the model, with hypothetical dam WSEs for the downstream boundary conditions.

- This research uses more recent data, which has been collected with more advanced technology, than the data used in Holly (2004).
- This research uses the industry-standard hydraulic modeling program, HEC-RAS 4.1.
- This research investigates the effects of the rule curve adjustment of dam WSEs from 741 ft PD to 743 ft PD, unlike Holly (2004), which investigated the effect of changing the power pool elevation from 741 ft PD to 745 ft PD.
- This research specifically focuses on the August 15 to September 15 time period relevant to the proposed rule curve adjustment, while the flood investigated in Holly (2004) occurred in June.

Therefore, while the conclusions in Holly (2004) are important and relevant, this thesis will be answering a related question, yet with more recent and more advanced data, as well as a more widely-accepted modeling program than the C1/C2 model used in Holly (2004).

2.1.4 Manders Research Project

A 2009 research project by Manders investigated a major flooding event that occurred in this watershed in July 2007. This study contributed elevation datasets from flood locations that will be useful in calibrating a hydraulic model of the Neosho River. The study concluded that backwater effects are a likely contributor to the flooding at Miami, yet this conclusion is based on eyewitness observation and testimony, as well as the Holly (1999) report mentioned in Section 2.1.3 [Manders, 2009]. Because

Holly (2009) specifically studied floods from 1992-1995, additional hydraulic modeling research is necessary to adequately understand the primary cause of the high water marks in the 2007 Miami flood.

2.2 Related Streamflow Analysis Literature

The streamflow analysis portion of this research involved both the collection of a large number of streamflow datasets, as well as a statistical analysis of those datasets. In the sections that follow, a literature review is provided concerning both the data collection methods and the statistical analysis methods used for this research.

2.2.1 Available Stream Gauge Data

Some of the tributaries that contribute to water levels at Miami, OK have been equipped with USGS stream gauges [USGS, 2012]. These gauges were used to calibrate and validate the hydraulic model used in this research. Figure 2.1 represents the locations of each stream gauge. Two relevant time-varied datasets are available from most stream gauges: discharge and stage. Table 2.1 summarizes the available datasets from each USGS gauge used in this research. In Figure 2.1, note that two of the gauge markers have dots in the middle of the marker. These gauges are used for calibration purposes, as the stage elevation is available for historic rainfall events. Calibration of the hydraulic model to these historic gauge stages is a necessary component of hydraulic modeling in order to capture the unique and complex physical characteristics of the region, as represented by parameters in the model.

Table 2.1. USGS stream gauge information.

Stream	Location	USGS No.	Stage	Discharge
Neosho River	Commerce, OK	07185000	✓	✓
Neosho River	Miami, OK	07185080	✓	
Spring River	Quapaw, OK	07188000	✓	✓
Elk River	Tiff City, MO	07189000	✓	✓
Tar Creek	Miami, OK	07185095	✓	✓
Pensacola Dam	Langley, OK	07190000	✓	

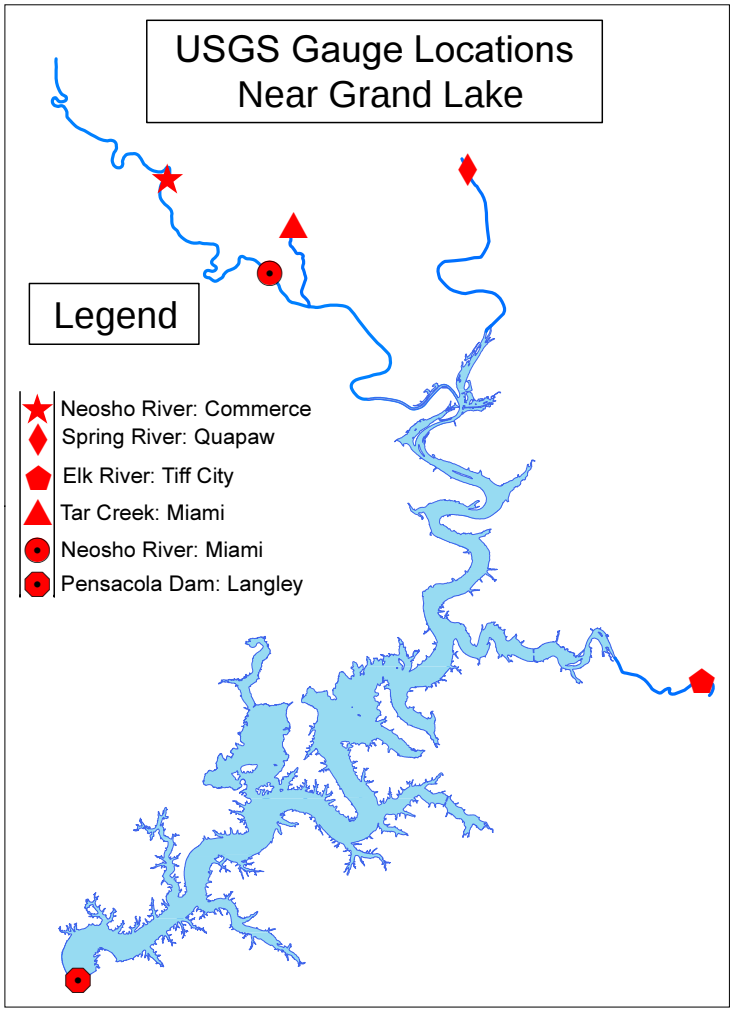

Figure 2.1. USGS Gauge Locations Relative to Grand Lake [USGS, 2012].

2.2.2 Bulletin 17B

In 1981, Bulletin 17B (B-17B) was published by the Water Resources Council, within the U.S. Department of the Interior. This document provides guidelines for determining flood flow frequency in the United States [USGS, 1982]. It also contains a glossary that is used to provide consistency of terms throughout this thesis. The B-17B recommends using the log-Pearson Type-III (LP3) probability distribution for estimating extreme flows when using annual maxima datasets. The LP3 distribution uses the Pearson Type-III (PE3) equation, but the parameters are calculated using the log-transform of the data. The probability density function (PDF) for the PE3/LP3 distribution is represented in equation 2.1.

$$f(x) = \frac{\left(\frac{x-\zeta}{\beta}\right)^{\alpha-1} \exp\left(-\frac{x-\zeta}{\beta}\right)}{|\beta\Gamma(\alpha)|}, \quad x > \zeta \text{ for } \beta > 0, \quad \text{or } x < \zeta \text{ for } \beta < 0 \qquad (2.1)$$

The three parameters in the LP3 distribution are α, (the shape parameter), β, (the scale parameter,) and ζ, (a shift parameter that makes the LP3 distribution unique from the Gamma probability distribution) [Wilks, 2011, pp. 95-103]. $\Gamma(\alpha)$ represents the gamma function[2] evaluated at α [Wilks, 2011, pp. 96]. The use of the log-transform of the data is the only difference between the LP3 and the PE3, mentioned in Section 2.2.4. More information about the methodologies involved with using the B-17B guidelines are found in Section 3.1.

The B-17B guidelines have been analyzed by many hydrologists in the more than 30 years since they were published, and many have found ways that the guidelines could be improved [Lim and Voeller, 2009; England Jr and Cohn, 2007]. Specifically for the context of this research, there are no guidelines included in the B-17B for

[2]The gamma function is a mathematical representation of the factorial function for numbers more complex than a positive integer [Wilks, 2011, pp. 78].

performing a flood-frequency analysis for a single month of the year, such as the August 15 - September 15 time period investigated in this research. For this reason, in this thesis, the B-17B standard annual maxima method is performed and compared to another data sampling method called "partial duration" data sampling. B-17B confirms that partial duration, or "peaks-over-threshold" datasets may be used in flow estimation, but that more care is required in determining the best fit distribution for the dataset [USGS, 1982]. Section 3.1.2 discusses the procedure used to ultimately choose between the two data sampling methods.

2.2.3 Partial Duration Data Sampling Literature

As described in B-17B, data sampling can be accomplished by two methods: either 1) using the annual maxima streamflows from the recorded datasets ("AM" method), or 2) using all of the streamflow measurements that are peaks over a certain threshold ("POT"[3] method) [Wilks, 2011]. The POT method is able to utilize a larger set of the historical data because multiple peaks-over-threshold may occur in any given year. This is specifically useful for streams which do not have a long history of recorded data. This condition is evident for Tar Creek in this research, which has less than 20 years of data on record.

Several authors have tested and confirmed the applicability of the POT method in streamflow analysis [Adamowski, 2000; Cunnane, 1973; Ekanayake and Cruise, 1993; Pham et al., 2013]. According to these studies, the POT method is more accurate than the AM method only if the number of peaks used is ≥ 1.65 times the number of years on record. This means that the peaks must be identified, and then at least the top $1.65 \times N$ (with N being the number of years on record) peaks are used for the statistical analysis [Cunnane, 1973]. For this thesis, M refers to the number of

[3]Although the POT method is more commonly referred to as the partial duration method, for the purpose of this thesis, the abbreviation "POT" will be used so as to not confuse the abbreviation "PD" with Pensacola Dam or Pensacola Datum.

peaks used and the ratio M/N is referred to as k. Therefore, k represents the average number of peaks extracted per year from the historical dataset.

When using the AM method, meteorologic independence of events is not a concern because only one event is extracted per year. However, independence of meteorological events must be taken into consideration with POT datasets [Wilks, 2011]. With multiple peak events per year being used by the POT dataset, some care must be taken to ensure that the peaks are indeed independent [Wilks, 2011]. The method used to ensure independence in this research is described in Section 3.1.2.

Fitting distributions to the POT datasets is completed in a similar manner to fitting distributions to AM datasets, but the probability quantiles are different for a particular return period because the number of data points is greater than the number of years on record ($M > N$). The process outlined in Section 3.1.6 must be followed to calculate the probability quantile associated with a particular return period derived from a probability distribution fitted to a POT dataset [Wilks, 2011].

2.2.4 Extreme Value Distributions Literature

Determining what streamflow to use for the hydraulic model involves calculating a probable "extreme value" of the distribution of historical floods. The probability theory of this process is outlined in *Statistical Methods in the Atmospheric Sciences*, by Wilks (2011). Although streamflow itself is not an atmospheric phenomenon, the primary cause of flooding is rainfall runoff, which is an atmospheric phenomenon and follows atmospheric statistical patterns. Section 3.1 explains the process of parameter fitting that was used to fit various probability distribution functions to the observed POT streamflow data. Eight probability distributions were chosen for POT analysis based on the literature cited in the following paragraphs.

Gamma and Log Pearson Type-III Distributions

The two-parameter Gamma-distribution is commonly used for precipitation modeling in the United States. The gamma distribution's probability density function (PDF) is represented by equation 2.2. The two parameters in the Gamma distribution are α, the shape parameter, and β, the scale parameter.

$$f(x) = \frac{(x/\beta)^{\alpha-1}\exp(-x/\beta)}{\beta\Gamma(\alpha)}, \quad x, \alpha, \beta > 0 \tag{2.2}$$

The Pearson Type-III distribution is a form of the gamma distribution that uses an additional shift parameter, ζ [Wilks, 2011, pp. 95-103]. The PDF for the Pearson Type-III distribution is the same as equation 2.1 in the B-17B explanation above. The Pearson Type-III differs from the LP3 in that it does not use the log-transform of the parameters.

The Gamma distribution, the non-transformed Pearson distribution (PE3), and the LP3 distribution were all included in this POT analysis to investigate whether any may apply to this specific research context.

Generalized Extreme Value (GEV), Gumbel, Weibull, and Generalized Pareto Distributions

The three-parameter GEV distribution is used to derive the two-parameter Gumbel and Weibull distributions. The GEV distribution is also the foundation for the generalized Pareto distribution, which is used specifically for POT datasets. In Wilks (2011), the GEV distribution is linked to the study of extremely large precipitation

events that may cause flooding. The GEV PDF is represented in equation 2.3, where κ, ζ, and β are the shape, location, and scale parameters, respectively.

$$f(x) = \frac{1}{\beta}\left[1 + \frac{\kappa(x-\zeta)}{\beta}\right]^{1-\frac{1}{\kappa}} \exp\left\{-\left[1 + \frac{\kappa(x-\zeta)}{\beta}\right]^{\frac{-1}{\kappa}}\right\}, \quad 1 + \kappa(x-\zeta)/\beta > 0 \tag{2.3}$$

The GEV distribution can be integrated analytically, yielding the cumulative distribution function (CDF) in equation 2.4.

$$F(x) = \exp\left\{-\left[1 + \frac{\kappa(x-\zeta)}{\beta}\right]^{\frac{-1}{\kappa}}\right\} \tag{2.4}$$

The Gumbel distribution is a form of the GEV distribution in which the shape parameter (κ) approaches zero. This distribution is also known as the Fisher-Tippett Type 1 distribution, but will be referred to as the Gumbel distribution for this research. The Gumbel distribution PDF, represented in equation 2.5, may be integrated analytically yielding the CDF represented in equation 2.6 [Wilks, 2011, p. 106]. The parameters of the Gumbel distribution are identical to the GEV, but κ is not included.

$$f(x) = \frac{1}{\beta}\exp\left\{-\exp\left[-\frac{(x-\zeta)}{\beta}\right] - \frac{(x-\zeta)}{\beta}\right\} \tag{2.5}$$

$$F(x) = \exp\left\{-\exp\left[-\frac{(x-\zeta)}{\beta}\right]\right\} \tag{2.6}$$

The Gumbel distribution has been used to model extreme streamflow in Mujere (2011), which applied the traditional method of moments to fit the Gumbel distribution to extreme streamflow on the Nyannyadzi River in Zimbabwe [Mujere, 2011].

The Weibull distribution (also known as the Fisher-Tippett Type III distribution) is the form of the GEV distribution in which the shape parameter is less than zero and the shift parameter equal to zero. The PDF for the Weibull distribution is shown

in equation 2.7 [Wilks, 2011, p. 107]. The parameters for the Weibull distribution are the shape (α) and scale (β), similar to the Gamma distribution.

$$f(x) = \left(\frac{\alpha}{\beta}\right)\left(\frac{x}{\beta}\right)^{\alpha-1} \exp\left[-\left(\frac{x}{\beta}\right)^{\alpha}\right], \quad x, \alpha, \beta > 0 \tag{2.7}$$

Singh (1987) investigates the applicability of the Weibull distribution to various hydrologic applications. This research concluded that the Weibull distribution is inaccurate for the hydrologic applications of rainfall depths and durations [Singh, 1987]. However, Ekanayake and Cruise (1993) compared the Weibull and exponential distributions in application to flood modeling and found the Weibull distribution to be superior.

The generalized Pareto distribution is a form of the GEV function that is specifically designed to work with POT datasets [Wilks, 2011, pp. 109]. Hosking and Wallis (1987) affirm that the generalized Pareto is useful specifically for POT datasets [Hosking and Wallis, 1987]. Ashkar and Ouarda (1996) demonstrate the use of the generalized Pareto distribution in modeling extreme flooding events [Ashkar and Ouarda, 1996]. The PDF of the generalized Pareto is represented in equation 2.8 and the CDF for this distribution is represented in equation 2.9.

$$f(x) = \frac{1}{\sigma^*}\left[1 + \frac{\kappa(x-u)}{\sigma^*}\right]^{-\frac{1}{\kappa}-1} \tag{2.8}$$

$$F(x) = 1 - \left[1 + \frac{\kappa(x-u)}{\sigma^*}\right]^{-1/\kappa} \tag{2.9}$$

In equations 2.8 and 2.9, the value u represents the threshold used for sampling the POT dataset, κ is the shape parameter for the distribution, and σ^* is the scale parameter [Wilks, 2011].

3-parameter Lognormal Distribution

The 3-parameter lognormal distribution (LN3) is a logarithmic power-transformation of the Gaussian distribution [Wilks, 2011, p. 92]. The PDF for the LN3 distribution is shown in equation 2.10.

$$f(x) = \frac{1}{(x-\gamma)\sigma_y\sqrt{2\pi}} \exp\left\{-\frac{\left[\ln(x-\gamma)-\mu_y\right]^2}{2\sigma_y^2}\right\}, \quad x > 0 \tag{2.10}$$

where σ_y and μ_y are the standard deviation and mean, respectively, of the log-transformed variable, $y = \ln x$ [Wilks, 2011]. In the LN3 distribution used in this thesis, γ represents the lower bound of the data. Vogel and Wilson (1996) compare the lognormal distribution to the GEV and LN3 distributions at various streamflow sites across the U.S. and conclude that the LN3 distribution is a viable model for predicting streamflow with POT datasets.

Usage of Probability Distributions

Each of the aforementioned probability distributions has been shown to be relevant to streamflow analysis; therefore, they were all included in the POT streamflow analysis for this research. Each distribution was fit to the historical observed POT dataset, and then analyzed to find the "best-fit" distribution for the extreme rainfall events. This process is described in detail in section 3.1 of the Methods chapter of this thesis.

2.3 Hydraulic Modeling Background

Hydraulic models can be evaluated in either one-dimensional (1D) or two-dimensional/ three-dimensional (2D/3D) computational procedures. Although 2D/3D models provide many advantages over 1D models, they are more complicated to use for large stream reaches, as well as more computationally expensive. Furthermore, for many

river flood studies, 2D/3D models may not provide a significant increase in accuracy [Merwade et al., 2008]. Therefore in this research, the hydraulic model utilized will be HEC-RAS (Hydraulic Engineering Center's River Analysis System), which is a 1D hydraulic model developed by the USACE. For both 1D and 2D/3D models, Geographic Information Systems (GIS) may be used to assist in managing the input data as well as spatially rendering the results.

2.3.1 One Dimensional (1D) Modeling Literature

HEC-RAS is a 1D, physics-based hydraulic modeling program created by the USACE to model open channel flow [Brunner, 2010]. There are various case studies available for review that use HEC-RAS to model flooding (e.g., Knebl et al. [2005]; Haghizadeh et al. [2012]). HEC-RAS is the recommended by the Federal Emergency Management Agency (FEMA) for floodplain modeling and hydraulic analysis [FEMA, 2012]. The HEC-RAS model iteratively solves a system of equations and outputs WSEs along a stream channel at user-defined cross section locations.

The HEC-RAS modeling program is capable of modeling two types of flow scenarios: steady-state and unsteady flow routing. The main difference is that unsteady flow routing is time-dependent, while steady-state flow has no time component in the water surface calculations.

Steady-state flow computations in HEC-RAS

The basic computational procedure used by HEC-RAS for the steady-state flow calculation is based on the solution of the 1D energy equation [Brunner, 2010], which is shown in equation 2.11.

$$Z_2 + Y_2 + \frac{\alpha_2 V_2^2}{2g} = Z_1 + Y_1 + \frac{\alpha_1 V_1^2}{2g} + h_e \tag{2.11}$$

where,

Z = Channel bottom elevation above datum,

Y = WSE above datum,

V = Average velocity,

α = Kinetic energy correction factor,

g = Gravitational constant, and

h_e = Head loss term, defined in equation 2.12

$$h_e = LS_f + C\left|\frac{\alpha_2 V_2^2}{2g} - \frac{\alpha_1 V_1^2}{2g}\right| \tag{2.12}$$

where,

L = discharge weighted reach length (based on geometry of both channel and flood-plain),

S_f = friction slope (based on Manning's-n),

C = expansion or contraction loss coefficient (user input)

The HEC-RAS procedure for steady-state flow WSE computation is as follows:

1. For subcritical flow (known WSE at downstream control point), assume a WSE at the immediate upstream cross section from the control point;
2. Based on that value, calculate the total conveyance and velocity head;
3. Calculate S_f based on values from step 2, and solve for h_e using equation 2.12;
4. Solve the energy equation (Eq. 2.11) for Y at the upstream cross section (WSE);
5. Compare calculated WSE with assumed WSE, and iterate until error is less than the tolerance level, which is either 0.01 ft by default, or else user defined.

The momentum equation is used for certain situations in the steady flow procedure where the flow may be temporarily rapidly-varied. These situations include bridge

contractions and expansions, abrupt changes in slope, and river confluences [Brunner, 2010].

Steady-flow results represent the dynamic equilibrium stage of the system, subject to a constant forcing. For this reason, for any flow magnitude, Q_0, a steady flow simulation will produce higher water surfaces, in general, than an unsteady flow with a peak of Q_0. Moreover, the steady flow simulation is convenient for determining WSEs for floods and statistically extreme flows because these are often single discharge values (the peak) and not flow vs. time hydrographs.

Unsteady flow routing in HEC-RAS

Two laws govern unsteady fluid flow in HEC-RAS calculations [Brunner, 2010]:

- Conservation of Mass, i.e., accumulation in a reach is equal to mass in minus mass out, and
- Conservation of Momentum, i.e., the time rate of change of momentum in a control volume is equal to the sum of the forces acting on the water in the control volume.

The 1D equation for conservation of mass for this context is:

$$\frac{\partial A_T}{\partial t} + \frac{\partial Q}{\partial x} + q_l = 0 \tag{2.13}$$

where,
$\frac{\partial A_T}{\partial t}$ = rate of change in fluid storage in a control volume,
$\frac{\partial Q}{\partial x}$ = net rate of fluid flow into the control volume, and
q_l = the lateral fluid flow entering the control volume, per unit length.

The 1D conservation of momentum equation is shown in equation 2.14. The left side of the equation represents the sum of all forces acting on a control volume in the

direction of flow, and the right side of the equation represents the momentum flux, or time rate of change of momentum in the control volume.

$$\sum F_x = \frac{dM}{dt} \tag{2.14}$$

The discrete equation for the sum of all forces in the direction of flow, for this context is represented in equation 2.15:

$$\sum F_x = -\rho\frac{\partial QV}{\partial x}\Delta x - \rho g A\frac{\partial h}{\partial x}\Delta x - \rho g A\frac{\partial z_0}{\partial x}\Delta x - \rho g A S_f \Delta x \tag{2.15}$$

where,

$\sum F_x$ = sum of all forces in the x-direction on a control volume

$\rho\frac{\partial QV}{\partial x}\Delta x$ = momentum flux through the control volume

$\rho g A\frac{\partial h}{\partial x}\Delta x$ = pressure forces on the control volume

$\rho g A\frac{\partial z_0}{\partial x}\Delta x$ = gravitational forces on the control volume, and

$\rho g A S_f \Delta x$ = boundary drag associated with the control volume

The discrete equation for the momentum flux acting on the control volume is represented in equation 2.16.

$$\frac{dM}{dt} = \rho\Delta x\frac{\partial Q}{\partial t} \tag{2.16}$$

In the limit, equations 2.14, 2.15, and 2.16 become the differential balance of momentum, represented by equation 2.17.

$$\frac{\partial Q}{\partial t} + \frac{\partial QV}{\partial x} + gA\left(\frac{\partial z}{\partial x} + S_f\right) = 0 \tag{2.17}$$

Equations 2.13 and 2.17 are solved simultaneously in the HEC-RAS unsteady flow routing solver based on a four-way iterative process involving two spatial (x) nodes

and two temporal (t) nodes, which is outlined in detail in Brunner (2010). The process yields a WSE for each cross section at each time step during the flow simulation.

Unsteady flow routing is especially useful for conditions where historical observed datasets have been recorded and can be input into the system as a flow vs. time or stage vs. time hydrograph.

2.3.2 2D/3D Modeling Literature

The most relevant literature available using the 2D approach is Merwade et al. (2008). This article outlines the use of a 2D hydraulic modeling technique using GIS on three rivers in the United States. The article addresses issues that the 2D approach encounters with geometric data. The traditional 1D approach, according to Merwade et al. (2008), does not accurately model the water behavior in the case of large-scale extreme events, such as over-500-year return period flooding or glacial outbursts. The purpose of the Merwade paper was to provide guidelines for incorporating surveyed channel data with surrounding Digital Elevation Models (DEMs). While it is helpful to know that this 2D/3D approach is an option, the traditional 1D approach will be used in this thesis research for three reasons:

1. The intended application does not include over-500-year return period flooding or dam breaks;

2. 1D modeling is the approach utilized and accepted by the USACE and the Federal Emergency Management Agency (FEMA) [Brunner, 2010; Buckley, 2001]; and

2.3.3 Geographic Information Systems Literature

Hydraulic modeling programs may be used in conjunction with GIS to develop maps that delineate the floodplain of a channel during a flood event [Yang et al., 2006]. This

enables the user to visually represent the flood and, also, to store information about the flood in a format that is useful for many different applications. A tool native to the GIS program ArcMap 10, called HEC-GeoRAS, is designed to aid the user in using GIS in conjunction with HEC-RAS [ESRI, 2011; Ackerman, 2009]. The flood maps created with HEC-GeoRAS may be compared with the existing (FEMA) floodplain maps in order to note differences and investigate the reason for the differences.

CHAPTER 3

Methods

There are three major segments involved in the methodology of this research: 1) a statistical streamflow analysis; 2) the building of the hydraulic model; and 3) HEC-RAS modeling.

3.1 Statistical Streamflow Prediction Methods

In order to conduct a hydraulic analysis of the Grand Lake region, extreme streamflow conditions are required for use as upstream boundary conditions for the model. A statistical analysis of the data is necessary for extrapolation of a probability distribution beyond the limits of the 74 years of recorded streamflows in order to estimate flood-frequency streamflows of lower probability events, such as the 100-year flood.

3.1.1 Approach

There are two acceptable and widely-used approaches to the flood-frequency prediction problem [Bedient et al., 2013]. The approaches differ in their method of defining the streamflow dataset at the boundary of the hydraulic model. The first approach is to set up a hydrologic model of the watershed for the all of the parameters that contribute to runoff (the "physics-based" approach). These parameters include historic rainfall patterns, land use, infiltration capacity, watershed storage, and evaporation. After calibration of these parameters, the hydrologic model is then used to simulate the expected runoff that would occur at the boundary of the hydraulic model. The process is repeated for many rainfall scenarios, and the resulting flow dataset is used

to estimate flood-frequencies. The second approach is to use the stream gauges that are located on the streams in the immediate vicinity of the study area to perform the flood-frequency analysis (the "stream gauge" approach) [Bedient et al., 2013]. Stream gauges act as an integration of all the upstream hydrologic parameters; therefore, the gauges output the cumulative result of all that is happening upstream. The historical datasets from these gauges are analyzed to produce statistical probabilities of the streamflow magnitudes.

There are advantages and disadvantages associated with each approach. One advantage of the physics-based approach is that representation of the actual contributors to runoff may be isolated and calibrated. For example, a model can take into account particular releases from upstream dams, seasonal infiltration capacities of the soil on the contributing watershed, recent changes in upstream land use, as well as historical rainfall events. The disadvantage of this approach is that it requires a very large amount of spatial and temporal data, especially for a watershed as large as the Grand Lake watershed.

An advantage of the stream gauge approach is that the data processing is simpler. For example, stream gauges have been collecting datasets on the Neosho, Elk, and Spring rivers since 1939. These datasets have essentially integrated the upstream hydrologic behavior for 70+ years. One disadvantage of this approach is that specific contributors to streamflow cannot be isolated (e.g., dam release upstream, infiltration capacities of the soil, etc.). Another disadvantage is that it depends on having a long enough period of record (e.g., this approach would not be viable with only 5 years of recorded data).

Given the relatively long period of record, the acceptance of the second approach in the floodplain modeling community, and the well-defined objectives of this research project, the second approach is used in this research. Time-series streamflow datasets

from the Neosho, Spring, and Elk Rivers and Tar Creek have been statistically analyzed in order to predict flood-frequency streamflow values [Bedient et al., 2013].

3.1.2 Data Collection

The datasets used for the statistical streamflow prediction of the Neosho, Spring, and Elk Rivers and Tar Creek were the observed August 15 to September 15 daily-mean streamflows at the streams' USGS gauges nearest Grand Lake, as shown in Table 3.1.[1]

Table 3.1. USGS stream gauges used for statistical streamflow prediction.

Stream	Location	USGS Gauge No.	Begin Date of Discharge Data
Neosho River	Commerce, OK	07185000	10/01/1939
Spring River	Quapaw, OK	07188000	07/12/1939
Elk River	Tiff City, MO	07189000	10/01/1939
Tar Creek	Miami, OK	07185095	01/01/1984

Bulletin 17B mentions two methods of data sampling techniques [USGS, 1982]. The two methods are each very prevalent in the hydrologic literature, and can be summarized as the following:

1. using the maximum annual streamflow from the recorded data (known as the annual maxima (AM) method), or

2. using all of the streamflow measurements that are peaks over a certain threshold (POT method) [Wilks, 2011].

B-17B does not recommend a particular method of data sampling for the purpose of predicting the extreme streamflow for a certain month of the year, as is the case for this research. Because no specific guidelines are given for this case, both methods

[1] The Tar Creek Miami gauge historical dataset has a gap of 9 years from 10/1/1993 to 5/27/2004, so there are only $N = 20$ years of data available for this location.

are employed for analysis of the Neosho River, Commerce gauge data, and the most conservative method is chosen for calculating flood frequencies of each stream for use in the model application phase of the research.

Averaging streamflow values over a 24-hr window will suppress the peak discharge values, particularly if the peak flow only occurred for a period of time less than 24-hrs. This suppression of peak discharge values is referred to as streamflow dampening. Accounting for streamflow dampening is necessary in order to accurately predict the extreme flood events, particularly on the smaller streams such as Tar Creek, which produce peaks that are completely contained within a 24-hr time period. In order to account for streamflow dampening in the daily-average datasets available from the USGS, the following procedure is used to convert the daily-average peaks to synthetic instantaneous-peak streamflow values.

1. First, the annual instantaneous-peak streamflow values for each gauge station are retrieved from USGS (2012).

2. The daily-average peak values associated with each annual instantaneous-peak are retrieved from the daily-data section of the same website.

3. A "peaking factor" is calculated for each peak value by dividing the instantaneous-peak by the daily-average peak.

4. An average peaking factor is calculated for each gauge station using the entire period of record.[2]

5. The daily-average peaks for the August 15 - September 15 time period are multiplied by the respective gauge peaking factor and those modified values used for input in the statistical analysis.

[2]These values are shown in Table 4.1 in Section 4.1.

3.1.3 Statistical analysis of the AM datasets using PEAKFQ

A program developed by USGS, PEAKFQ, is utilized to determine the statistically extreme streamflows for the streams included in this study [Flynn et al., 2014]. The users' manual outlines the computing codes used to follow the B-17B procedures exactly. PEAKFQ uses a specific input file of a form that is available from the USGS National Water Information System [USGS, 2012]. The file is available for download for the annual peak streamflow events on a gauge station webpage, provided that gauge station records historic streamflow data. This file is accessed for each of the four streamflow gauges used in this thesis, and the file is modified to include the maximum streamflow for each August 15 - September 15 on record, with the peaking factors applied.

The PEAKFQ program uses the historical datasets in the input file to calculate the parameters for the LP3 distribution in the precise method outlined in B-17B. The program provides an output file including the details of the statistical analysis as well as probable extreme value estimates calculated from the fitted LP3 distribution. The program also provides a graphical output representing the observed gauge data (or "systematic data") and the fitted LP3 distribution with its 95% confidence interval [Flynn et al., 2014]. This program is used to determine the statistically extreme streamflows used for each of the four upstream streamflow input locations in the hydraulic model.

3.1.4 Statistical analysis of the POT datasets using L-moment parameter estimation

The following method is used to compile the POT dataset from the historical datasets for each stream:

1. First, all of the historical datasets were entered into a spreadsheet.

2. The datasets from each year's August 15 to September 15 period were isolated.

3. Individual peaks were identified for each year, with an independence criteria of 7 days between peaks[3]

4. The highest $M = N \times k$ peaks[4] were ranked from highest to lowest.

5. Those M peaks were used for fitting the probability distributions in the statistical analysis portion of the research.

Probability distributions of type Gamma, GEV, Generalized Pareto, Gumbel, Lognormal, PE3, LP3, and Weibull were fit to the observed POT datasets using parameter fitting methods. A discussion of each distribution can be found in Section 2.2.4.

The method of L-moments is used to estimate parameters for each distribution. Hosking (1990) presents a concise summary of L-moments and their applicability to parameter estimation [Hosking, 1990]. L-moments are analogous to traditional statistical moments, but they are linear combinations of order statistics. L-moments have been used to estimate probability distribution parameters in additional research since Hosking's (1990) paper [Adamowski, 2000; Vogel and Wilson, 1996; Ilorme and Griffis, 2013]. A detailed explanation of L-moment theory is not included in this thesis, but may be found in Hosking (1990). Hosking created and maintains an R package entitled "L-moments," which is used in this research to calculate the L-moments and fitted parameters for each probability distribution [Hosking, 2014; R Core Team, 2013].

After fitting the probability distributions to the observed POT datasets, probability plotting-positions are calculated for the observed datasets. The plotting positions

[3]The independence criteria of 7-days between peaks is based on methods outlined in Ashkar and Ouarda (1996).

[4]See Section 2.2.3 for definitions of $M, N,$ and k

are used to compare the fitted distributions' probability quantiles to the probability quantiles of the observed datasets [Makkonen et al.; Hirsch, 1987; Weibull, 1939].

3.1.5 Choosing a "Best-fit" Distribution

In order to determine which distribution is the "best fit" to the POT dataset, a root-mean-square-error (RMSE) analysis is applied comparing each fitted distribution to the observed dataset [Ritter and Muñoz-Carpena, 2013]. The RMSE equation is represented by equation 3.1. RMSE is a valuable statistic for this application because it naturally weights errors in the highest flow values more than in the lower flow values.

$$RMSE = \sqrt{\frac{\sum (y_i - \hat{y}_i)^2}{n}}, \tag{3.1}$$

where,

y_i = the observed value at a probability plotting-position,

$\hat{y}_i$ = the distribution value at the matching probability quantile, and

n = the number of observed data points.

The RMSE values are compared for each distribution using a bootstrapping confidence interval (CI) of the RMSE. Bootstrapping is a method of data analysis known as "resampling with replacement" [Efron and Tibshirani, 1986]. Bootstrapping is advantageous in streamflow analysis because the true underlying probability distribution is unknown, and bootstrapping is a simple method for deriving the CI for a statistical property of the data. For this research, the RMSE was bootstrapped 5,000 times for each {simulation vs. observation} dataset. The RMSE CI's may be used to determine, with confidence, which probability distribution is the "best fit" of the observed data.

3.1.6 Calculation of Extreme Streamflow Values Using Fitted Distributions

In order to calculate extreme streamflow values, the probability distributions are extrapolated beyond the extent of the highest streamflow values recorded in the observed dataset. The calculation of probability is simple for the AM method, and slightly more complicated for the POT method. For example, with N=74 prior years of data using the AM method, the most extreme value (rank = $r = 1$) would have an $r/(N+1) = 1/75 \approx 0.0133$ probability of occurring in any given year [Makkonen et al.; Weibull, 1939]. Using the AM method, to calculate a 100-year storm the probability distribution was extrapolated to a 0.01, or 1/100 probability value. A 200-year storm would have a 1/200, or 0.005 probability of occurrence in a given year, a 500-year storm would have a 1/500, or 0.002 probability of occurrence, and so on [Wilks, 2011]. This process is included in the computations completed by the PEAKFQ program for calculating flood-frequency values for the AM dataset.

When using the POT method, however, an alteration must be made in order to calculate quantiles for extrapolating the probability distributions. Equation 3.2 is used to calculate the CDF quantile "$F(x)$" associated with a particular return period for a POT dataset. For example, for the most extreme value in the recorded POT dataset for the Neosho River, Commerce gauge (where $M = 124$), the return period T' would be equal to the number of years on record ($N = 74$), and the probability quantile would be $F(x) \approx 0.9919355$.

$$F(x) = 1 - \frac{1}{T'k} \tag{3.2}$$

where,

$F(x)$ = CDF probability quantile

T' = Return period for POT dataset

k = Ratio of number of POT data points to number of years on record (M/N)

3.1.7 Choosing a Distribution to Use for Estimating Flood Frequency Values for This Thesis

The probability quantiles for the 2-, 10-, 20-, 50-, 100-, 200-, and 500-yr return intervals were calculated for the Neosho using the method described above. The method that produces the most conservative flood frequency estimates (i.e. highest streamflow values) is used to calculate extreme streamflow estimates on all other streams. These extreme streamflow values are used to "force" the model in the sensitivity analysis and model application portion of the research, as described in section 3.3.2.

3.2 Hydraulic Model Development

3.2.1 Data Collection

In order to build an accurate hydraulic model using the best-available data, information had to be compiled from many sources. These datasets then had to be "normalized" for use in a consistent model. Herein, normalization means combining datasets that may be in different forms into a single form which can be used in a consistent model. These different data sources all use a different data organization method, and normalization allows the model to be able to read all of the datasets consistently. The "topography," as defined in this paper, are the areas of bare-earth elevations that were not underwater at the time of the data collection. The underwater areas are referred to as "bathymetry."

A major issue encountered in the normalization of the datasets is that there are many vertical datums used to record elevation data. A diagram developed by USGS for understanding datums in this region is shown in Figure 3.1(a). The graphical

portion of the figure represents the data transformation process for converting between datums. The physical representation of the datums would be reversed, with PD as the highest datum and NAVD88 as the lowest datum. For example, suppose a particular water surface has an elevation of 741 ft above PD. To convert to NAVD88, according to the text in Figure 3.1(a), 1.4 ft is added to the elevation. Therefore, the same water surface is 742.4 ft above NAVD88. Visually, the physical representation of the datums is shown in Figure 3.1(b).

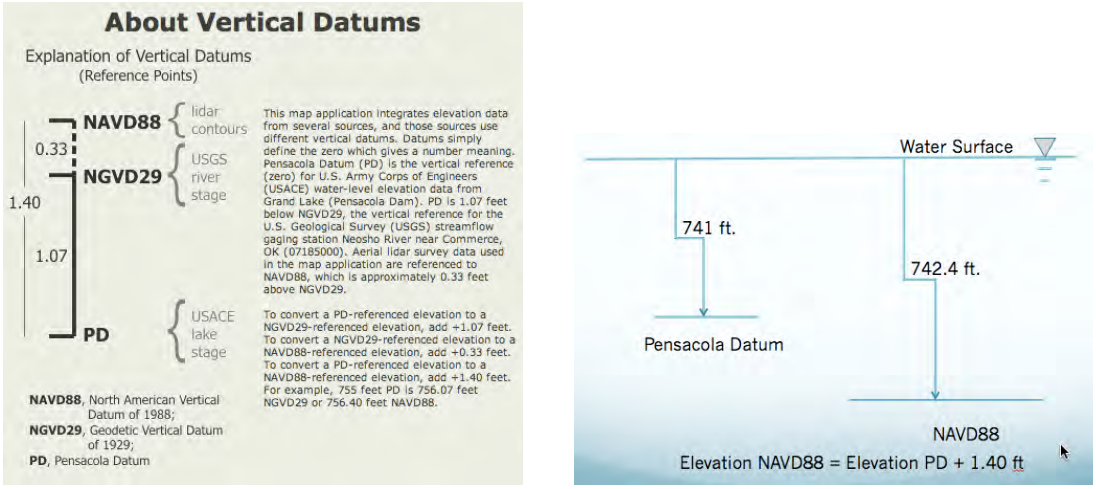

(a) USGS Figure (b) Physical Representation

Figure 3.1. Graphical representation of the complexity of converting between various vertical datums. USGS Figure taken from USGS (2012).

Topographic Data

The topographic datasets provide information about the floodplain for a hydraulic model. Detailed topographic datasets are currently publicly available from the National Elevation Dataset (NED), which is provided by the USGS. The most recent detailed dataset for the Grand Lake region was collected in 2008. Details about this dataset may be accessed from the dataset's metadata, available from the NED website [Gesch, 2007]. The relevant details for this thesis are as follows:

- The dataset is downloaded as raster files in .img format.

- The dataset is downloaded in sections of 0.25° longitude × 0.25° latitude.
- The resolution of the raster is about 3 meters.
- The elevation data points are stored in SI units and relative to the NAVD88 vertical datum.
- The data points were collected using Light Detection and Ranging (LiDAR) technology.
  - LiDAR is extremely accurate for vertical elevations (~10 cm accuracy[5]).
  - LiDAR does not collect bathymetric data points because the light emitting device reflects off the surface of the water.

Bathymetric Data

The bathymetric datasets for the Grand Lake region originate from many sources. Four different sources were collected and combined for use in the hydraulic model, spanning various collection methods and ages of the datasets.

1. The Oklahoma Water Resources Board (OWRB) collected a bathymetric dataset for the entire Grand Lake reservoir in 2009 [OWRB, 2009].
   - The bathymetric data points were collected using an acoustic doppler device, which is not as accurate as the aforementioned LiDAR, but is still very accurate, with a published accuracy to within ~16 cm in the vertical direction for the entire dataset[6].

[5]This accuracy of 10 cm vertically is the maximum expected difference between the measured topography and the actual topographic conditions. This discrepancy is likely found at locations where the topography changes drastically over a short distance (e.g., cliffs). Although this dataset is not perfectly accurate, a certain amount of error is present in any dataset, and this is the best currently available dataset. An identical geometry file is used in each hydraulic model run for this thesis. Therefore, the accuracy of the dataset does not affect the calculation of the WSE differences representing the proposed rule curve adjustment.

[6]See footnote 5. This concept applies to the bathyemtric dataset as well.

- The bathymetric elevation data points are stored in U.S. customary units and relative to the Pensacola Datum.
- The OWRB bathymetric study does not extend into the river channels of the Neosho or Spring Rivers upstream of Twin Bridges or to the USGS gauge location at Tiff City on the Elk River. Additional bathymetric datasets are required for these sections of the river channel.

2. USGS updates cross sectional datasets for the river channels at USGS gauge station locations periodically, and these channel cross section datasets were used to interpolate between the end of the OWRB bathymetry availability and the gauge station locations on the Spring and Elk Rivers. The Quapaw gauge is used for the Spring River and the Tiff City gauge for the Elk River. These cross section elevations are collected using acoustic doppler technology similar to that used by OWRB in the reservoir bathymetry study [Strong, 2014].

3. A channel bathymetry dataset for the Neosho River between Twin Bridges and the USGS Commerce gauge was collected as surveyed cross sections along the floodplain in 1997 by the USACE. This dataset was received in the form of a HEC-RAS geometry file from the USACE [Wyckoff, 2014]. This channel bathymetry dataset is sufficiently accurate for this research (i.e., determining the effect of Pensacola Dam on upstream flooding), but not nearly as accurate as the aforementioned acoustic doppler technique used by OWRB for the reservoir [OWRB, 2009]. The vertical datum for this dataset is not cited, but it was determined to be relative to the NAVD88 datum[7]. The data points are stored in U.S. customary units.

[7]This assumption is made based on the USACE datasets in relation to another dataset received from USGS for the same cross section locations [Smith, 2013]. The USGS dataset was received as an excel spreadsheet with cross section station/elevation datasets. The topography portion of these cross sections is apparently extracted from the LiDAR data in the NED dataset (Gesch (2007)), but the bathymetry is generalized as a single point in the middle of the river channel. This single point matches up precisely (i.e., to the hundredths digit) with the USACE dataset in its original form. The USGS dataset is clearly cited as relative to the NAVD88 vertical datum. For this reason, it

4. Bathymetry data points were required for the section of Tar Creek south of the Highway 10 bridge in Miami, where the water is several feet deep even on days with little flow. GRDA provided spot-depth data points for this section of Tar Creek in May 2014 using a sonar depth reader. These data points were provided as coordinates and depths from the water surface in U.S. customary units.

Bridge Data

Physical datasets about the relevant bridges in the study area were provided by the USACE in the HEC-RAS geometry file previously mentioned as the source of channel bathymetry data for the Neosho River [Wyckoff, 2014]. These datasets include bridge deck elevations, pier locations and geometry, as well as all necessary bridge modeling information, such as weir coefficients and pier-loss coefficients. These datasets are manually input into the HEC-RAS model created for this research.

3.2.2 Data Normalization and TIN Creation

The raw datasets collected for this research are referenced to different datums and units as per the needs of the specific agency that collected the datasets. Because the NED topography is the largest dataset, its units and datum provide the base for normalizing the topographical and bathymetric datasets. The normalized datasets are then combined in order to create a type of terrain model, called a Triangulated Irregular Network (TIN), that is used by HEC-GeoRAS for the extraction of a hydraulic model.

---

can be reasonably assumed that the original USACE dataset is in reference to the NAVD88 vertical datum.

Normalization Procedures

The normalization of the datasets requires a series of step-by-step procedures in the ArcMap GIS program. The details of these procedures are included in Appendix B. The main structure of the procedure is outlined in the following list.

1. Normalizing the NED dataset

    a. The original raster form of the dataset has a resolution of ~3 meters in the horizontal direction. The vertical accuracy, however, is about 10 cm. The dataset is compressed so that data points within 10 cm vertically of one another are excluded, creating a much smaller file size that still maintains the vertical accuracy of the original dataset.

    b. The original dataset also includes false data points at locations that were covered by water at the time of the data collection. In order for these data points to not interfere with the OWRB dataset, the points within the boundary of the OWRB study are removed from the NED dataset.

2. Normalizing the OWRB dataset

    a. The OWRB data points are received in U.S. customary units referenced to the Pensacola Datum. These data points are converted to SI units referenced to the NAVD88 datum in order to match the larger NED dataset.

    b. The OWRB bathymetry dataset is then merged with the normalized NED dataset to create a dataset including both topography and bathymetry.

3. The NED floodplain topography and OWRB reservoir bathymetry are then compiled into a triangulated irregular network (TIN), which is the type of DEM from which HEC-GeoRAS (see section 2.3.3) is able to extract elevation data points for the hydraulic model. This TIN will henceforth be referred to as "Grand TIN."

4. In order to include the bathymetry dataset for the Neosho River channel upstream of Twin Bridges, the cross sections acquired from the USACE are introduced to Grand TIN. These cross section data points are already in U.S. customary units and referenced to the NAVD88 vertical datum, so no conversion is necessary in that regard.

5. A tool created by Dr. Venkatesh Merwade of Purdue University is used to interpolate the channel bathymetry between the coarsely-spaced USACE cross sections [Merwade et al., 2008]. The interpolated bathymetry is then input into Grand TIN.

6. The Tar Creek channel bottom depths from GRDA are converted to channel bottom elevations using recorded WSEs at a nearby USGS gauge station. These channel bottom elevations are added to Grand TIN as individual points.

7. The channel bottom elevations for the Spring and Elk Rivers require interpolation between the furthest extent of the OWRB (2009) study and the USGS gauge station cross sections, but that process is completed in the HEC-RAS program instead of ArcMap, and it is explained in section 3.2.3.

8. After compiling all the available datasets using ArcMap, Grand TIN requires clean up to remove residual false data points from the NED representation of water surfaces.

3.2.3 Data Extraction Using HEC-GeoRAS

With the Grand TIN complete and all of the bathymetry and topography datasets normalized and merged, the process of exporting the data from ArcGIS to HEC-RAS begins. The tool created by the USACE for communication between ArcMap 10.1 and HEC-RAS is called HEC-GeoRAS 10.1. HEC-GeoRAS is a toolbar that may be downloaded from the internet and installed into ArcMap [Ackerman, 2009].

The documentation in the HEC-GeoRAS users manual is helpful for a step-by-step guide to using the tool. Merwade's personal website also contains a helpful step-by-step walkthrough of generating a HEC-GeoRAS output from a TIN [Merwade, 2014]. HEC-GeoRAS has several capabilities that are particularly useful for this research. These capabilities are explained below according to the feature classes that HEC-GeoRAS requires.

- River and River 3D: These feature classes contain the stream centerline datasets for the river reaches that will be modeled in HEC-RAS. The features are "measurable," and the measures along the routes are the source of HEC-RAS' station assignments for each cross section.

- Banks: The banks feature class is used by HEC-GeoRAS to identify the bank location for each cross section. This information distinguishes the left overbank (LOB) and right overbank (ROB) floodplain section from the channel section, allowing for different Manning's n values in each section.

- Flowpaths: The flowpath feature class is made up of three lines for each reach: left, right, and center path lines. The feature measures are used to calculate the downstream reach lengths for the LOB and ROB (as they can differ for meandering streams).

- XSCutlines and XSCutlines3D: The cross-section cutline feature class is arguably the most important and valuable feature exported by HEC-GeoRAS. Cross sections can be drawn at any location the user desires, and the HEC-GeoRAS program exports all of the information about the cross section (reach lengths, elevations, bank stations, Manning's n, ineffective flow areas, blocked obstructions, etc.) to HEC-RAS. This process could consume a large amount of time resources to complete manually, especially with a large area like the Grand Lake project, and, more importantly, manual extraction is more prone

to human error. Nearly 1000 cross sections were exported for this research using HEC-GeoRAS.

- Bridges and Bridges3D: The ability to draw bridge locations in ArcMap and then export them to HEC-RAS is limited in its usefulness because topographic datasets do not typically have bridge deck elevations included. However, exporting the bridge locations with HEC-GeoRAS makes the upstream and downstream cross sections pre-marked for the user to go in and manually add surveyed bridge data using HEC-RAS.

- IneffAreas: Ineffective flow areas are areas in which water enters during a flood scenario, but would not be considered part of the flow path due to nearby upstream or downstream obstructions. Small stream inlets or areas upstream and downstream of bridge embankments are the most commonly used ineffective flow areas in this research. The ineffective flow areas are represented as 2D polygons in the GIS, but exported as locations intersecting the cross sections in HEC-RAS.

- BlockedObs: Blocked obstructions are locations that do not allow water to flow through a part of a cross section. These could be buildings, or, in this context, the water treatment facility near Riverview Park in Miami. The blocked obstructions are represented in HEC-RAS similarly to the ineffective areas.

- Manning's n table: Manning's n is the one parameter in HEC-RAS that is not based purely on geometry of the area. Land use typically determines Manning's n values, but vegetation and other seasonal changes in the landscape can change Manning's n values as well. In a basic HEC-RAS model, Manning's n values are assigned to the LOB, channel, and ROB as a generalized value. With HEC-GeoRAS, a land use map may be included that assigns Manning's n values to

different sections along a cross section, based on that section's intersection with a land use polygon.

A land use map is available for this region as a downloadable shapefile from the USGS website [Price et al., 2007]. This shapefile includes land use descriptions for the different land use polygons in Oklahoma, and the Manning's n values shown in Table 3.2 are assigned to the land use descriptions based on recommendations given in Chow (2009). Manning's n values for the channels of each river are assigned based on channel description and values used in the Holly reports [Holly Jr., 2004]. This method of assigning Manning's n values is much more refined than the typical LOB-channel-ROB method, but also adds complexity when calibrating the model to different flows and seasonal conditions.

Table 3.2. Manning's n For Each Land-Use [Arcement Jr. and Schneider, 1984].

Land Use	**Manning's *n***
Transportation	0.013
Strip mines	0.02
Water Bodies	0.035
Wetland	0.04
Urban	0.05
Farming	0.06
Forestland	0.08

- After assigning datasets from the model to all of the HEC-GeoRAS GIS layers and telling the program what TIN to use for extracting elevations, the program runs a code to convert all the information into a format that is able to be read by HEC-RAS. This file is then imported into HEC-RAS in preparation for the hydraulic modeling portion of the research.

3.3 HEC-RAS Modeling Procedure

The process of producing meaningful results with the hydraulic model is a multi-step, iterative process. Before using the model, the data extracted from GIS using HEC-GeoRAS requires clean-up and validation to the existing datasets. The model is then calibrated to make sure that it accurately represents a historical August 15 to September 15 flood. After calibration, the model is validated using various historical streamflows other than the one used for calibration. In the case that the model does not behave sufficiently in the validation stage, the parameters are slightly adjusted based on the information gathered in each step, and the process is repeated until sufficient results are achieved. After the final validation step, the model is ready for addressing the main question of this research project: "Do the changes in water surface elevations due to the proposed rule curve adjustment for the August 15-September 15 time period have an effect on major flooding levels upstream of Twin Bridges and, primarily, the city of Miami, OK?" The model is then verified by comparing the application results to the results of existing research. Finally, a sensitivity analysis is conducted in order to determine what phenomena to which the model is most sensitive (e.g., Spring River flow, Dam WSE, Neosho River roughness values, etc.). The results of the sensitivity analysis help to qualify the confidence one may have in the application results.

3.3.1 Correlation of GIS Extractions to Previously Existing Datasets

Several aspects of the model require slight corrections after the export of data from the GIS to HEC-RAS. One of the issues encountered is that the land-use map did not distinguish channel locations from LOB and ROB locations along the cross sections. The channel Manning's n values, therefore, are input manually. The Manning's n values used for each channel are shown in Table 3.3. Note that these are the a priori

values used to set up the model. These values were calibrated during the calibration phase (see Section 3.3.3). These Manning's n values were chosen based on both a) investigation of prior models of this area [Holly Jr., 2004; Wyckoff, 2014], and b) expected values for the channel conditions that typically exist during the relevant season [Chow, 2009].

Table 3.3. Manning's n for each stream channel.

Stream	**Manning's *n***
Neosho River	0.03
Spring River	0.025
Elk River	0.03
Tar Creek	0.035

Another task that is required before running the model is representing the bridges in HEC-RAS, as mentioned in section 3.2.1. All of the necessary bridge modeling datasets were included in the USACE geometry file, but the stationing along the cross sections required correction in the updated model [Wyckoff, 2014].

For the Spring and Elk Rivers, the channel depth requires interpolation between the USGS gauge station locations and the furthest upstream extent of the OWRB (2009) study. This is accomplished using a HEC-RAS tool that creates cross sections with user-defined side slopes and channel bottom widths along a linear slope. This process channelizes the horizontal plane created by the LiDAR technology reflecting off of the water surface along the stream channel, and removes the sharp drop-off in channel bottom elevation caused by the transition from the NED topography dataset to the OWRB bathymetry dataset.

3.3.2 Model Forcing and Boundary Conditions

Detailed historical hydrologic datasets are available at USGS stream gauge locations from the USGS National Water Information System [USGS, 2012]. Therefore, these

gauge locations are used in the model as the upstream boundary conditions for streamflow on each river reach. Figure 2.1 in Section 2.2.1 contains a map of the locations used as upstream forcing points for this research.

The symbols without black dots in the middle are those used as upstream forcing points, (i.e., the furthest upstream point of the model for each river reach). The octagon shaped symbol marked with a black dot is the location of the downstream model forcing boundary condition. This location represents the dam location, and the historical information provided by GRDA for dam operations is the source of the datasets used as downstream boundary conditions for historical streamflow modeling.

The square and circle symbols with dots are gauge locations at which USGS keeps historical records of water stage elevations. These locations are used for calibration of the model to historical flood stage elevations.

3.3.3 Calibration of Model for August 15 to September 15 time period Using Historical Streamflow Data

In order to calibrate the model to represent what is actually occurring in the real world, the historical dataset from the September 2009 flood is compared to the model output. The September 2009 flood is used as the calibration flood for several reasons:

1. 15-minute increment time-varied data points are available from USGS for this flood event [USGS, 2012];

2. The flood peak occurred within the August 15 to September 15 time frame, which is ideal for calibrating the model to seasonal physical characteristics;

3. The event hydrograph is fairly uniform and independent of the effect of other flood events;

4. The event caused WSEs at the Neosho River Commerce gauge to exceed the "flood stage" of 15 ft above zero gauge, which is equal to 764.30 ft NAVD88 (762.90 ft PD) [NOAA, 2013; USACE, 1998];

5. The event caused the WSE in Miami, OK to approach the USACE easement elevation of 760.33 ft NAVD88 (758.93 ft PD) [Holly Jr., 2004];

USGS stream gauges are located in various locations around Grand Lake, as shown in Figure 2.1. These gauges are used to gather time-varied information about the streamflow in each river reach, as well as gauge heights for certain locations. In order to model the time-varied conditions available from USGS, the unsteady flow HEC-RAS procedure is used to calculate stage vs. time and flow vs. time hydrographs for each cross section location in the model. The default HEC-RAS tolerance level of 0.01 ft is used in the computational procedure (see Section 2.3.1).

The USGS gauge station no. 07185080 is located at Miami, and it is the only gauge station available for calibration purposes on the Neosho River. This gauge station provides data points in 15 minute increments, and the HEC-RAS output is calculated in 15 minute increments for comparison.

The HEC-RAS output consists of a flow vs. time and stage vs. time hydrograph for any location the user specifies. In this case, the model cross section 343647, located just downstream of the Highway 125 bridge, is closest to the location of the actual gauge station. The stage vs. time hydrograph from the observed dataset is compared to the stage vs. time hydrograph output by HEC-RAS at this location in order to calibrate the model to the September 2009 flood.

Due to the fact that HEC-RAS only has one parameter that is not determined by the geometry of the physical area (Manning's n), the calibration phase consists of adjusting the Manning's n of the area until the computed hydrograph matches the observed hydrograph. Manning's n is a type of lumped parameter for all the phenomena that affect hydraulic roughness. The calibration of this parameter involves

a certain degree of uncertainty, but the value of the parameter is not allowed to fall out of the expected range for major streams such as the Neosho River (0.025 to 0.20) [Chow, 2009].

The model is calibrated until the stage vs. time hydrograph from the HEC-RAS output matches up as close as reasonably possible with the observed stage vs. time hydrograph at that location. A certain degree of difference is expected because the model is a simplified portrayal of a very complex system. Therefore, exact agreement of the model to reality should never be expected. The Nash-Sutcliffe model efficiency coefficient (NSC) is used for comparison of the model output to the observed hydrograph at the calibration location [Nash and Sutcliffe, 1970]. This coefficient was developed in order to test the efficiency of hydrologic models, and has been used to test the efficiency of models for streamflow and water quality in various applications since its publication in 1970 [Moriasi et al., 2007; Farmer and Vogel, 2013; Santhi et al., 2001; Awawdeh, 2004]. The equation for the NSC efficiency, E is represented in Equation 3.3.

$$E = 1 - \frac{\sum_{t=1}^{T} (Q_o^t - Q_m^t)^2}{\sum_{t=1}^{T} (Q_o^t - \overline{Q_o})^2} \tag{3.3}$$

where,

Q_o represents observed streamflows,

Q_m represents the model output streamflows, and

$\overline{Q_o}$ represents the mean of the observed streamflows.

This efficiency, E, is compared for different calibrations of the model, and the calibration which yields the best efficiency is then tested for validation. NSC values of 0.75, or 75% efficiency, have been cited as a very high level of model efficiency in various literature [Farmer and Vogel, 2013; Santhi et al., 2001; Awawdeh, 2004]

3.3.4 Validation of Hydraulic Model with Historical Streamflows

Validation of the hydraulic model is an iterative process of comparing the calibrated model to historical observed datasets other than the dataset used in the actual calibration stage. Ideally, other floods that occurred during the period of August 15 - September 15 are used in this step in order for the model to remain consistent with seasonal phenomena such as channel roughness and flood magnitude. Flood datasets from 2008 to present are used because USGS makes that time period's streamflow datasets available in 15 minute increments. Datasets prior to 10/2007 are available in coarser time increments that dampen the peak streamflow values, making it difficult to calibrate the system to the real-world behavior.

The unsteady flow routing capability of HEC-RAS is utilized in this process as described in the calibration phase explanation in Section 3.3.3. The iterative process of calibration and validation is repeated until a model is developed that provides an adequate representation of reality. There is a degree of difference expected between the best possible computer model and the actual observed datasets because the simplified computer model cannot account for coarse data resolution or unrecorded phenomena.

The efficiency of the model to represent historical events was tested by the same coefficient, NSC, as was used in the calibration step [Nash and Sutcliffe, 1970]. The equation for the NCS is shown in equation 3.3. The validation process allows the researcher to be confident in the fact that the model is consistently and efficiently representing real-life phenomena under differing scenarios.

3.3.5 Application of the Model with Statistically Extreme August 15 - September 15 Streamflows

Using the statistically extreme streamflow values described in Section 3.1, the validated model is run in order to quantify the answer to the main research question of this project. The process of executing the HEC-RAS model is outlined in detail

in Brunner (2010). In order to determine the effect of the proposed rule curve adjustment, the steady state HEC-RAS model is run with the downstream boundary condition set at the existing rule curve WSE, and then the same flow is run using a downstream boundary set as the proposed rule curve WSE. The two scenarios are compared using the calculated WSEs of the flow at the priority locations described in Chapter 4.

The proposed rule curve change suggests lowering the WSE at Pensacola Dam from 744 ft PD to 743 ft PD from 8/1 to 8/15, and then holding a constant WSE from 8/15 to 9/15 (see Figure 1.3). The existing rule curve calls for the WSE lowering from 744 ft PD to 743 ft PD from 8/1 to 8/15, and then lowering from 743 ft to 741 ft PD from 8/15 to 8/31. The existing and proposed rule curves are identical up to 8/15, therefore the difference from 8/15 to 9/15 is used to test the rule curve changes. A downstream WSE of 744.4 ft NAVD88 (743 ft PD) is used to represent the proposed rule curve, and 742.4 ft NAVD88 (741 ft PD) is used to represent the existing rule curve. Although 741 ft PD is the minimum value of the drawdown of the existing rule curve, using this minimum value provides the most stark contrast between the effect of the proposed rule curve and existing rule curve.

3.4 Model Verifications and Sensitivity Analyses Methods

3.4.1 Hydraulic Model Verifications

The results of the application of the hydraulic model are verified by three processes:

1. Creating a simplified model to verify the qualitative pattern of the results;

2. Comparing steady-state results to similar unsteady-state model results for verification that steady-state model produces more conservative WSEs; and,

3. Qualitatively comparing the results from Holly (2004) to results calculated using the updated model and Holly's published roughness characteristics

Use of a simplified model to verify backwater pattern

In order to verify the qualitative pattern found in the application of the hydraulic model, a simplified model of the Grand Lake region is developed. This model follows the general channel-bottom slope pattern of the real model, but the sinuosity and acute fluctuations in channel bottom slope are removed. Four representative cross sections are used for the model: at river stations 0+00, 1870+00, 2760+00, and 3980+00. Cross-sections are interpolated between the user-defined cross sections at 1000 ft spacings. Downstream reach lengths are equal for channel, LOB, and ROB in order to create a simplified, non-sinuous hydraulic model. The hydraulic roughness values used in the simplified model coincide with the values published in Holly (2004).

For each of the flood-frequency values determined in the statistical analysis, the model is executed as if there were no dam (i.e., normal depth at the downstream boundary model boundary), vs. as if the dam were held at a constant 743 ft PD (i.e., a known WSE at the downstream model boundary), in order to represent the proposed rule curve adjustment. The streamflow values from the Neosho River alone are used in order to remove the impact of other streams acting as intermediate boundary conditions, affecting the WSE upstream.

The upstream backwater effect of the dam is investigated to determine at what location upstream of the dam the backwater effect is less than 0.10 ft. The backwater effect is defined as the difference in WSE between the no-dam conditions and with-dam condition for each streamflow. For this thesis, a 0.10 ft difference in WSEs is defined as the beginning of a backwater effect. Other research, such as USACE (1998), has defined "minimal backwater effect" as 0.20 ft. Therefore, 0.10 ft is a reasonable definition of the beginning of a backwater effect.

Comparison of steady-state model to similar unsteady-state model to verify conservativeness of steady-state procedure

As described in Section 2.3.1, the steady-state HEC-RAS calculations theoretically output a higher WSE for a given flow scenario than the unsteady flow calculations. This is verified by running the instantaneous-peak flow scenario from the September 2009 flood through HEC-RAS using the steady state model, and comparing the WSEs at the priority locations to the WSEs at the same locations using the peak scenario of the unsteady-flow model. The September 2009 flood is the flow used for this verification because it is the flow used for the model calibration in Section 3.3.3.

The representative steady-state flow used is the peak flow for the event at the Neosho River, Commerce gauge location, which occurred at 6:00 AM on 9/12/2009. The streamflow conditions at this time for each upstream boundary condition are used to run a steady-state model, and the WSEs at the priority locations are compared to the WSEs at the same location at the peak of the unsteady flow calculation for the September 2009 flood.

Comparison of qualitative results from this research to Holly's 2004 results

In order to verify that the results of this research are consistent with previous published research, the results of Holly (2004) are extracted from the published report and compared to the results found using the hydraulic model used in this research. The hydraulic model used in this research is modified to emulate Holly's model because Holly's model did not include Tar Creek, and it was calibrated to early-summer Manning's n conditions. The WSEs calculated using this modified model are compared, qualitatively, to Holly's results for the Priority 1 section of the research. In order to complete this task, the WSEs for the 742 to 745 PD comparison in the table in Appendix I of Holly (2004) are extracted from the report and compared to the same scenario in the current HEC-RAS model. The WSEs at the location of Riverview

Park in Miami are compared based on results from Holly's model and the hydraulic model used for this thesis.

3.4.2 Global Sensitivity Analysis

The objective of the global sensitivity analysis is to isolate different phenomena that contribute to the results of the experiment, and to rank those phenomena in terms of the degree of impact. A base scenario representing the final calibrated geometry and 100-yr flow conditions is used for comparing the various scenarios that are used in the sensitivity analyses. The steady-state computation procedure of HEC-RAS is used for the sensitivity analysis in order to model peak-flow scenarios. After developing a ranking of the model's sensitivity to the various phenomena with the global sensitivity analysis, a secondary sensitivity analysis is conducted. The secondary sensitivity analysis consists of systematically adjusting the phenomenon to which the model is most sensitive to determine whether the research conclusions are highly sensitive to changes in this phenomenon.

For this research, the following phenomena are studied for model sensitivity:

- Streamflow on the Neosho, Elk, and Spring Rivers, and Tar Creek
- WSEs at Pensacola Dam
- Roughness values summarized with Manning's n

The following scenario is used as a base for the sensitivity analysis:

- 100-year August 15 - September 15 streamflow on the Neosho, Spring, and Elk Rivers and Tar Creek
- A WSE of 743.9 ft NAVD88 (742.5 ft PD)[8] at Pensacola Dam

[8]This WSE is the average of the target WSEs of the existing and proposed rule curves for the August 15-September 15 time period.

- Bridges modeled as described in the USACE dataset
- Manning's n values as determined by the initial calibration iteration

The following alternative phenomena are used for building various scenarios during the sensitivity analysis:

- 2-, 10-, 20-, 50-, 100-, 200-, and 500-year statistical streamflows on the Neosho, Spring, and Elk Rivers and Tar Creek
- Water surface at the Dam from "normal depth" (as if there were no dam) to 758.4 ft NAVD88 (757 ft PD, the top of the dam)
- Manning's n values (based on acceptable ranges in Chow (2009)):
  - 0.01 to 0.10 in all channels
  - 0.02 to 0.20 in all floodplains

The sensitivity analysis process involves keeping all alternatives equal except one, and changing that one alternative through its entire physically plausible range, in order to create different scenarios. For example, for testing the sensitivity of the model to the streamflow on the Spring River, the boundary scenarios represented in Table 1, in Appendix A, are modeled in HEC-RAS. The table shows the process of changing the Spring River streamflow values to reflect alternative flow scenarios.

The output from these alternative scenarios is compared to the base scenario to determine how WSEs near Miami are affected by significant changes to the streamflow on the Elk River. The statistical value used for comparison is RMSE. The WSE for each alternative scenario is compared directly to the WSE of the base scenario at each cross section location, and all of the scenarios for one phenomenon are included in the representative sensitivity RMSE value. These results are separated based on priority locations and then ranked in order of degree of sensitivity to the research

question. These rankings allow the researcher to determine the level of sensitivity of the model to each phenomenon.

3.4.3 Specific Sensitivity Analyses

Determining the sensitivity of results to changes in Manning's *n*

Section 4.3 reveals that the highest ranked phenomenon for all priority sections is the roughness coefficient for the Neosho River channel. Although streamflow on the Neosho River is the second highest ranked phenomenon, it depends on the meteorologic conditions in the watershed, and is not user-defined. The roughness coefficient, or Manning's n value, for the Neosho River channel and floodplain is the user-defined phenomenon to which the model is most sensitive. Therefore, the Manning's n value for this section is varied across its possible range of values (as recommended by Chow (2009)) to determine the sensitivity of the results on this phenomenon. Table 3.4 shows the range of values used for this part of the sensitivity analysis. The ranges of possible values given in Chow (2009) are used and divided into quartiles to determine the range of sensitivity of results to Manning's n.

Table 3.4. Manning's n ranges used for sensitivity analysis of results.

Manning's *n*	low	25%	50%	75%	high
Neosho Channel	0.025	0.04375	0.0625	0.08125	0.10
Neosho Floodplain	0.025	0.06875	0.1125	0.15625	0.20

Determining the sensitivity of results to WSEs at the dam exceeding 743 ft PD

A further concern involved with estimating the effect of the proposed rule curve adjustment is the impact that the adjustment would have on WSEs at the dam rising above the target elevation. A study into this question was performed by the

USACE in May 2012, investigating the annual exceedance percentages for various WSEs at the dam [Daylor, 2012]. A reservoir routing program called RiverWare was employed to compare the existing rule curve to the proposed rule curve based on how much more percentage time, per year, the lake WSE would exceed specific WSEs. In order to test the sensitivity of the model application to the higher dam WSEs, the hypothetical higher dam WSEs are investigated compared to WSEs representing hypothetical existing rule curve conditions.

An unsteady flow model is conducted using high-dam conditions in order to verify that the steady-state and unsteady results are consistent. This was accomplished using the September 2009 flow scenario from the calibration phase, and adding two feet to the observed downstream WSEs representing Pensacola Dam. Although it is unlikely that a full two feet of difference in WSEs would be encountered under the proposed rule curve conditions, this represents a conservative estimate of the effects of the propose rule curve adjustment. The WSEs in the priority 1 location from the model using the observed downstream conditions are compared to the WSEs in the priority 1 location from the model using the hypothetical 2-ft higher dam WSEs. The differences (i.e., the effect of the proposed rule curve adjustment) is then compared to the results found in the steady-state analysis above to verify consistency between the steady and unsteady models.

In addition, a polynomial is fit to the daily-mean dam WSE data in order to determine whether an inline structure representation of the downstream model boundary is required rather than the known-downstream-WSE approach taken in Section 3.3.5. This polynomial interpolation procedure is completed using the "Interpolation" function in the Mathematica program [Wolfram Research, 2010]. The results from running the HEC-RAS model with the interpolated dam WSEs (3 hr time-increment) are then compared to the original results calculated using the daily-mean dam WSEs. This

comparison is conducted using the NSC efficiency value (c.f. Section 3.3.3 for an explanation of NSC).

Determining the sensitivity of results to the effect of structures constricting streamflow along the Neosho River

In the USACE (1998) Real-Estate Adequacy Study, the structures (bridges and low-water dam) along the Neosho River were cited as a possible contributor to increased upstream WSEs in the Miami area. Thus, the final sensitivity analysis in this thesis takes a preliminary look at the bridges' contributions to flooding. Although this thesis does not investigate the structures in-depth, the model is used to investigate whether they are a likely contributor to increased WSEs upstream. Ten structures were removed from the model in order to test the effect of the structures on upstream WSEs in the priority locations.

CHAPTER 4

Results and Analysis

This chapter contains both results and analysis of each of the research topics mentioned in the methods chapter. After completion of the initial model application, it was determined that further sensitivity analyses were required to adequately answer the research questions. Methodology, results and analysis from this additional sensitivity analyses are included at the end of this chapter.

In order to organize and highlight the results that are relevant to this thesis, the research area is divided into three "priority locations": These locations are described below and shown on a map in Figure 4.1.

1. Priority 1: The section of the Neosho River upstream of the confluence of the Neosho with Tar Creek that is adjacent to the city of Miami. This section spans from Neosho River XS 354400 to 337106.

2. Priority 2: The section of Tar Creek upstream of its confluence with the Neosho River that is adjacent to the city of Miami. this section spans from Tar Creek XS 21647 to 327.

3. Priority 3: The section of the Neosho River downstream of the confluence of the Neosho with Tar Creek to the confluence of the Neosho with Spring River (location of Twin Bridges). This section spans from Neosho River XS 335674 to 275762.

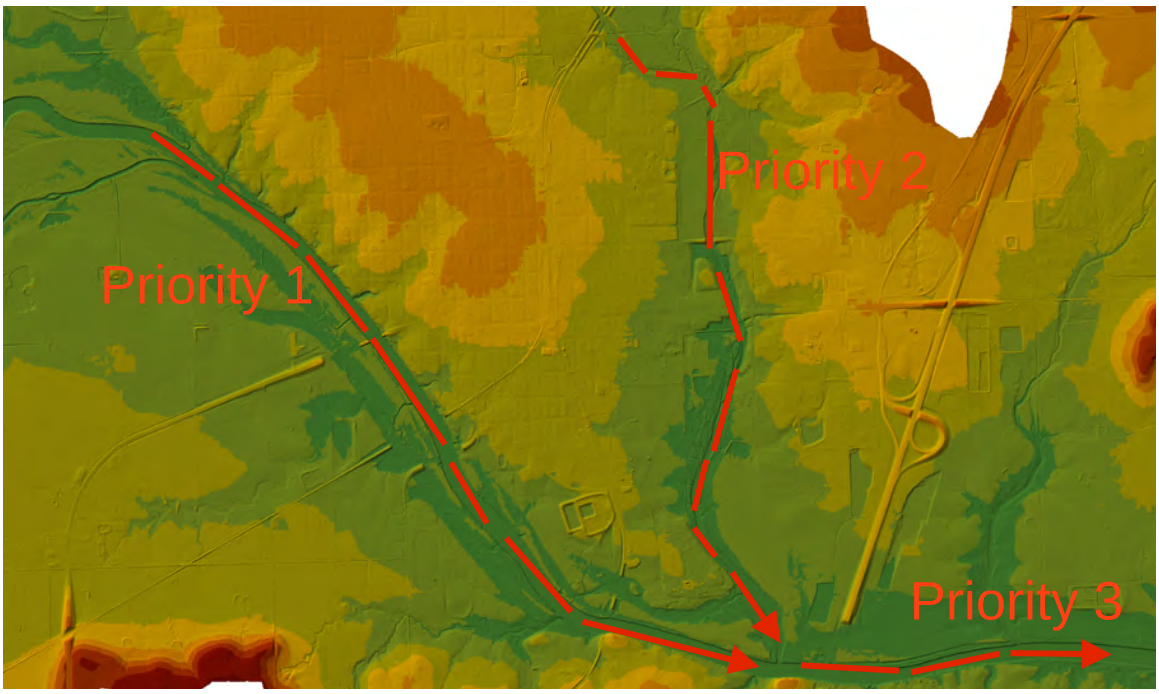

Figure 4.1. Map of priority locations used to separate relevant results in this section. Note: Priority 2 extends upstream a short distance and Priority 3 extends all the way to Twin Bridges.

4.1 Statistical Streamflow Analysis

4.1.1 Data Collection

The data available from the USGS National Water Information System for the August 15 - September 15 time period are daily-average data. In order to convert the daily-average peak dataset to an instantaneous-peak dataset, a peaking factor is necessary for each stream gauge [USGS, 2012]. The daily-mean peaks from both the AM and POT datasets were multiplied by the peaking factor for each stream in order to create synthetic instantaneous peaks datasets. This process ensures that the statistical streamflow analysis takes into account the peak streamflow conditions instead of the damped daily-mean values. Table 4.1 represents the peaking factors calculated for each stream gauge used in this research.

Table 4.1. Peaking factors calculated for each USGS gauge station.

USGS Gauge No.	River	Average Instantaneous Annual Peak	Average Daily-Mean Annual Peak	**Average Peaking Factor**
07185000	Neosho	46061	44268	1.048
07185095	Tar Creek	3670	2395	1.701
07188000	Spring	46170	41674	1.153
07189000	Elk	27268	18274	1.458

4.1.2 Analysis of Neosho River, Commerce gauge POT dataset

The lines in Figure 4.2 represent the eight probability distributions discussed in Section 2.2.4, fit to the POT dataset for the Neosho River, Commerce gauge. Note that PE3 and LP3 both use the Pearson Type-III distribution equation, but PE3 uses the non-log-transformed data and LP3 uses the log-transformed data (see Section 2.2.4 for a discussion of the differences between these two distributions). The LP3 distribution yields quantiles that require a re-transformation in order to be compared to the original data. This re-transformation is the inverse of the log-transformation, i.e., $10^{quantile}$.

The various probability distributions in Figure 4.2 were fit to the data using the L-moment parameter estimation method. The parameters calculated for each distribution are shown in Table 4.2.

Table 4.2. Parameters estimated using L-moments for each probability distribution.

	Parameter		
Distribution	*Shape*	*Scale*	*Location*
Gamma	0.642	12382	-
GEV	-0.410	3849	3135
Pareto	-0.264	5959	-154
Gumbel	-	6734	4061
Lognormal	0.999	8.603	-1025
PE3	2.816	10351	7948
LP3	0.211	0.539	3.602
Weibull	0.730	6247	336

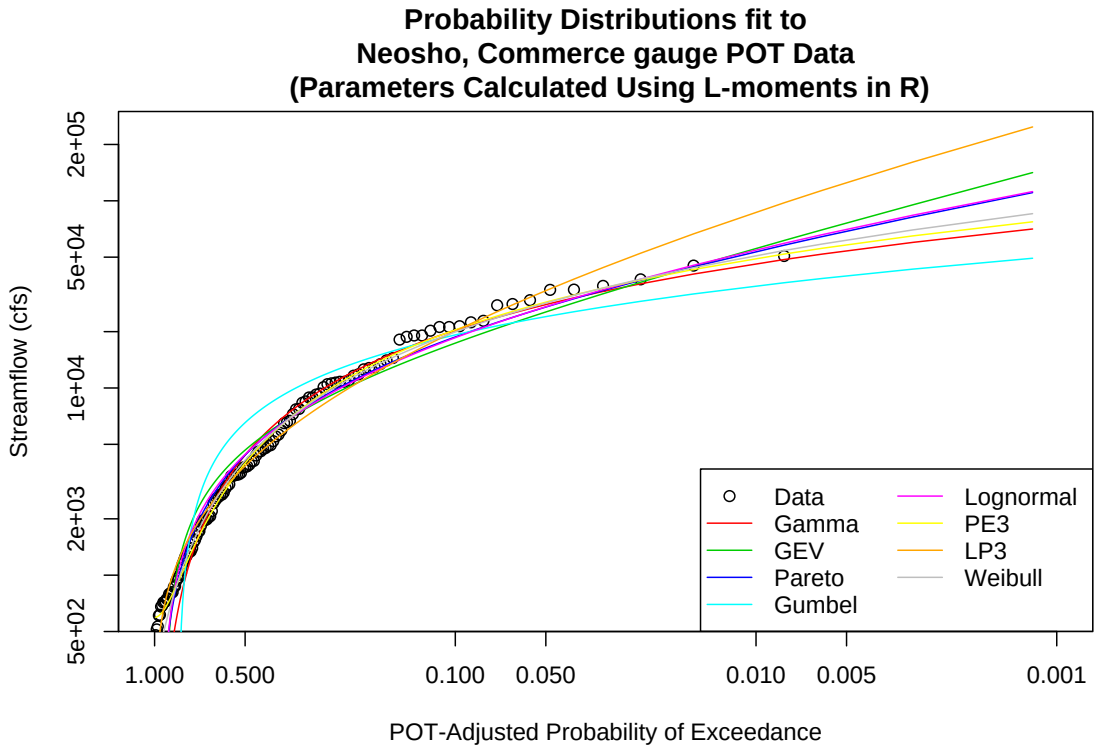

Figure 4.2. Probability distributions fit to POT dataset at Neosho River gauge.

After fitting the distributions to the data, it is apparent that some distributions fit the data better than others. An RMSE analysis was conducted to determine which distribution is the best fit of the data. Figure 4.3 is a simple bar chart of the actual RMSE values for the fitted distributions. Figure 4.4 shows the confidence intervals (CIs) for the RMSE values of each probability distribution compared to the observed data, calculated using a bootstrap analysis. Figure 4.5 isolates the CIs for the top 3 best-fitting distributions for the Neosho River, Commerce gauge POT dataset.

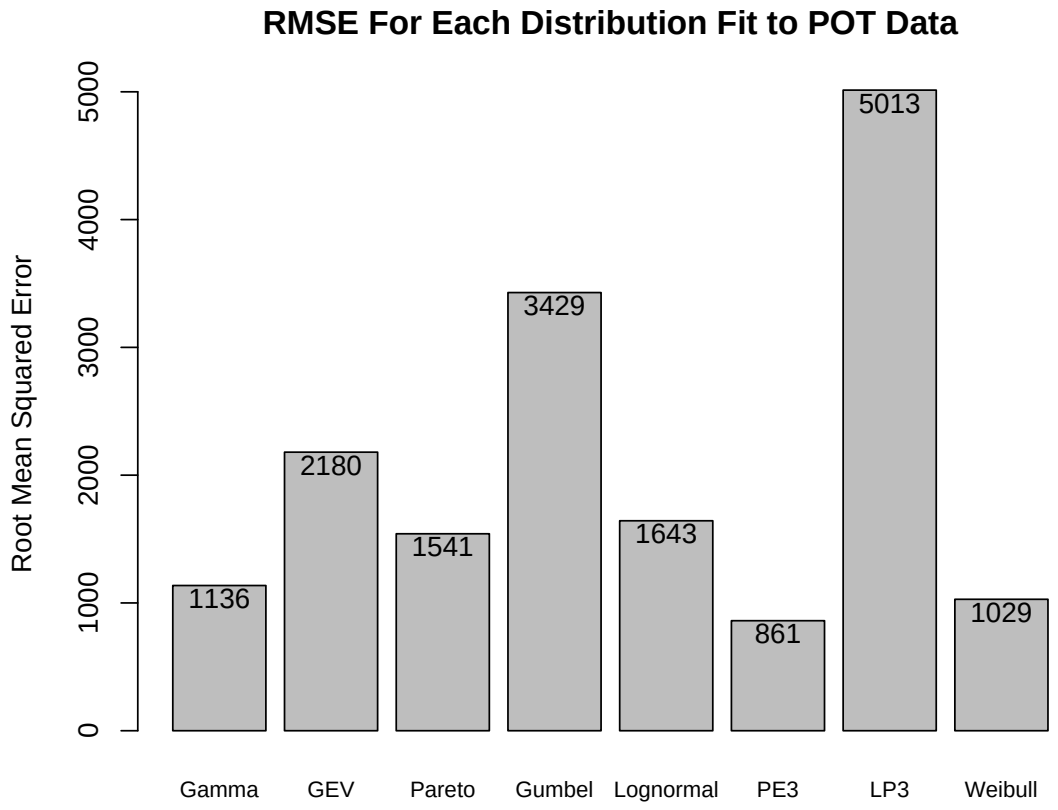

Figure 4.3. RMSE values for probability distributions fit to Neosho-Commerce POT observed dataset. RMSE value printed on each bar.

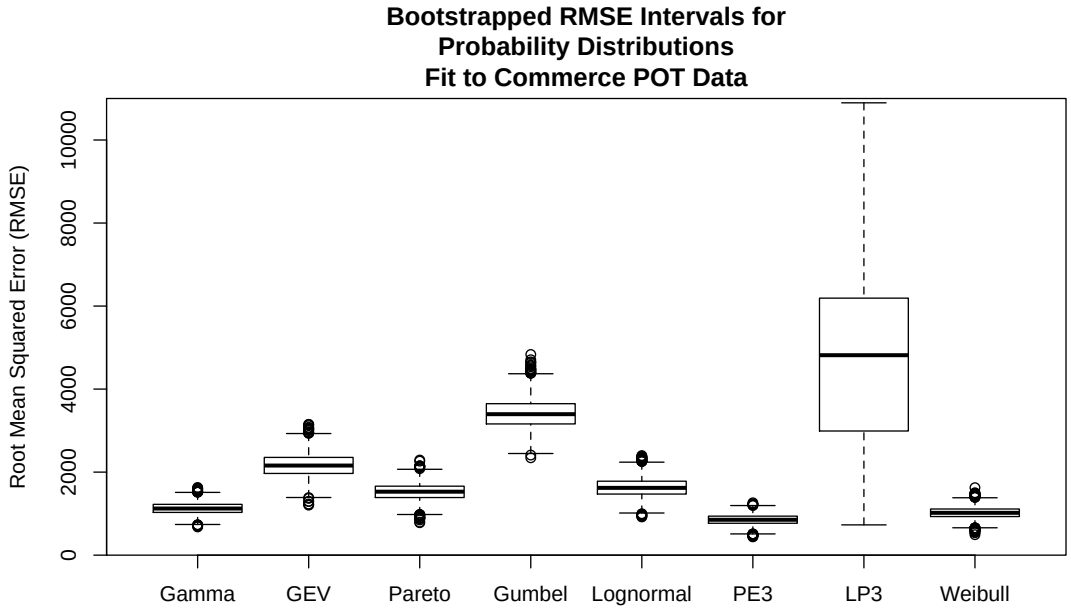

Figure 4.4. CIs for each probability distribution fit to Neosho-Commerce POT observed dataset. Black line represents median, box represents 90% CI, and whiskers represent 95% CI.

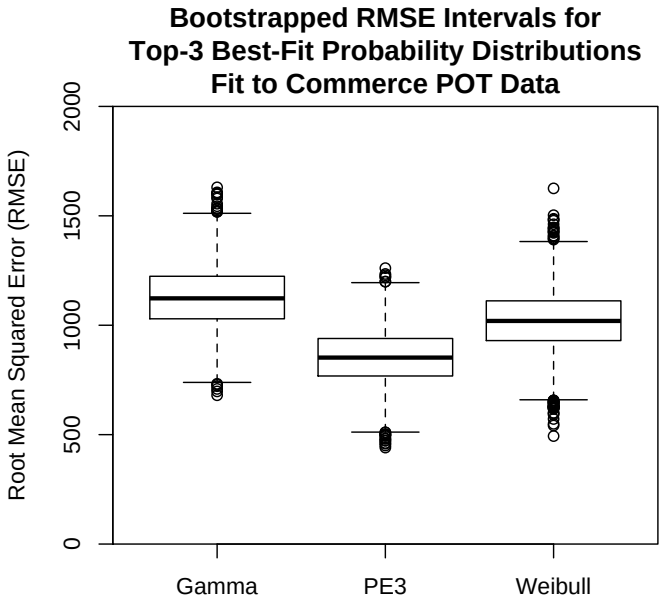

Figure 4.5. CIs for three best-fit probability distributions fit to Neosho-Commerce POT observed dataset.

The best-fit probability distribution for the Neosho River, Commerce gauge POT dataset according to Figure 4.5 is the non-log-transformed Pearson Type-III (PE3) distribution. The PE3 distribution, graphically fit to the observed data and extrapolated out to the 100-, 200-, and 500-year return intervals, is shown in Figure 4.6.

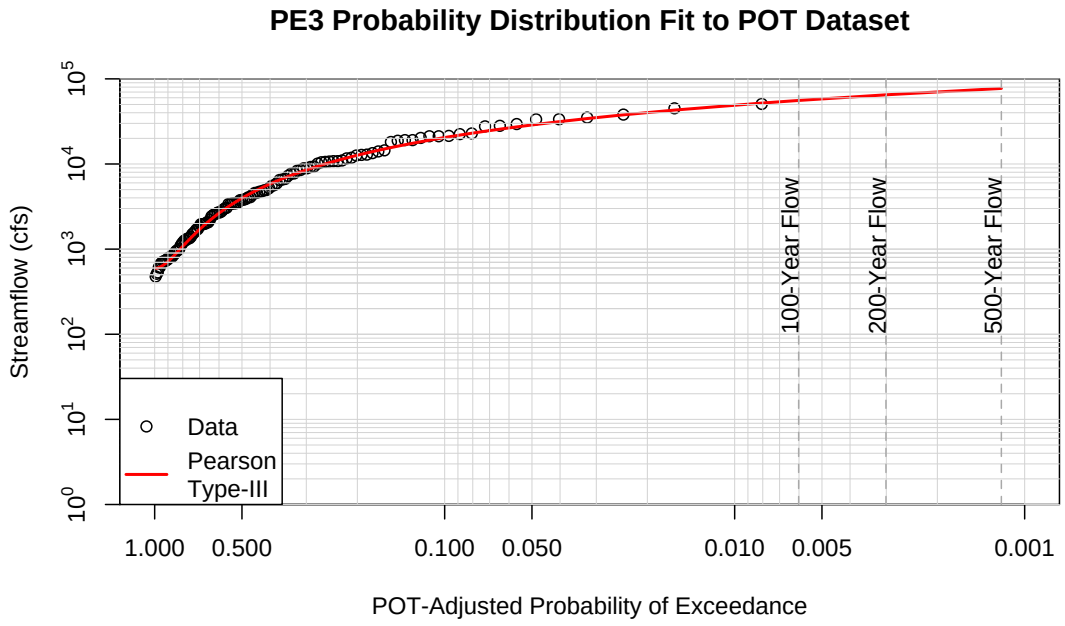

Figure 4.6. PE3 distribution fitted to the observed Neosho River, Commerce gauge POT dataset.

In order to quantitatively compare the results of this POT analysis to the AM analysis results, the return-period streamflows for the Neosho River, Commerce gauge were calculated from the fitted PE3 curve. The results are shown in Table 4.3. The quantitative comparison is included in Section 4.1.5.

Table 4.3. Return-period streamflow predictions for Neosho River, Commerce gauge, from POT analysis.

	Return-Period Streamflow (cfs)						
Gauge Location	2-yr	10-yr	20-yr	50-yr	100-yr	200-yr	500-yr
Neosho - Comm.	8488	26496	35052	46740	55782	64952	77226

4.1.3 Analyses of Neosho River, Commerce gauge AM dataset using B-17B method and PEAKFQ, with comparison to LP3 parameters estimated using L-moments

The B-17B method has been criticized for its use of manually-calculated moments using the method-of-moments (Section 2.2.2). The method of L-moment parameter estimation is compared to the B-17B method for the Neosho River Commerce gauge in order to qualitatively and quantitatively compare the two methods. The AM dataset for the Neosho Commerce gauge is created by multiplying the annual peak streamflow for each year on record by the peaking factors shown in Table 4.1. Using this AM dataset, the parameters of the LP3 distribution are calculated using both the B-17B guidelines and the L-moment method. Table 4.4 shows the LP3 parameters calculated by PEAKFQ for the B-17B method, and the LP3 parameters estimated using the L-moment method.

Table 4.4. Log-Pearson Type-III probability distribution parameters for Neosho River, Commerce gauge AM dataset.

Parameter Estimation Method	Mean of Logs	St. Dev. of Logs	Skewness
B-17B	3.4485	0.7760	-0.3630
L-Moments	3.4781	0.7838	-0.5937

An LP3 curve is fit to the AM data using the PEAKFQ program to precisely follow the B-17B guidelines for flood-frequency estimation. The PEAKFQ graphical output of this curve-fitting is shown in Figure 4.7. The red line in the graph represents the LP3 probability distribution fitted to the observed datasets. The blue lines in the graph represent the upper and lower limits of the 95% confidence interval (CI) for the fitted LP3 distribution.

The LP3 distribution fit to the AM dataset using parameters estimated by L-moments is compared to the B-17B output in Figure 4.8. The probability quantiles

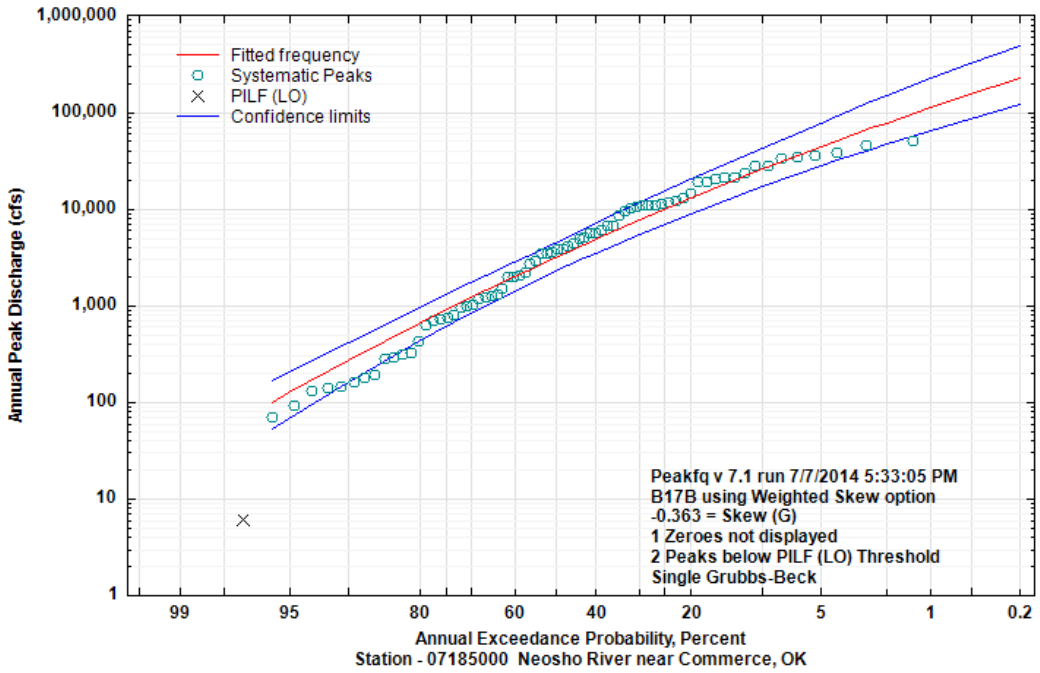

Figure 4.7. LP3 distribution fitted to observed Neosho River, Commerce gauge AM dataset using PEAKFQ.

represented by the 100-, 200, and 500-year statistical floods are shown on this figure as well.

The return-period streamflows for AM dataset of the Neosho River, Commerce gauge are shown in Table 4.5. This table may be used to compare the B-17B and L-moment methods of parameter estimation for fitting the LP3 distribution to the data.

Table 4.5. Return-Period Streamflow Predictions for Neosho River, Commerce gauge, from AM Analysis of August 15 - September 15 Time Period.

	Return-Period Streamflow (cfs)						
Est. Method	2-yr	10-yr	20-yr	50-yr	100-yr	200-yr	500-yr
B-17B	3128	25580	50750	77180	110800	152500	220900
L-Moments	8641	37404	55431	83921	108626	135702	174585

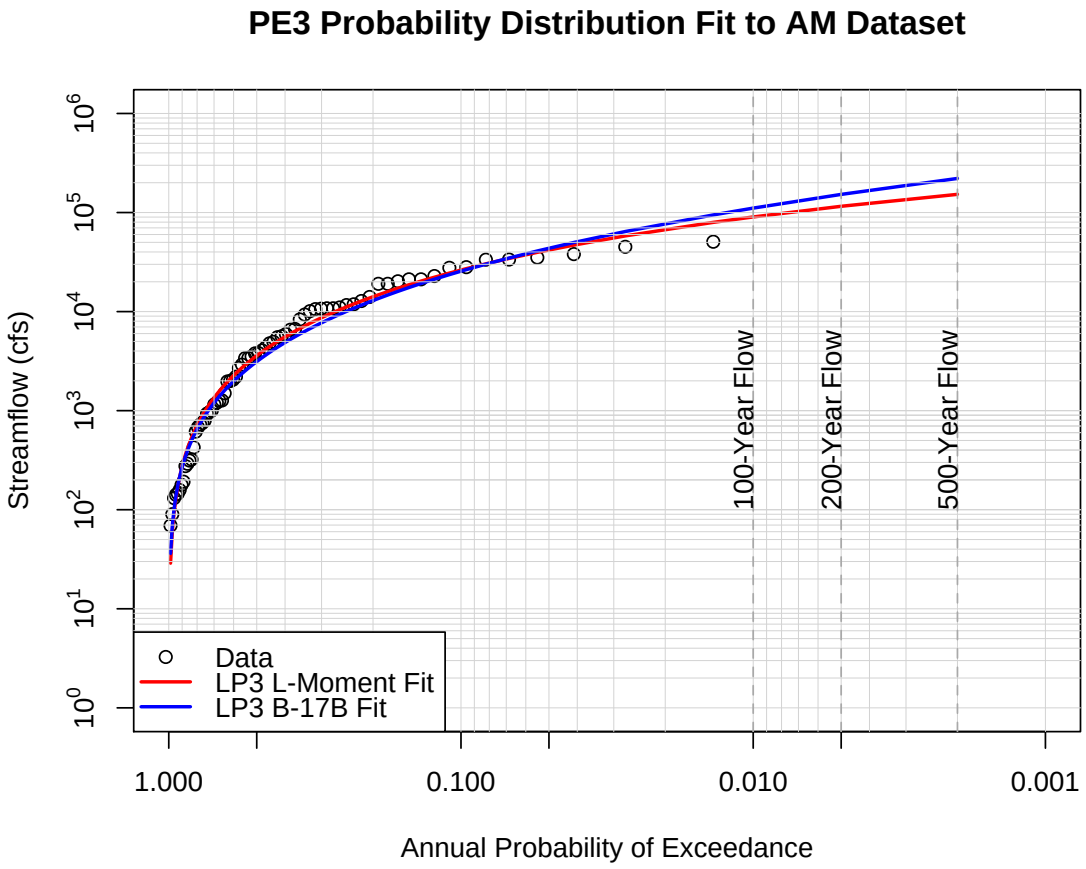

Figure 4.8. LP3 distribution fitted to the observed Neosho River, Commerce gauge AM dataset. The red line represents the LP3 distribution fit to the data using L-moment parameter estimation. The blue line represents the B-17B method of fitting the LP3 distribution to the data.

4.1.4 Comparison of degree of fit of PDF for POT vs. AM Methods of Streamflow Analyses

In order to compare the fitted probability distributions, an RMSE analysis is used to compare the PE3 fit of the POT dataset, the LP3 fit of the AM dataset using B-17B methods, and the LP3 fit of the AM dataset using L-moment parameter fitting. The RMSE values are shown in Figure 4.9, and the bootstrapped CIs of the RMSE values are shown in Table 4.6.

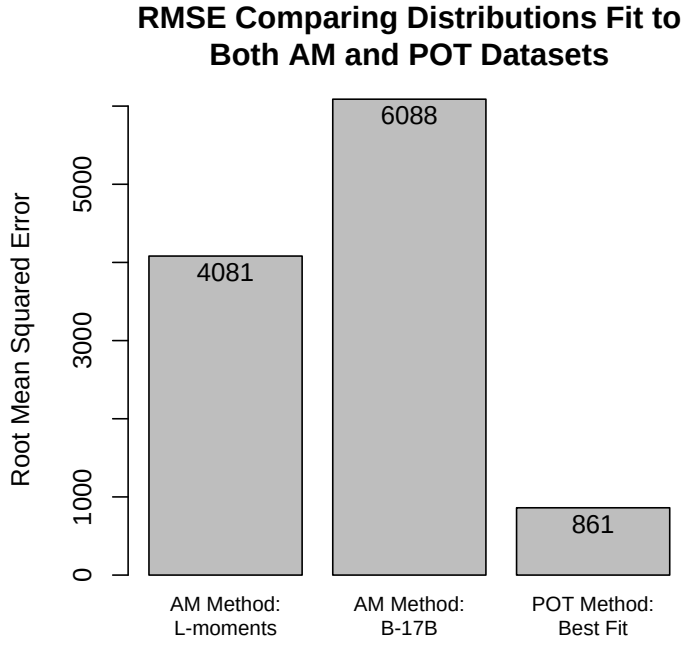

Figure 4.9. RMSE comparison of 3 final distributions chosen for comparison of AM and POT data extraction methods.

Table 4.6. Bootstrapped CIs of RMSE of 3 final distributions chosen for comparison of AM and POT data extraction methods.

Distribution Fitting Method	95% Confidence Interval for RMSE
AM Method: L-Moments	(1280 - 6590)
AM Method: B-17B	(1878 - 9863)
POT Method: Best Fit	(612 - 1100)

These figures show that the best fit probability distribution from the POT dataset is a far better fit to the actual observed data than either method used with the AM dataset. Analyzing the AM dataset alone, the L-moment parameter fitting method provides a better fit to the data than the B-17B method. This is an initial assessment of the data extraction and probability distribution-fitting methods. Further comparison is necessary in order to determine which method is most conservative.

4.1.5 Comparison of POT vs. AM Methods of Streamflow Analyses

A comparison of the conservativeness of the extreme return-period streamflows calculated using the POT vs. AM methods involves extrapolating the fitted distributions out to the extreme statistics and analyzing the magnitudes of the extreme values. Figure 4.10 is a graphical representation of the extreme streamflows calculated using each method.

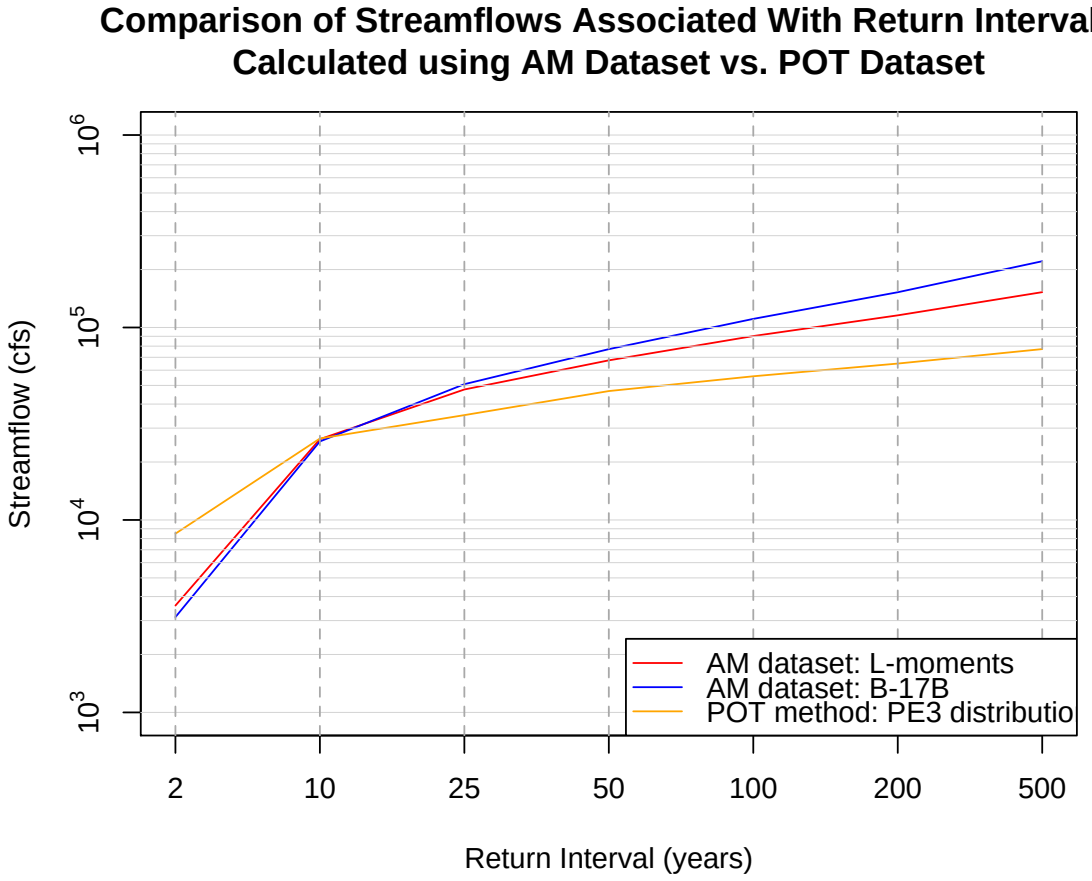

Figure 4.10. Comparison of flood frequency streamflows calculated using various estimation methods.

The 100-, 200-, and 500-year flow estimates for each of the 3 chosen distributions representing the AM and POT datasets are shown in Table 4.7.

Table 4.7. Comparison of Extreme Return-Period Streamflow Predictions between POT and AM datasets.

	Return Period Streamflow (cfs)		
Fitting Method	100-yr	200-yr	500-yr
AM: L-moments	108626	135702	174585
AM: B-17B	110800	152500	220900
POT: Best Fit	55782	64952	77226

According to this assessment of the conservativeness of the return-period streamflows calculated using the AM and POT methods, the AM data extraction method and B-17B parameter-fitting methodologies are the most conservative. This method estimates streamflows 2-3 times greater than the values calculated using the POT method, depending on the degree of extreme flow. Due to the conservativeness of streamflows calculated by the B-17B methods, and the recommended approach given by USGS (1982) for flood frequency prediction in the United States, the B-17B methodologies are chosen for flood-frequency prediction in this research.

4.1.6 Final Results of Streamflow Analysis

As described in Section 2.2.2, the B-17B guidelines provide a strict procedure for fitting the Log-Pearson Type-III distribution to the AM dataset for a given stream. The values shown in Table 4.8 are the parameters calculated by the PEAKFQ program for each stream, according to the B-17B guidelines.

Table 4.8. Log-Pearson Type-III probability distribution parameters calculated using B-17B methodologies.

USGS Gauge No.	River	Mean of Logs	St. Dev. of Logs	Weighted Skewness
07185000	Neosho	3.4485	0.7760	-0.3630
07185095	Tar Creek	1.8938	0.9476	0.0510
07188000	Spring	3.4012	0.6065	0.1570
07189000	Elk	2.7356	0.5541	0.3910

The output shown in Figure 4.11 is a graphical representation of the fitted probability distributions—completed by PEAKFQ according to the B-17B guidelines—for each gauge station. The red lines in the graphs represent the LP3 probability distribution fitted to the observed datasets. The blue lines in the graphs represent the upper and lower limits of the 95% confidence interval (CI) for the fitted LP3 distribution. The Tar Creek gauge station had only 19 years of observed data, therefore the CI is broader for that station than any of the other stations. There is an especially stark contrast between the width of the Spring River gauge CI and the Tar Creek gauge CI because the Spring River gauge contains 74 years of observed data with no outliers, allowing for a higher degree of confidence in the computed LP3 distribution.

The statistically extreme streamflows calculated by PEAKFQ are shown in Table 4.9. These values are calculated according to the methods outlined in B-17B, the industry standard for calculating conservative streamflow estimates. These values are the streamflows used for the flood-frequency flows henceforth in this thesis.

Table 4.9. Statistical Streamflow Predictions from AM Analyses using B-17B guidelines and PEAKFQ.

	Return Period Streamflow (cfs)						
Gauge Location	2-yr	10-yr	25-yr	50-yr	100-yr	200-yr	500-yr
Neosho - Comm.	3128	25580	50750	77180	110800	152500	220900
Tar Crk. - Miami	77	1298	3710	7345	13610	24010	47900
Spring - Quapaw	2428	15420	31270	49830	76210	113000	183300
Elk - Tiff City	501	2916	5969	9682	18980	31070	58000

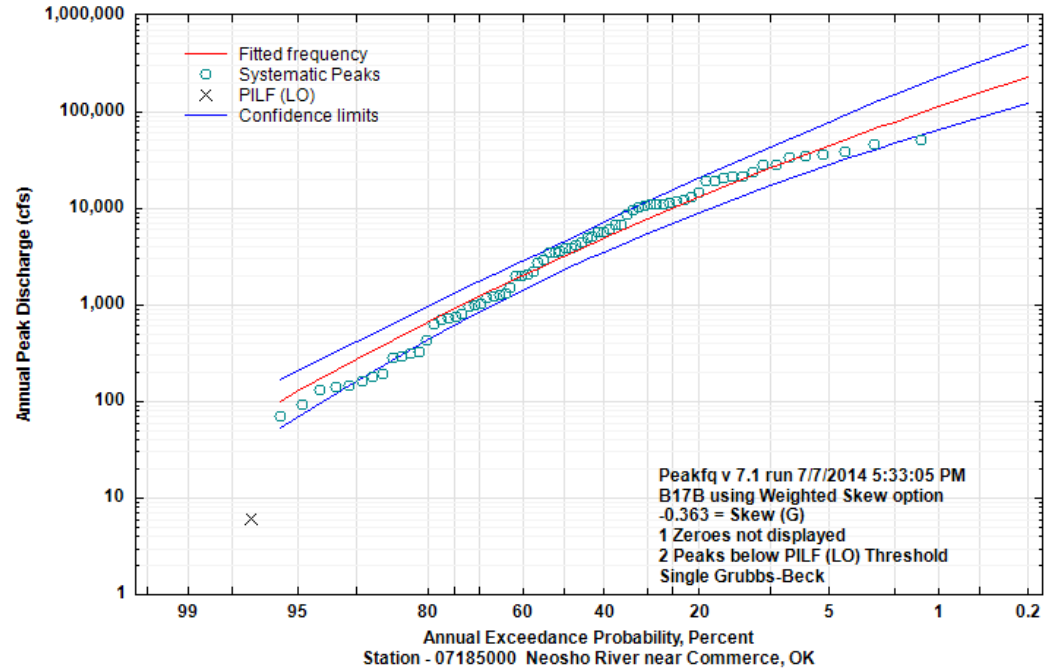

(a) Neosho River, Commerce Gauge

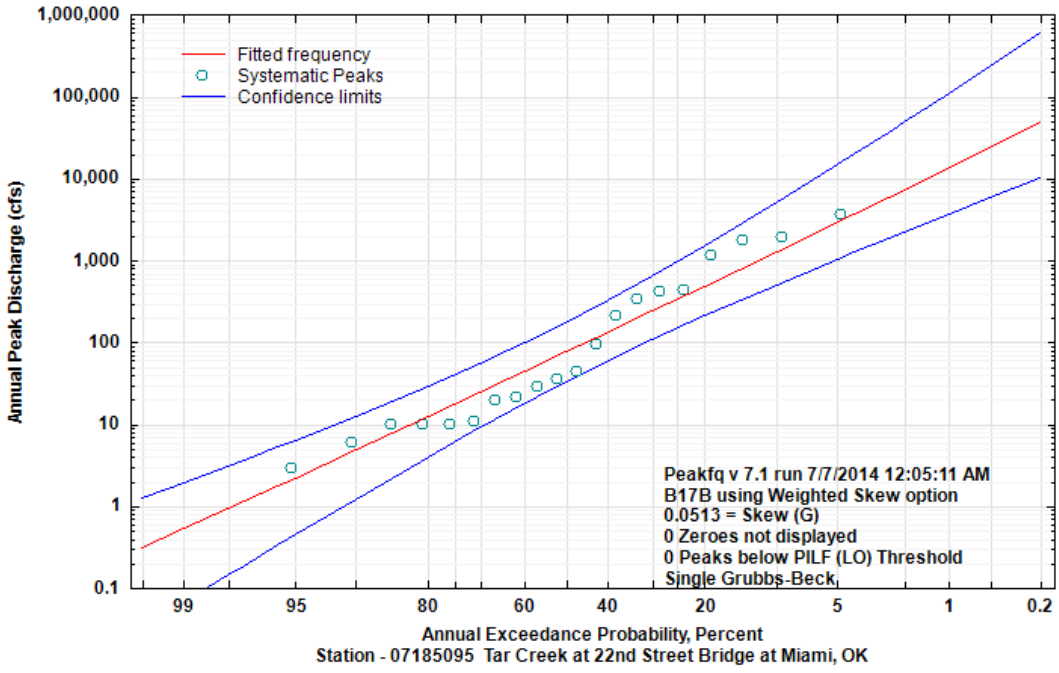

(b) Tar Creek, 22nd St Bridge Gauge

Figure 4.11. PEAKFQ output of frequency analysis using August 15- September 15 AM datasets for each stream.

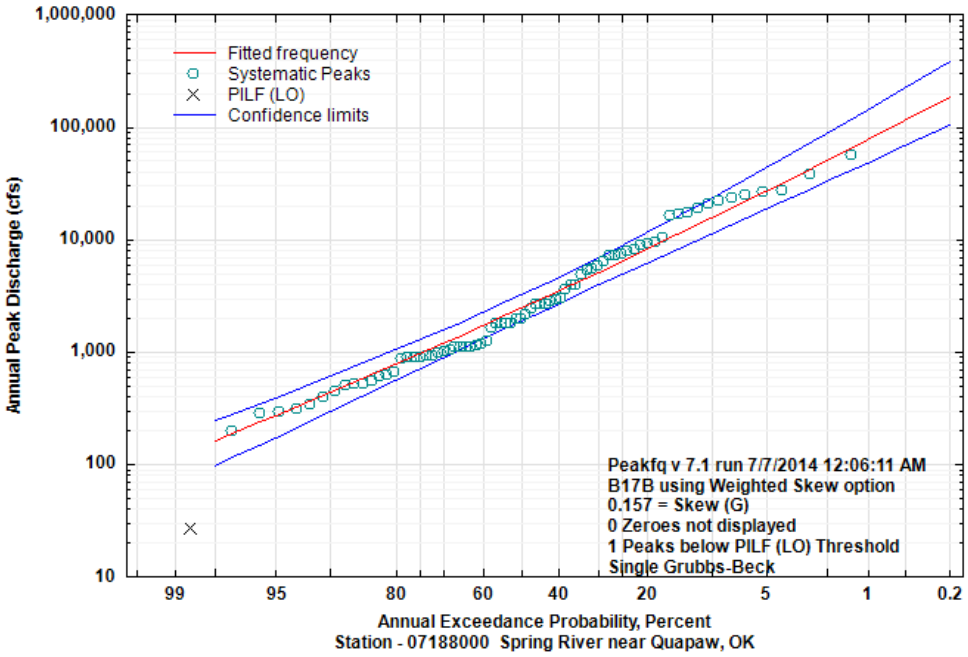

(c) Spring River, Quapaw Gauge

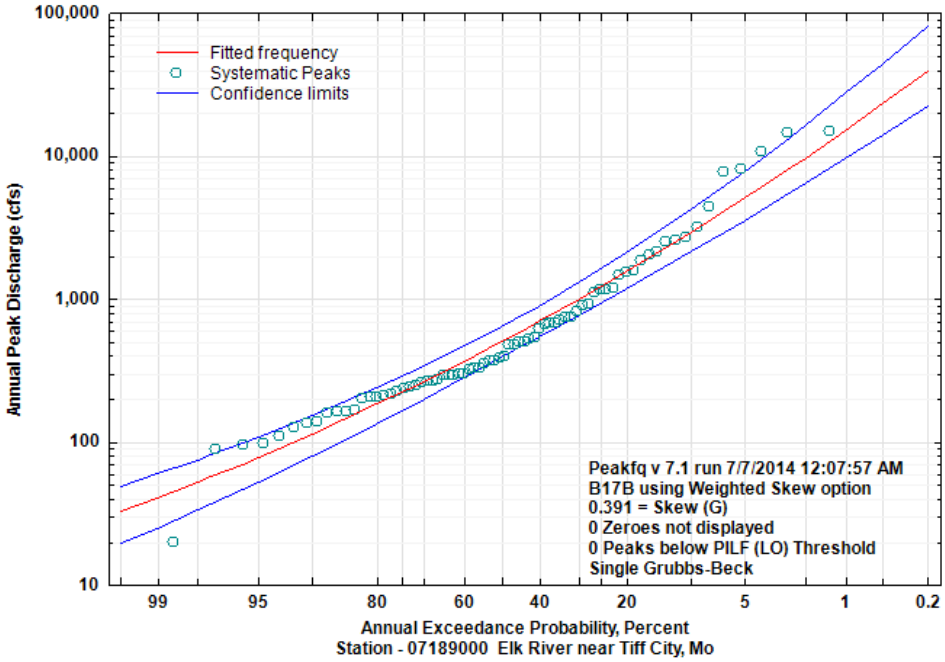

(d) Elk River, Tiff City Gauge

Figure 4.11. PEAKFQ output of frequency analysis using August 15- September 15 AM datasets for each stream. (cont.)

4.2 Model Geometry Setup

The merged TIN, referred to as Grand TIN in Section 3.2, is a 3D representation of the best-available data for the Grand Lake region. Figure 4.12 is a picture of Grand TIN in the location of Miami, OK before the bathymetry of the Neosho River channel was added. The Neosho channel appears very shallow in this location because the LiDAR technology returns an elevation data point when a water surface is scanned [Gesch, 2007]. Figure 4.13 is a picture of Grand TIN in the location of Pensacola Dam. The dam is located at the bottom left part of the picture. This figure provides a perspective on the detail the Grand TIN contains after the merging of the topographic and bathymetric datasets. Figure 4.14 is a picture of the entire extent of Grand TIN after the merging of the NED dataset and the OWRB bathymetric study [Gesch, 2007; OWRB, 2009].

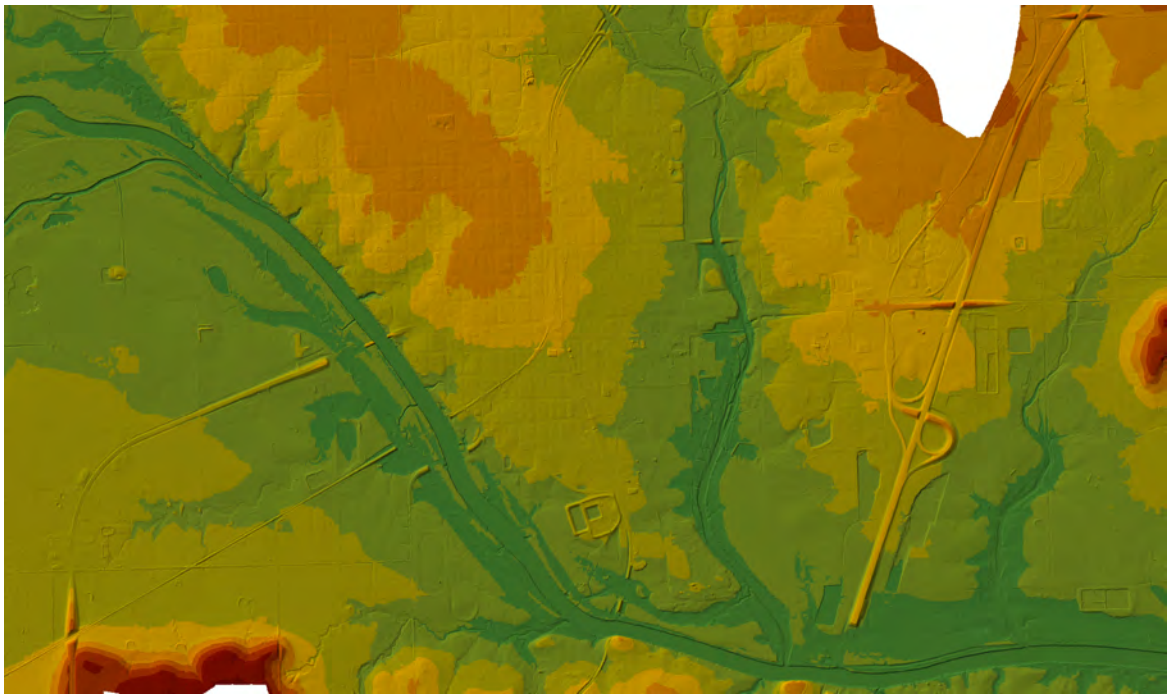

Figure 4.12. Picture of TIN at confluence of Neosho River and Tar Creek showing lower elevations in green and higher elevations in red.

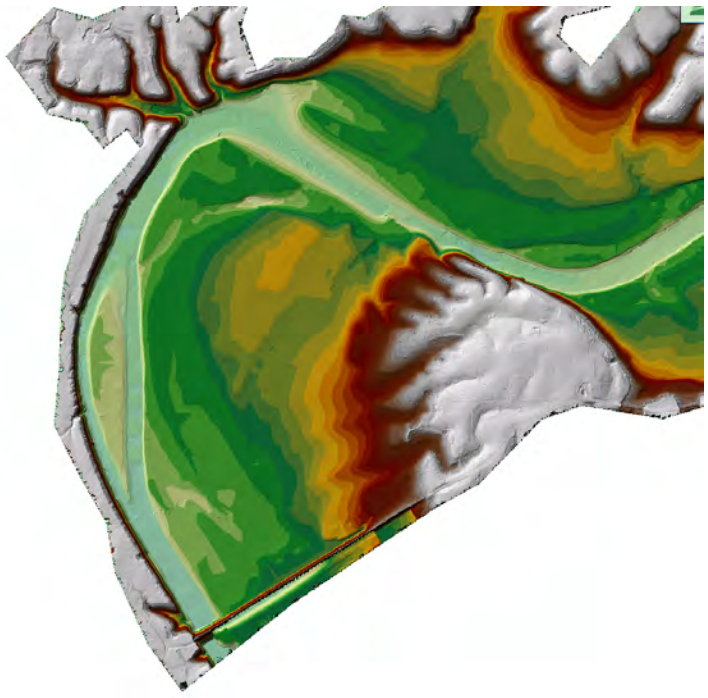

Figure 4.13. Picture of merged TIN at location of Pensacola Dam; lower elevations in blue and higher elevations in white.

A 3D picture of Pensacola Dam and historic Neosho River channel near the location of the modern dam is shown in Figure 4.15. Figure 4.16 is a 3D representation of the TIN in the Miami area. Note that these are representations of the topography as if there were no water present in Grand Lake and Neosho.

The final model exported to HEC-RAS is represented in Figures 4.17 and 4.18. Figure 4.17 shows the HEC-GeoRAS cross sections drawn on a satellite image of the area, and Figure 4.18 is the HEC-RAS representation of the same cross sections. Comparing this updated HEC-RAS with the HEC-RAS geometry of the region received from Wyckoff (2014), shown in Figure 4.19, the degree of complexity added by the model building technique outlined in this thesis is obvious.

Figure 4.14. Picture of TIN for full study area with merged topography and bathymetry; lowest elevations in blue and highest elevations in red.

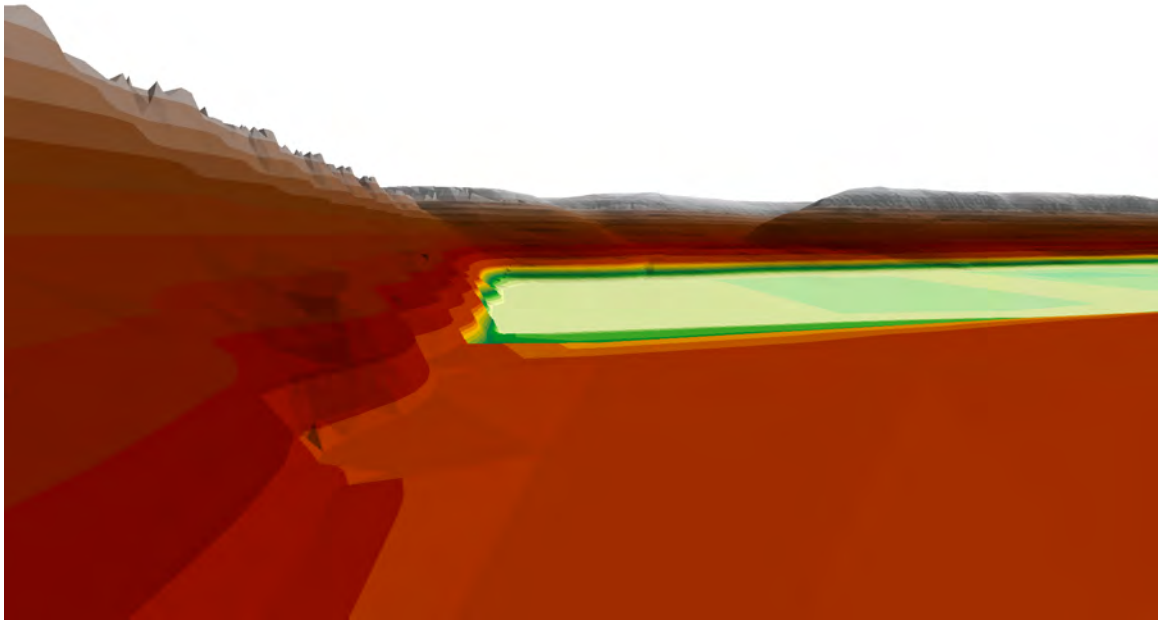

Figure 4.15. 3D representation of merged TIN near location of Pensacola Dam. Looking southwest from the lake side of the dam, with the dam on the left of the picture.

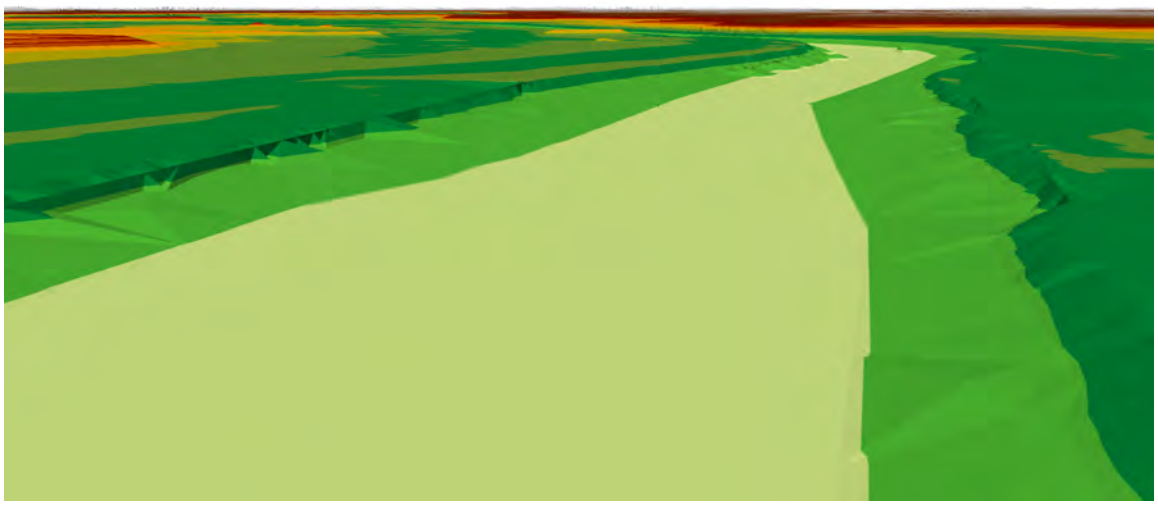

Figure 4.16. 3D representation of merged TIN near location of Miami. Looking downstream from Hwy 125 Bridge.

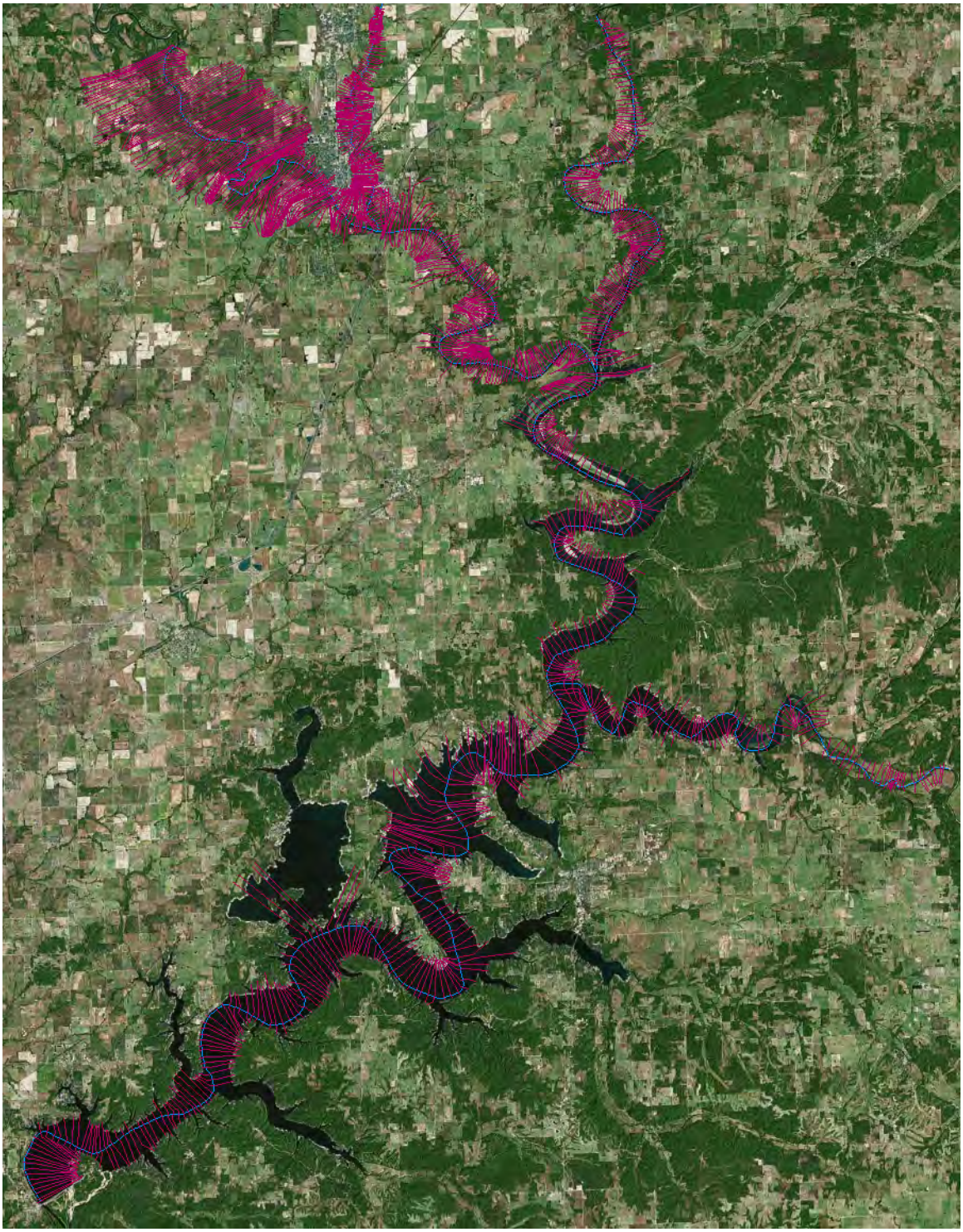

Figure 4.17. Picture taken in ArcMap of HEC-GeoRAS cross sections drawn on a satellite image of the Grand Lake region.

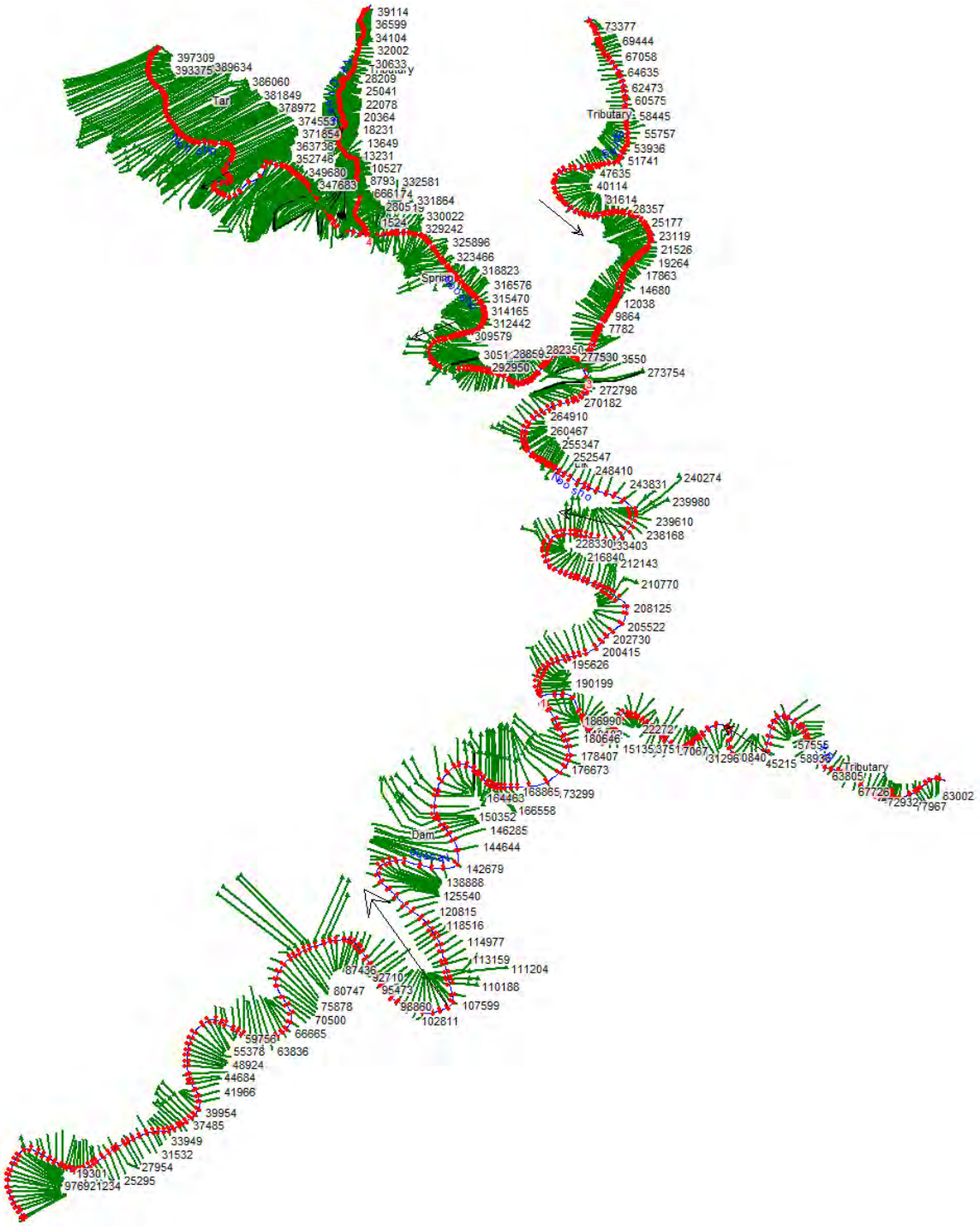

Figure 4.18. Final Geometry model in HEC-RAS depicting Grand Lake model cross sections.

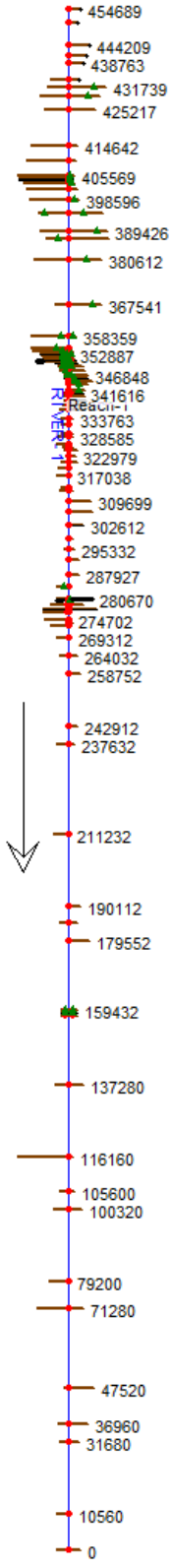

Figure 4.19. Original HEC-RAS Geometry model supplied by the USACE, depicting Grand Lake model cross sections. Compare this model to Figure 4.18. The richness of modern datasets allows for a more realistic description of this complex system.

4.3 Model Hydraulics Setup

4.3.1 Calibration Phase

The flood event used for calibration of the hydraulic model was the August 1 to October 7, 2009 (68-day) hydraulic event. The peak event of this storm occurred between September 9-16, 2009. The details of this event are listed below:

- Peak streamflow occurred on September 12, 2009
- Peak streamflow at Neosho River, Commerce gauge: 44,600 cfs
- Peak stage at Neosho River, Miami gauge: 758.47 ft NAVD88
- NSC for calibrated model, full modeled time period: 0.9790
- NSC for calibrated model, peak event: 0.9774
- Peak stage at Neosho River, Miami gauge for model: 758.55 ft NAVD88 (0.08 ft higher than observed peak)
- At time of peak of observed data, model stage: 758.52 ft NAVD88 (0.05 ft higher than observed peak)
- Model peak occurs 2 hours after observed peak, during a 68 day simulation

The graphical representation of the observed dataset vs. the model output for the full 68 day simulation is shown in Figure 4.20. The model output of the peak September 9-16 event compared to the observed dataset is shown in Figure 4.21.

The NSC values (both greater than 0.97) are particularly excellent levels of model fidelity, according to research cited in Section 3.3.3. In order to achieve the very accurate NSC values for the model, the Manning's n values along the Neosho River floodplain were slightly adjusted from the land-use map used to set the initial parameters (see Section 3.2.3). In particular, the Manning's n values in the Neosho

River floodplain upstream of Twin Bridges to the model boundary were reduced by 30% from the values imported using the land-use map in order to achieve the results shown. The reduced values are still well within the bounds of reasonable Manning's n values outlined in Chow (2009): 0.025 to 0.1 for natural floodplains with top-width at flood stage >100 ft.

While Holly's model used higher Manning's n values, that model used a much coarser discretization, it did not include Tar Creek in the model geometry, and it was calibrated to Manning's n values for early-summer. The Manning's n values used in this model require additional calibration based on the application for which the model will be used in future research.

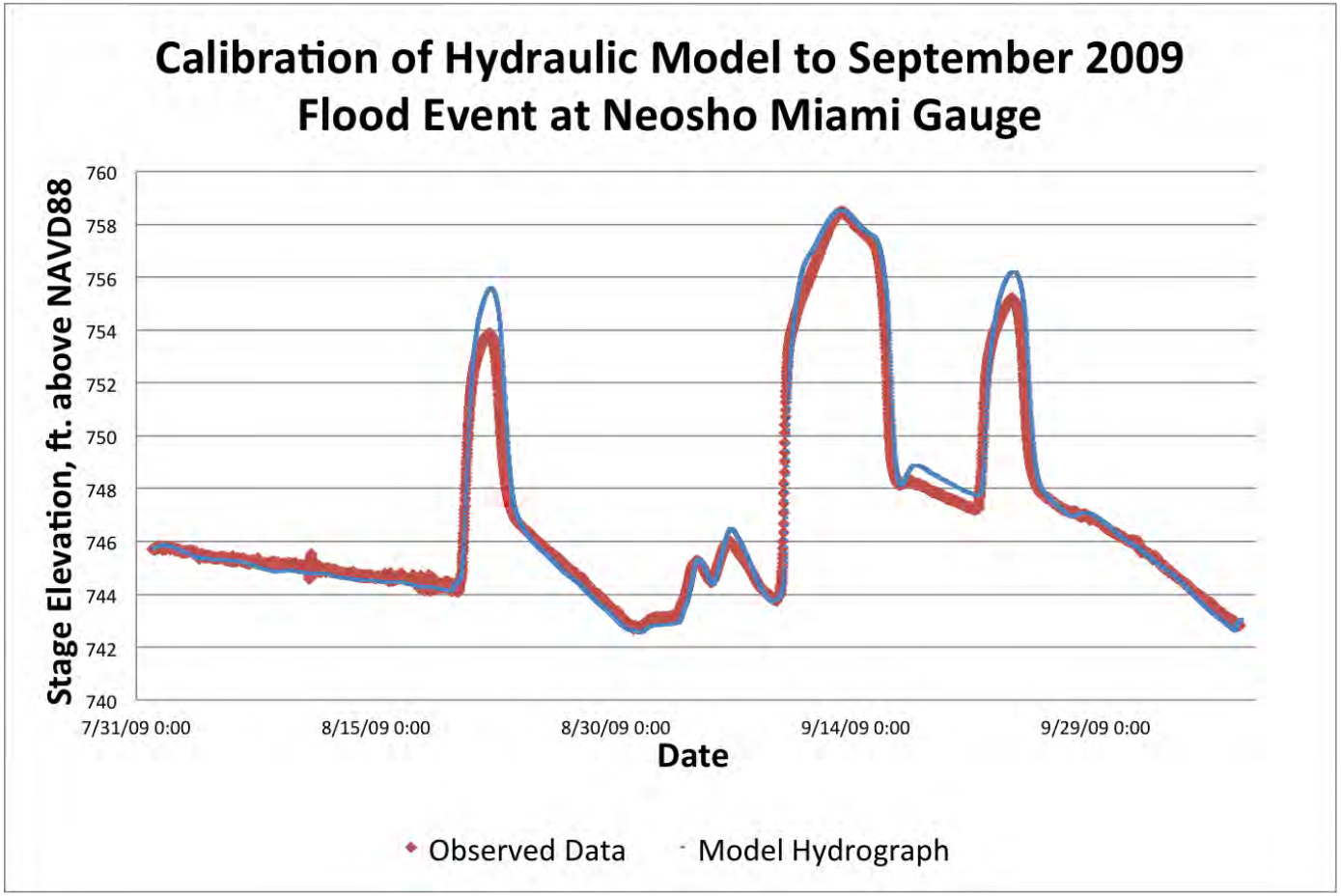

Figure 4.20. Full modeled extent of September 2009 event; Observed dataset compared to model output.

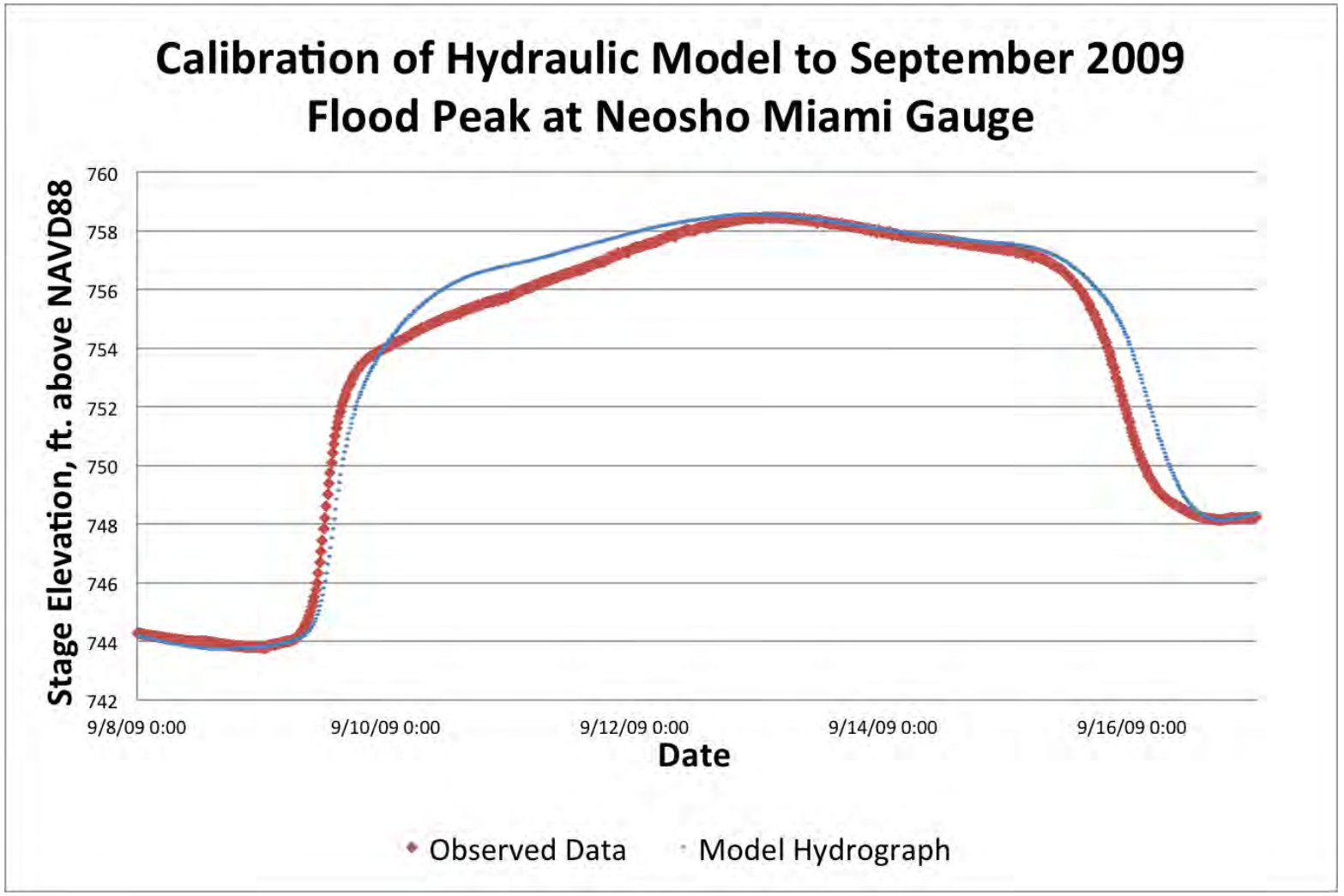

Figure 4.21. Peak flood of September 2009 event; Observed dataset compared to model output.

4.3.2 Validation Phase

As discussed in Section 3.3.4, the NSC efficiency coefficient is applied to the model output for several other relevant historic streamflow events in order to validate the hydraulic model. A historic streamflow event is considered relevant if it occurred within the months of August or September and the flood waters approached the USACE easement of 760.33 ft NAVD88. Streamflow events from 2008 to present are used because time series datasets are available for this period in 15-minute increments [USGS, 2012]. The following events are included in the validation:

1. September 12-15, 2008; Peak streamflow at Neosho River, Commerce gauge: 34,700 cfs; Peak stage at Neosho River, Miami Gauge: 757.96 ft above NAVD88

2. September 15-20, 2010; Peak Streamflow at Neosho River, Commerce gauge: 19,800 cfs; Peak stage at Neosho River, Miami Gauge: 750.84 ft above NAVD88

3. August 4-14, 2013; Peak Streamflow at Neosho River, Commerce gauge: 34,700 cfs; Peak stage at Neosho River, Miami Gauge: 757.47 ft above NAVD88

The NSC efficiency values calculated for each of these events, without any further adjustments of Manning's n, are shown in Table 4.10. The NSC for the full time period modeled is included as well as the NSC isolated to the main peak of the flood event. Note that these NSC values of >0.90 are sufficiently accurate for streamflow modeling, according to literature cited in Section 3.3.3.

Table 4.10. Nash-Sutcliffe efficiency coefficient values for validation events.

Validation	Dates		NSC Efficiency
2008	Full:	8/28 - 10/15	0.9888
	Peak:	9/12-9/19	0.9871
2010	Full:	8/14 - 10/9	0.9494
	Peak:	9/15 - 9/20	0.9183
2013	Full:	7/15 - 8/19	0.9785
	Peak:	8/4 - 8/14	0.9590

The figures included on the following pages (Figures 4.22, 4.23, and 4.24) show the observed hydrographs for the validation flood events compared to the model output for these events. The observed hydrographs are depicted with a red line and the model output with a blue line, as shown in the legend on each figure. Based on the excellent agreement of model to observations for these three validation events, it was determined that no further model calibrations was necessary.

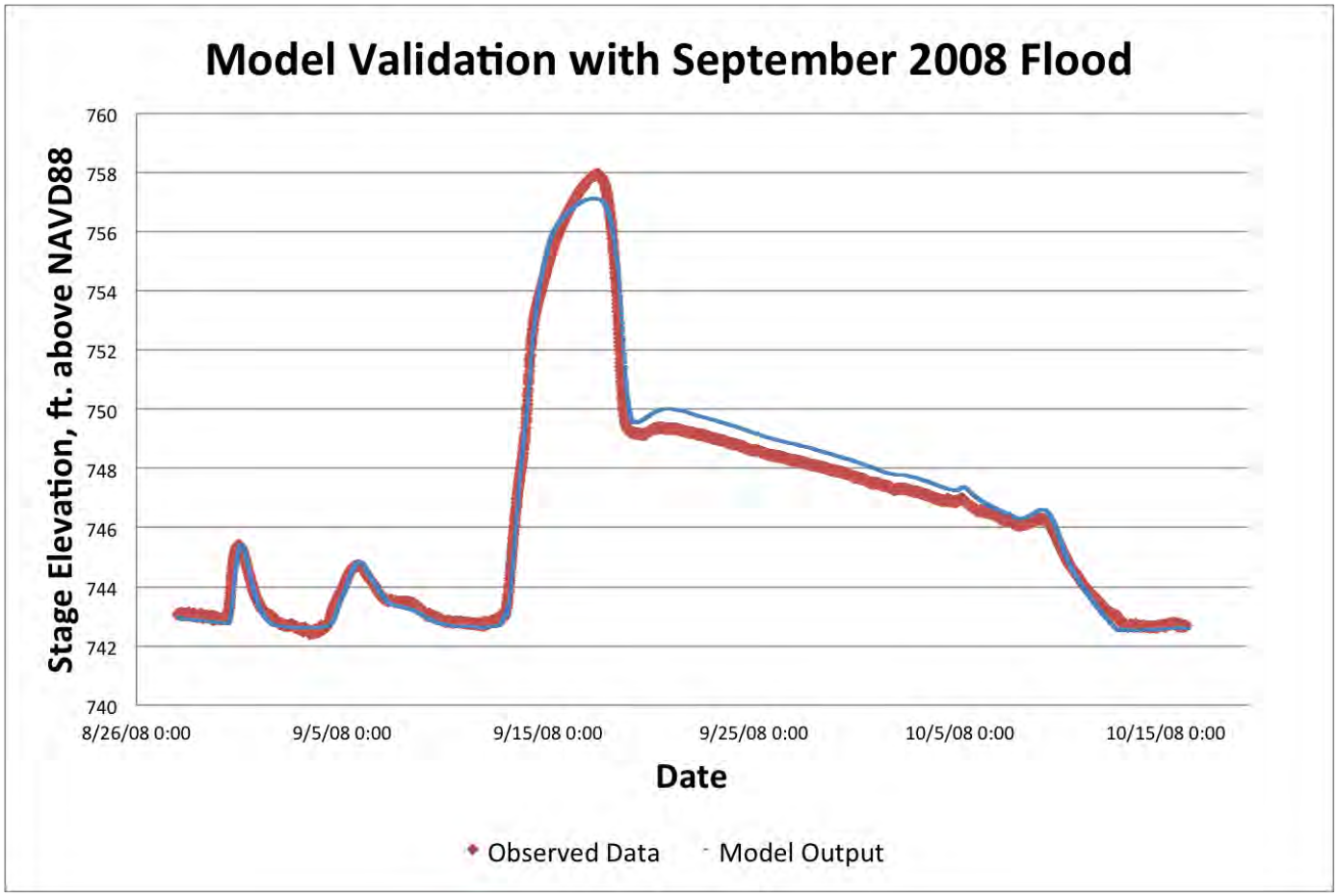

Figure 4.22. Full modeled extent of September 2008 flood event, observed dataset compared to model output.

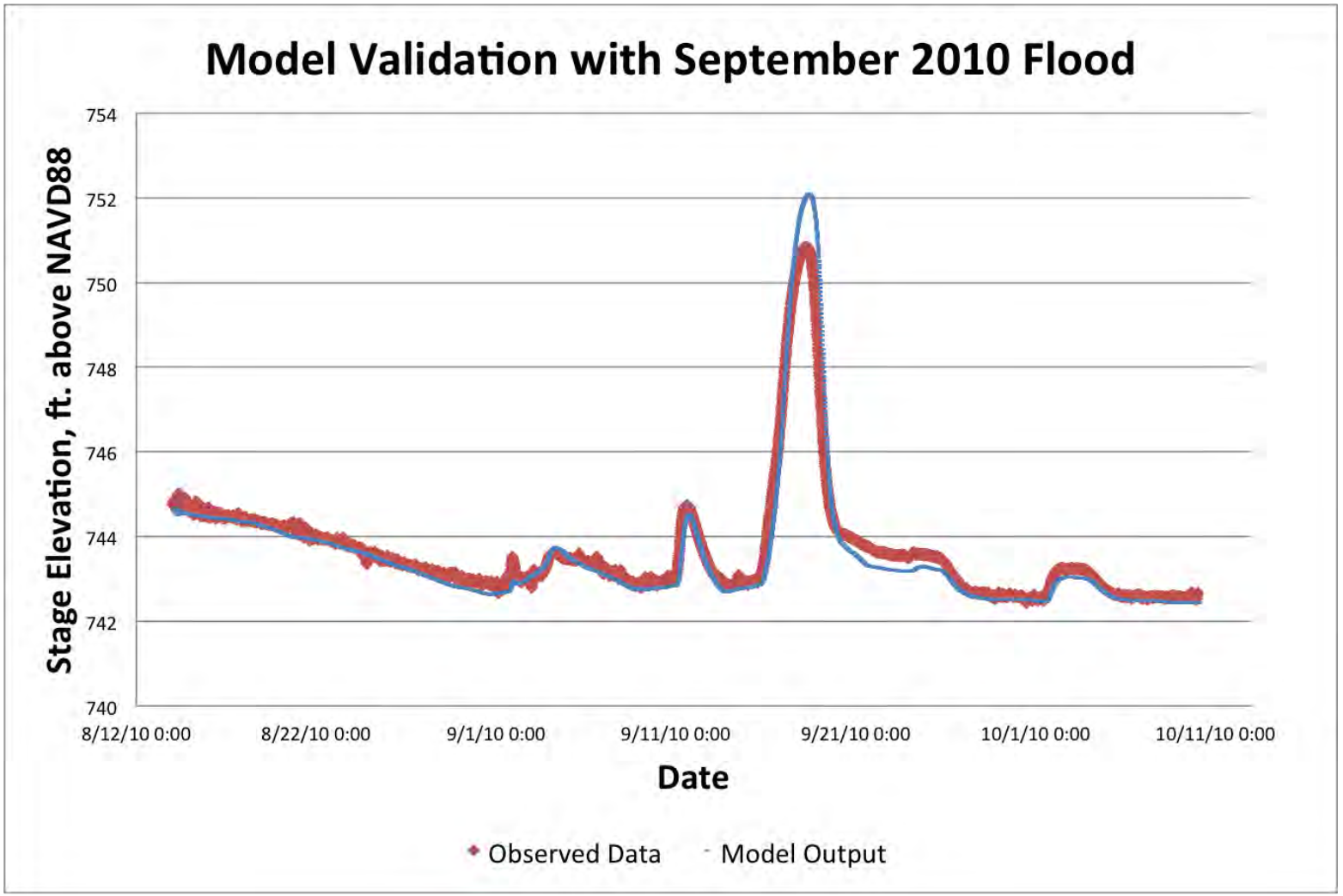

Figure 4.23. Full modeled extent of September 2010 flood event, observed dataset compared to model output.

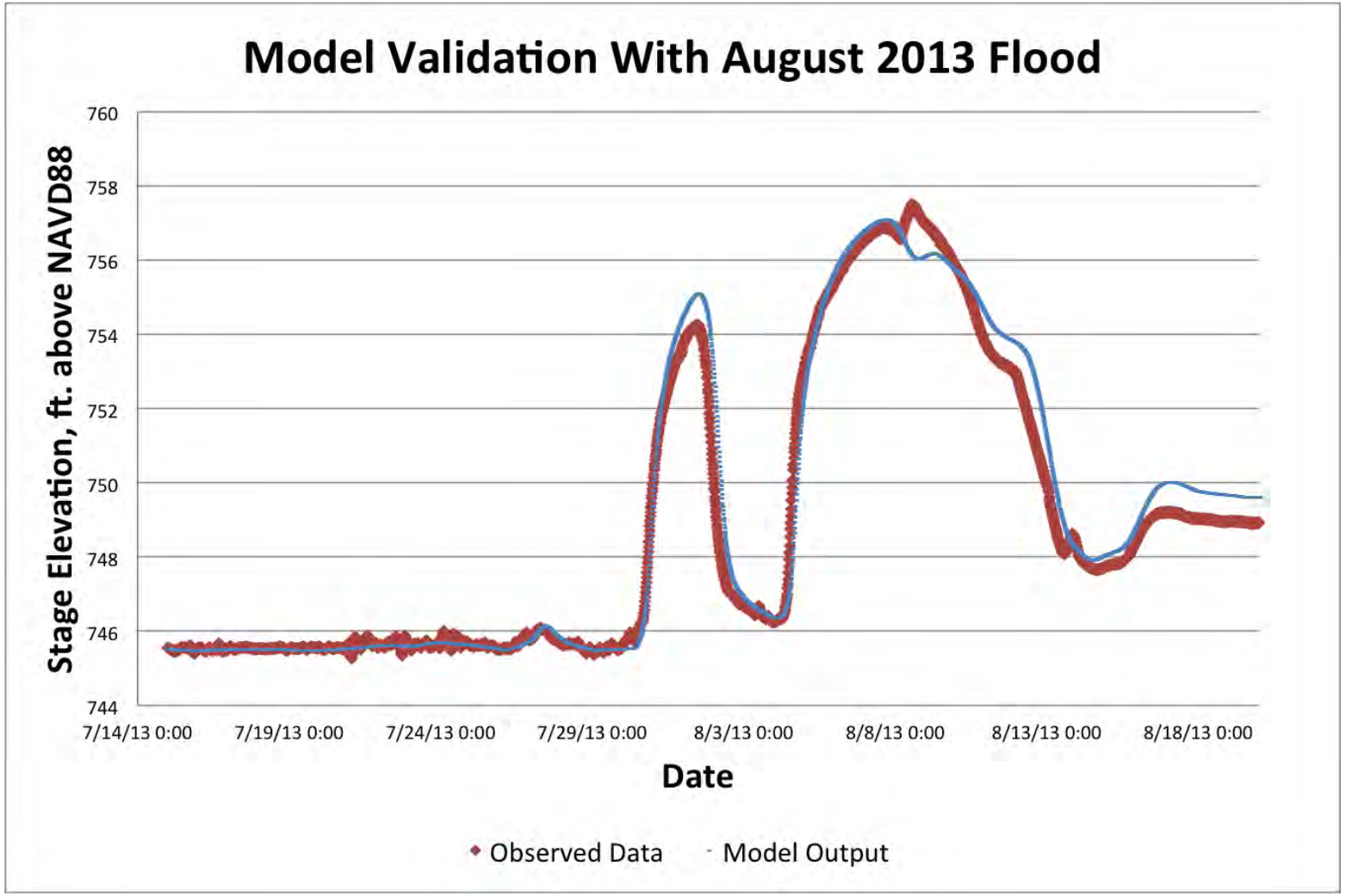

Figure 4.24. Full modeled extent of August 2013 flood event, observed dataset compared to model output.

4.3.3 Model Application

The table and figures included in this section represent the HEC-RAS model's predicted effect of the proposed rule curve adjustment (i.e., a change in downstream boundary conditions) on upstream flooding in the priority locations described in the beginning of this chapter. Table 4.11 shows the maximum WSE calculated for each priority location under the proposed rule curve conditions. This table should be used to determine what flow conditions cause the WSEs to exceed the USACE easement of 760.33 ft NAVD88 in the priority locations. Table 4.12 is a summary of the effects of the proposed rule curve adjustment on WSEs in the priority sections for the streamflow scenarios shown. Graphics representing the spatial distribution of the percent changes in depth and top-width can be found in Appendix C.

Figures 4.25, 4.29, and 4.30 represent the physical changes in WSE due to the proposed rule curve adjustment at each priority location for each flood-frequency streamflow determined in Section 4.1.6. The figures are grouped by priority location, and there are seven sets of figures for each flood-frequency. The figure on the left is a representation of the entire priority section, including the channel bottom elevations. The figure on the right is a zoomed-in version of the same figure, accentuating the difference between the WSE levels for the different dam conditions. Note that the zoomed-in figures each use very different scales on the y-axis.

Table 4.11. Table summarizing model application phase. Maximum WSEs calculated in each priority section under the proposed rule curve conditions are shown.

Return Period Flow on All Streams	*Priority 1* Max WSE (ft)	*Priority 2* Max WSE (ft)	*Priority 3* Max WSE (ft)
2-yr	746.24	769.09	745.80
10-yr	757.26	773.77	754.67
25-yr	763.27	776.36	760.72
50-yr	767.79	778.07	765.25
100-yr	772.30	779.88	769.31
200-yr	776.00	781.52	773.75
500-yr	781.18	784.07	779.71

Table 4.12. Table summarizing model application phase. The difference in WSE caused by the proposed rule curve adjustment (PRCA) is the PRCA effect. Positive values indicate a higher WSE under the proposed rule curve conditions. The left-hand column refers to the return period flow on each stream in the model. The average PRCA effect in the priority location is shown in the "Avg" row, and the maximum PRCA effect in the priority location is shown in the "Max" row.

		Priority 1 PRCA effect (ft)	*Priority 2* PRCA effect (ft)	*Priority 3* PRCA effect (ft)
All 2	Avg	1.76	0.34	1.91
	Max	1.83	1.84	1.96
All 10	Avg	0.15	0.07	0.47
	Max	0.20	0.19	0.68
All 25	Avg	0.04	0.02	0.14
	Max	0.05	0.06	0.24
All 50	Avg	0.03	0.02	0.08
	Max	0.03	0.04	0.14
All 100	Avg	0.02	0.01	0.05
	Max	0.03	0.03	0.09
All 200	Avg	0.00	0.01	0.02
	Max	0.01	0.01	0.05
All 500	Avg	0.01	0.01	0.02
	Max	0.02	0.02	0.05

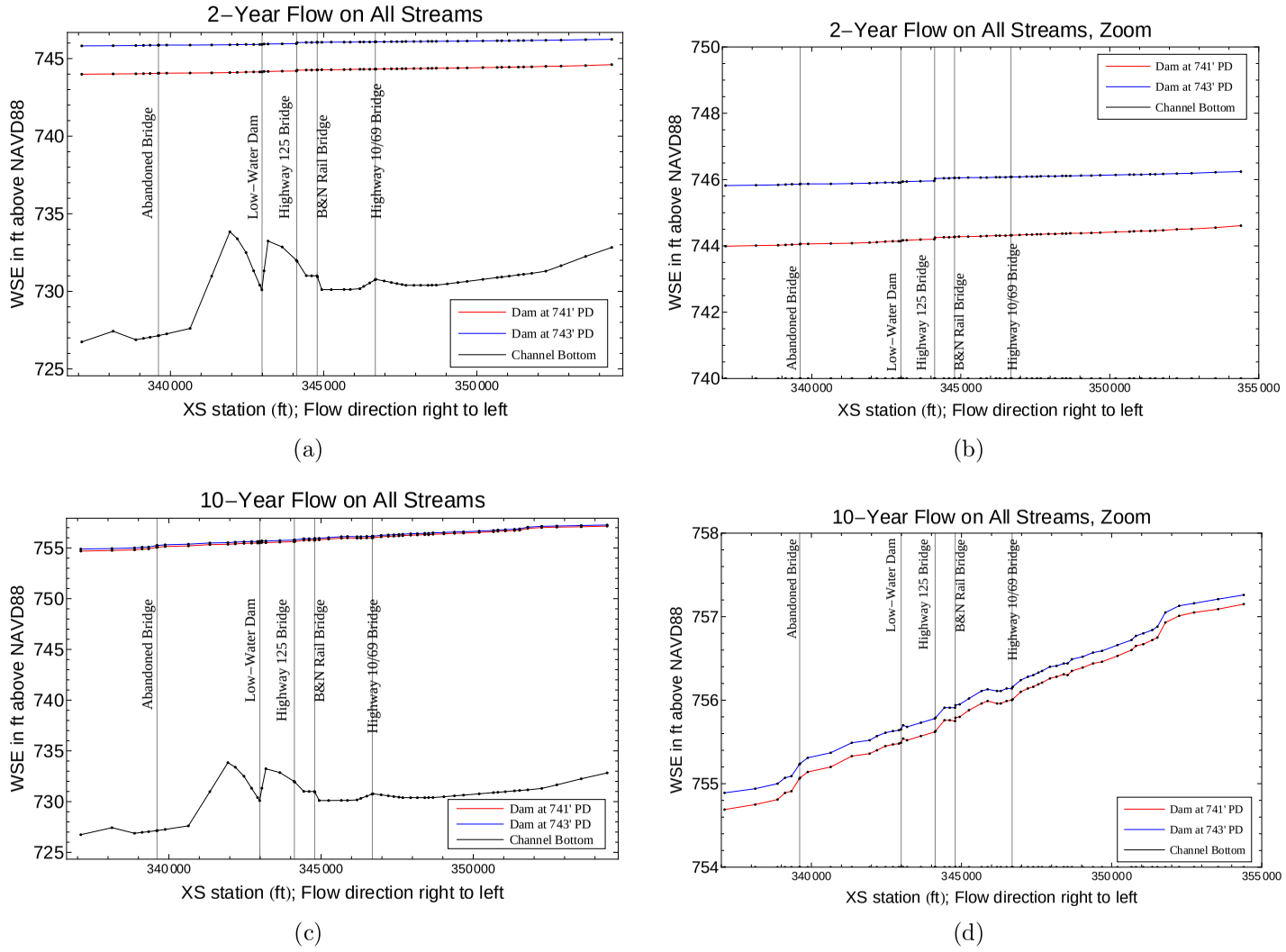

Figure 4.25. Physical changes in WSEs for priority 1 locations due to changing boundary condition at dam from 741 to 743 ft PD for 2- and 10-yr return periods. Figures on left are full vertical scale including channel bottom elevations, and figures on the right are zoomed in figures.

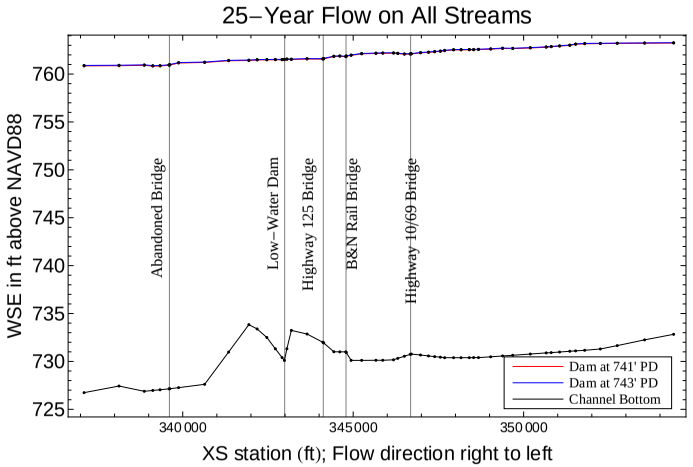

(e)

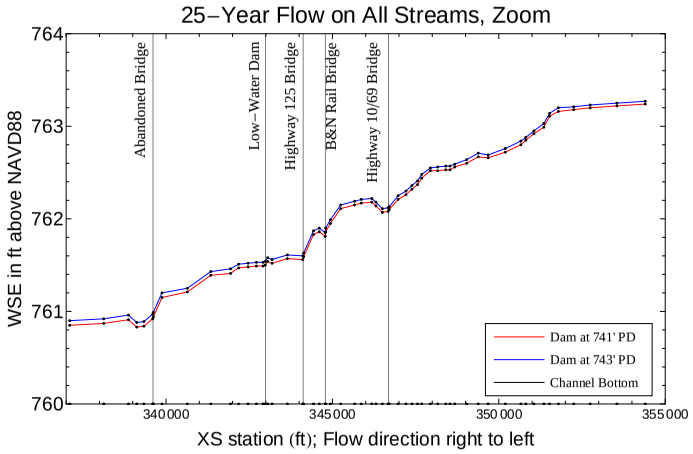

(f)

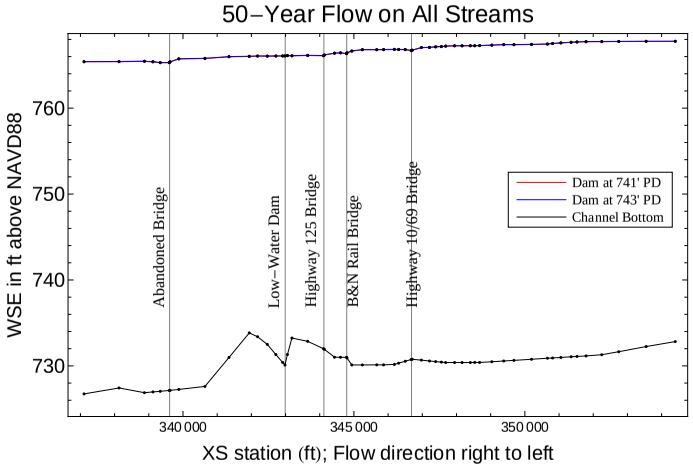

(g)

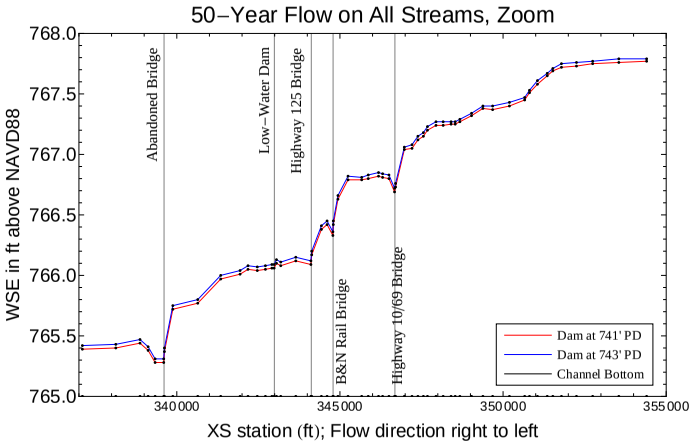

(h)

Figure 4.25. Physical changes in WSEs for priority 1 locations due to changing boundary condition at dam from 741 to 743 ft PD for 25- and 50-yr return periods. Figures on left are full vertical scale including channel bottom elevations, and figures on the right are zoomed in figures.

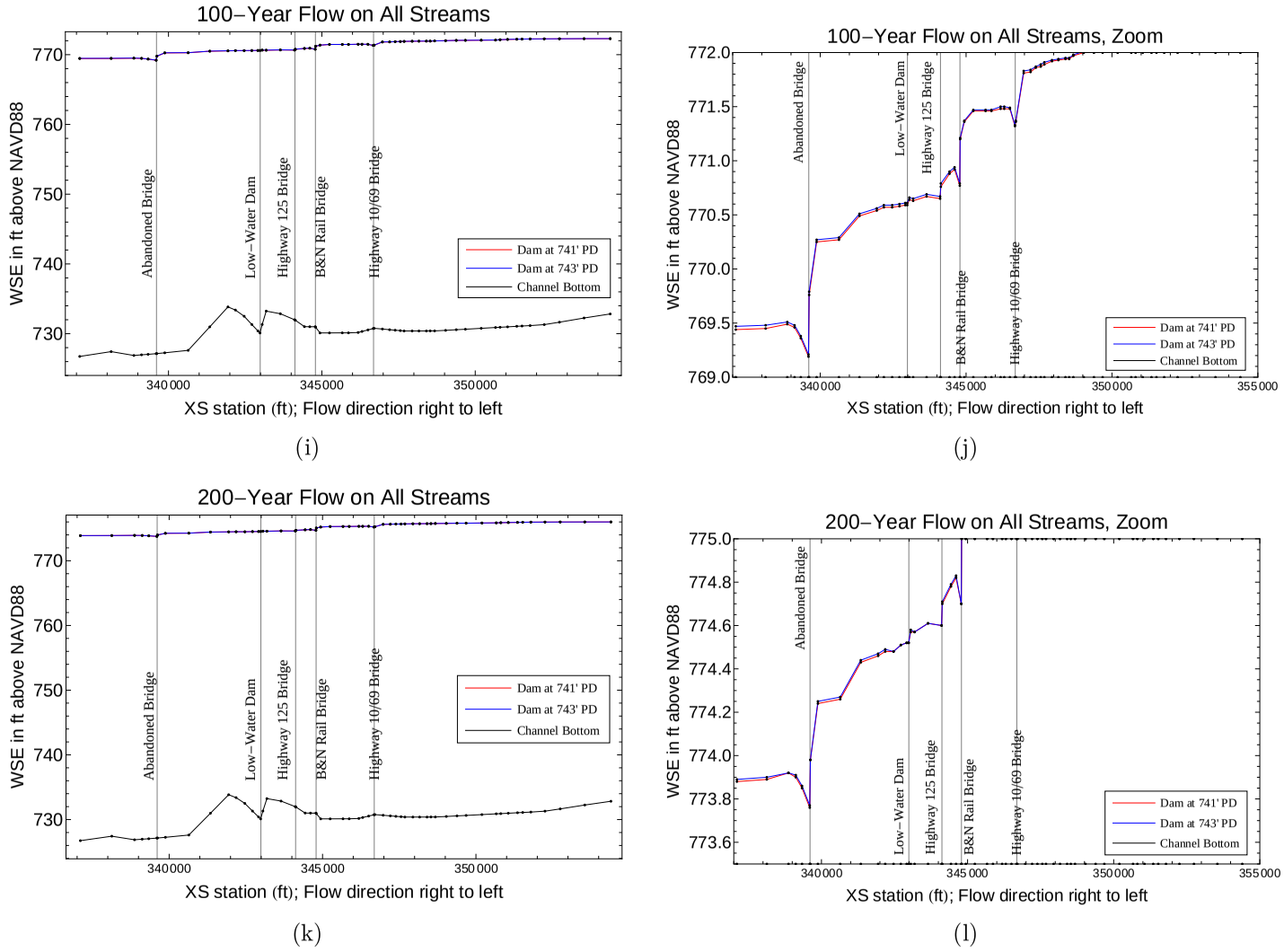

Figure 4.25. Physical changes in WSEs for priority 1 locations due to changing boundary condition at dam from 741 to 743 ft PD for 100- and 200-yr return periods. Figures on left are full vertical scale including channel bottom elevations, and figures on the right are zoomed in figures.

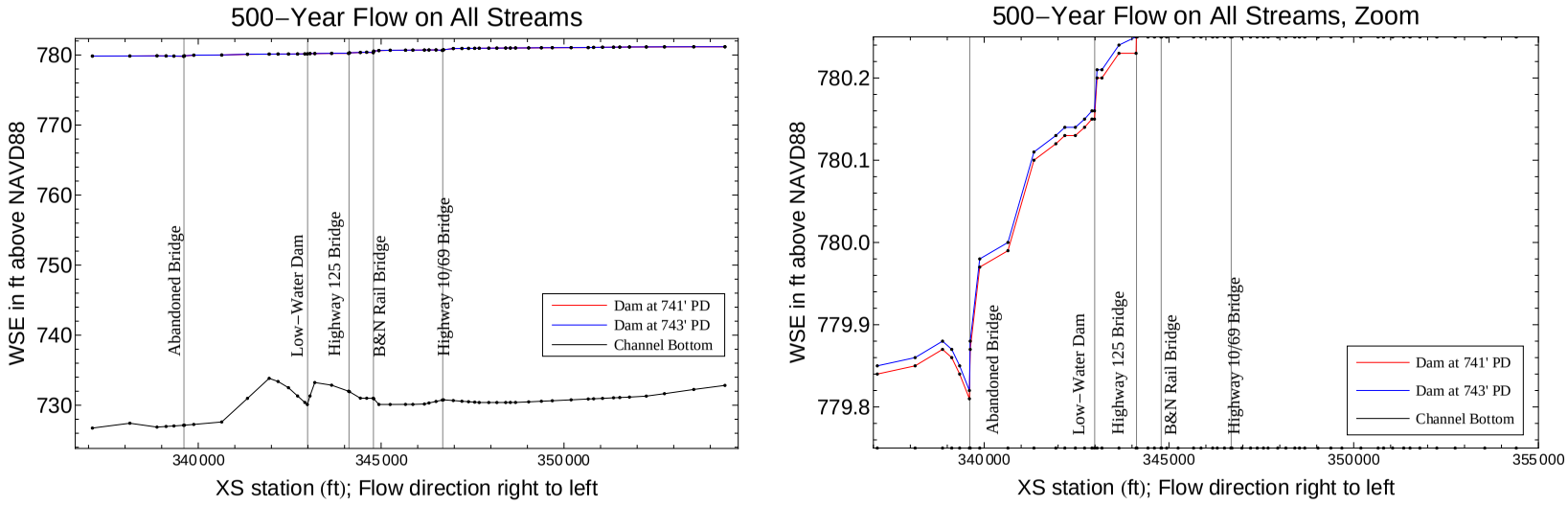

Figure 4.25. Physical changes in WSEs for priority 1 locations due to changing boundary condition at dam from 741 to 743 ft PD for 500-year return period. Figure on left is full vertical scale including channel bottom elevations, and figure on the right is zoomed in figure.

The location of Riverview Park (RP) is the first location to flood in the priority locations during a flood event, according to the National Weather Service's (NWS) description of flooding in this area [NOAA, 2013]. The model station of RP along the Neosho River is near 3436+47, just downstream of the Highway 125 bridge in Miami. The USACE easements at this location extend to an elevation of 760.33 ft NAVD88 [USACE, 1998]. Flooding in RP occurs when WSEs exceed the USACE easements, therefore the 760.33 ft NAVD88 elevation is considered "flood-stage." The location of RP is shown during various flood events in Figures 4.26, 4.27, and 4.28.

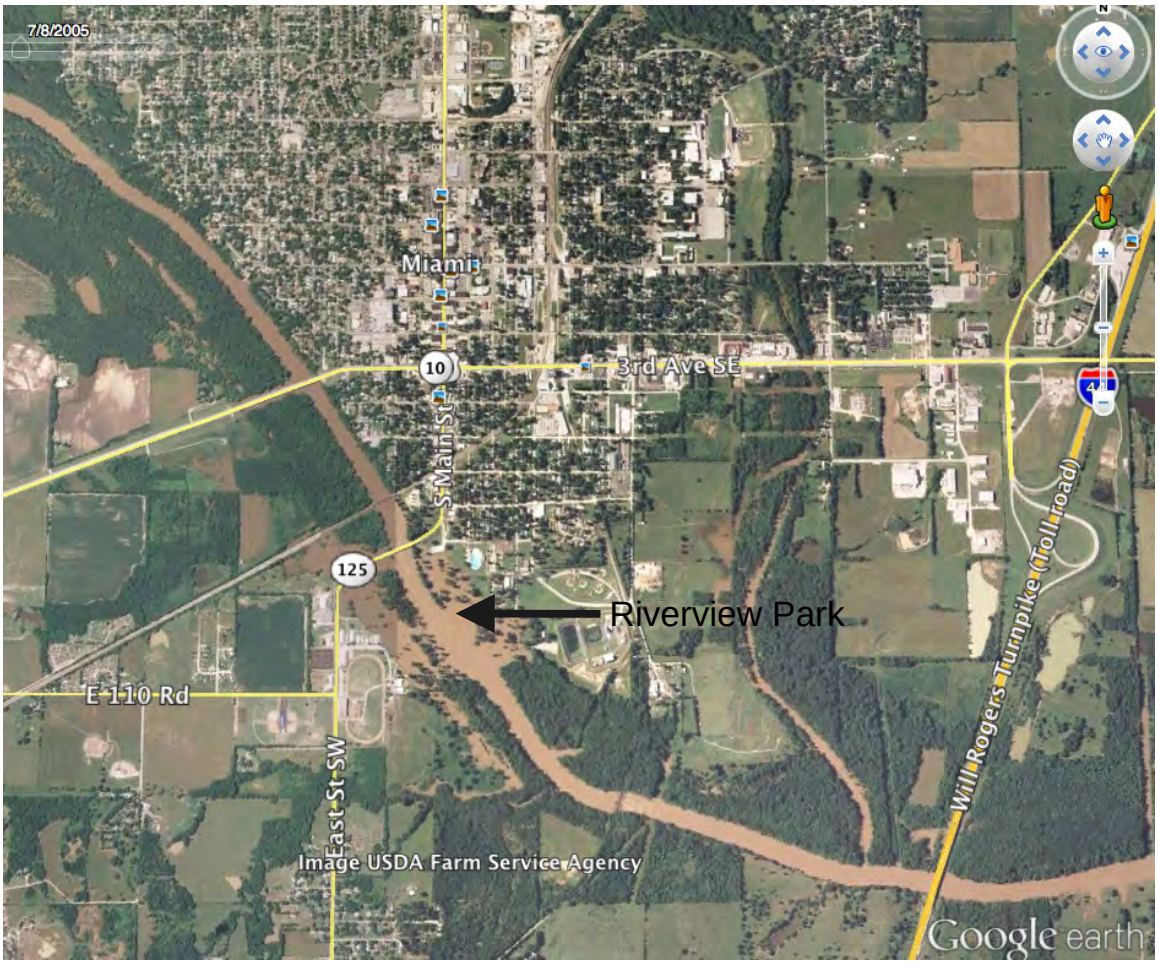

Figure 4.26. Location of Riverview Park in reference to Miami. Flood event from July 2005. Picture used from Google Earth.

Figure 4.27. Picture of Riverview Park during the June 2009 flood event.

Figure 4.28. Picture of Riverview Park during the August 2013 flood event.

An analysis of the results shown in Table 4.11 and Figure 4.25 reveals that WSEs exceed flood stage near RP at a flow between the 10- and 25-year return period flows. Table 4.12 show that the proposed rule curve adjustment would cause between 0.04 and 0.20 ft of increased WSEs at RP under a flow between the 10- and 25-yr return interval. The difference of 0.20 is the maximum predicted increase in WSEs by the HEC-RAS model under the proposed rule curve adjustment for WSEs that exceed flood stage in the priority locations.

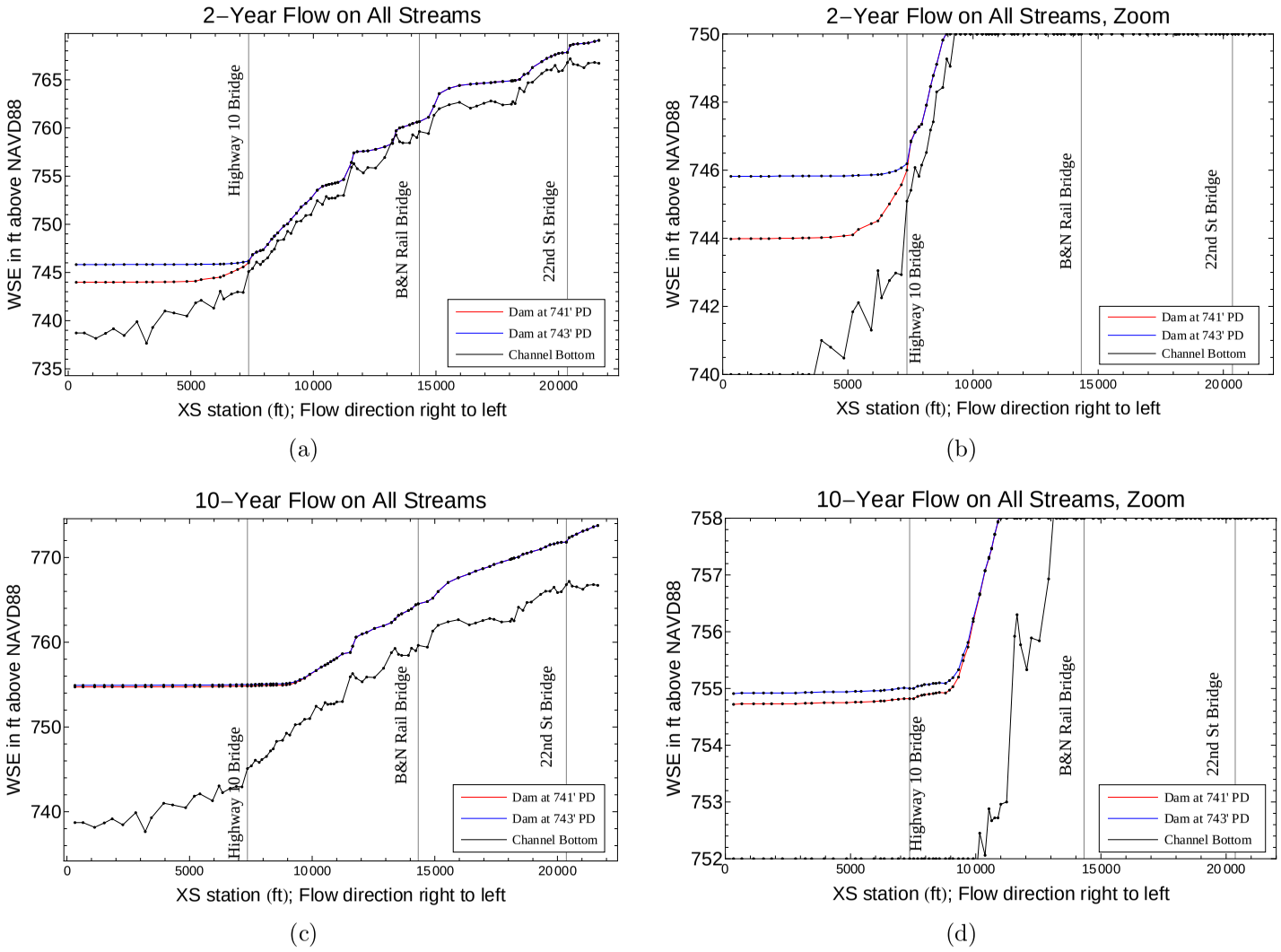

Figure 4.29. Physical changes in WSEs for priority 2 locations due to changing boundary condition at dam from 741 to 743 ft PD for 2- and 10-yr return periods. Figures on left are full vertical scale including channel bottom elevations, and figures on the right are zoomed in figures.

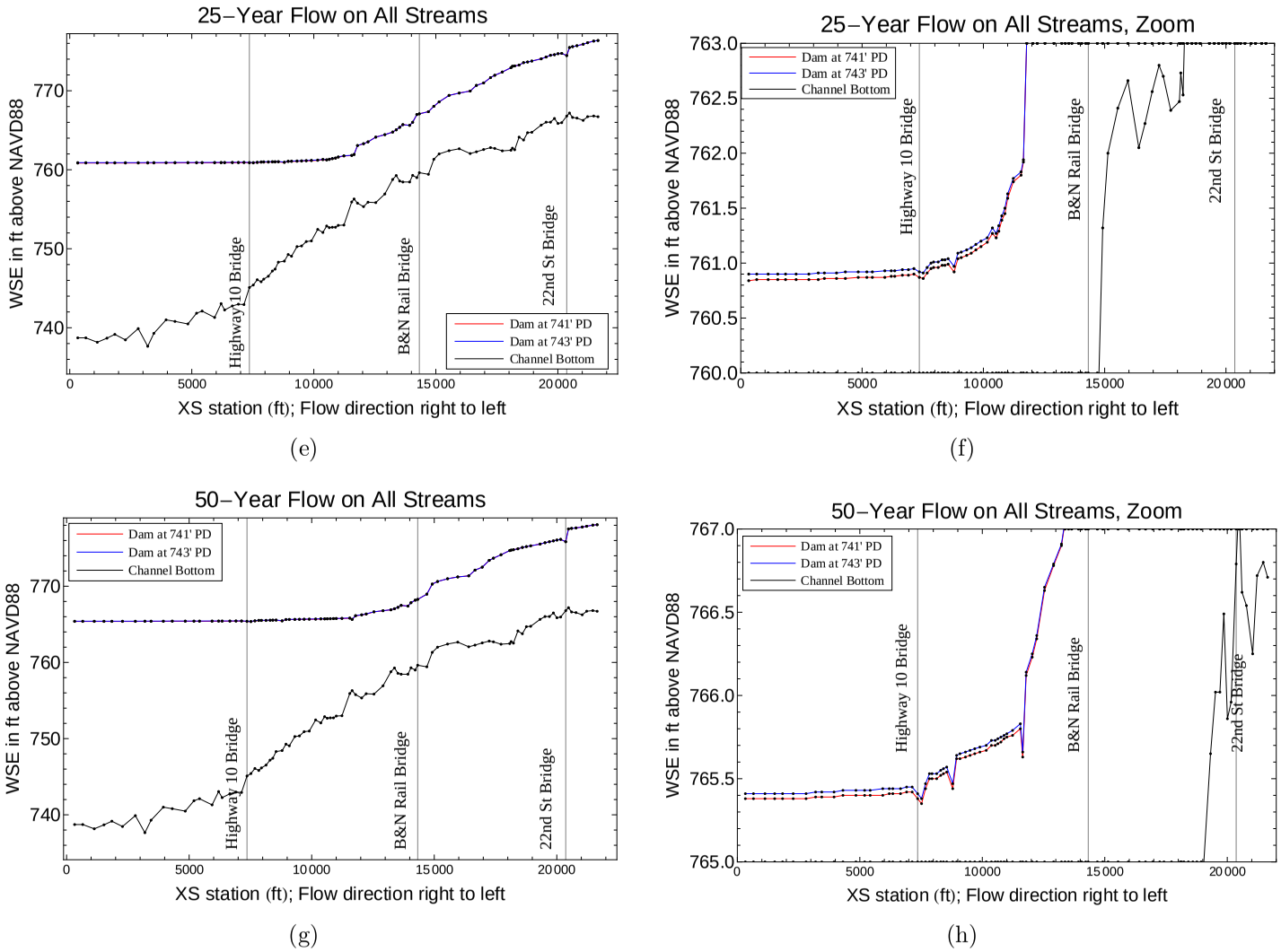

Figure 4.29. Physical changes in WSEs for priority 2 locations due to changing boundary condition at dam from 741 to 743 ft PD for 25- and 50-yr return periods. Figures on left are full vertical scale including channel bottom elevations, and figures on the right are zoomed in figures.

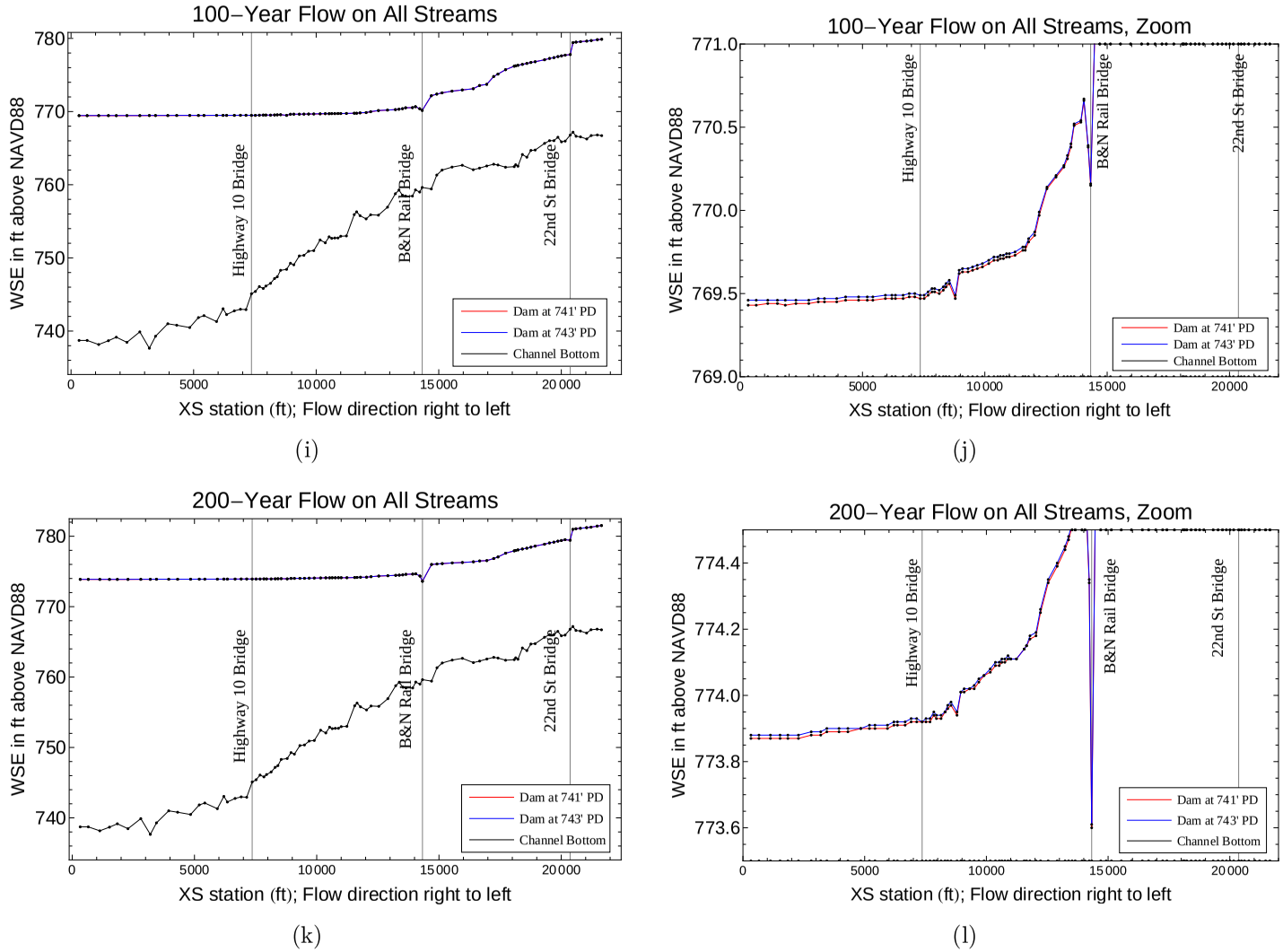

Figure 4.29. Physical changes in WSEs for priority 2 locations due to changing boundary condition at dam from 741 to 743 ft PD for 100- and 200-yr return periods. Figures on left are full vertical scale including channel bottom elevations, and figures on the right are zoomed in figures.

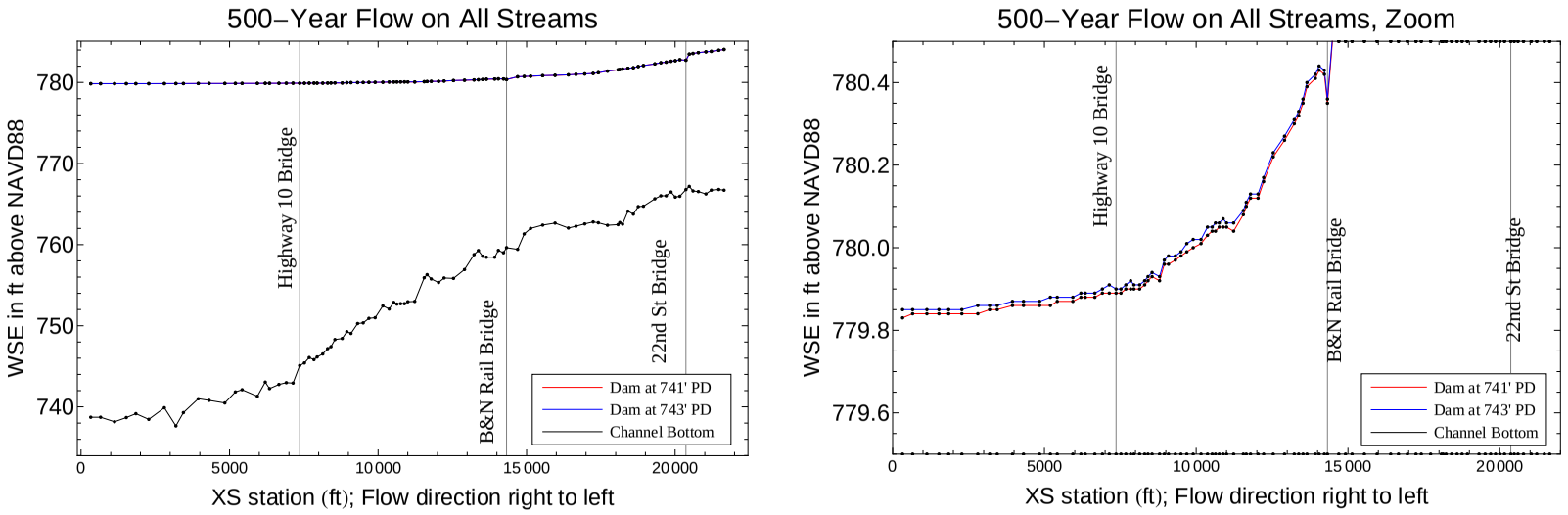

Figure 4.29. Physical changes in WSEs for priority 2 locations due to changing boundary condition at dam from 741 to 743 ft PD for 500-yr return period. Figure on left is full vertical scale including channel bottom elevations, and figure on the right is zoomed in figure.

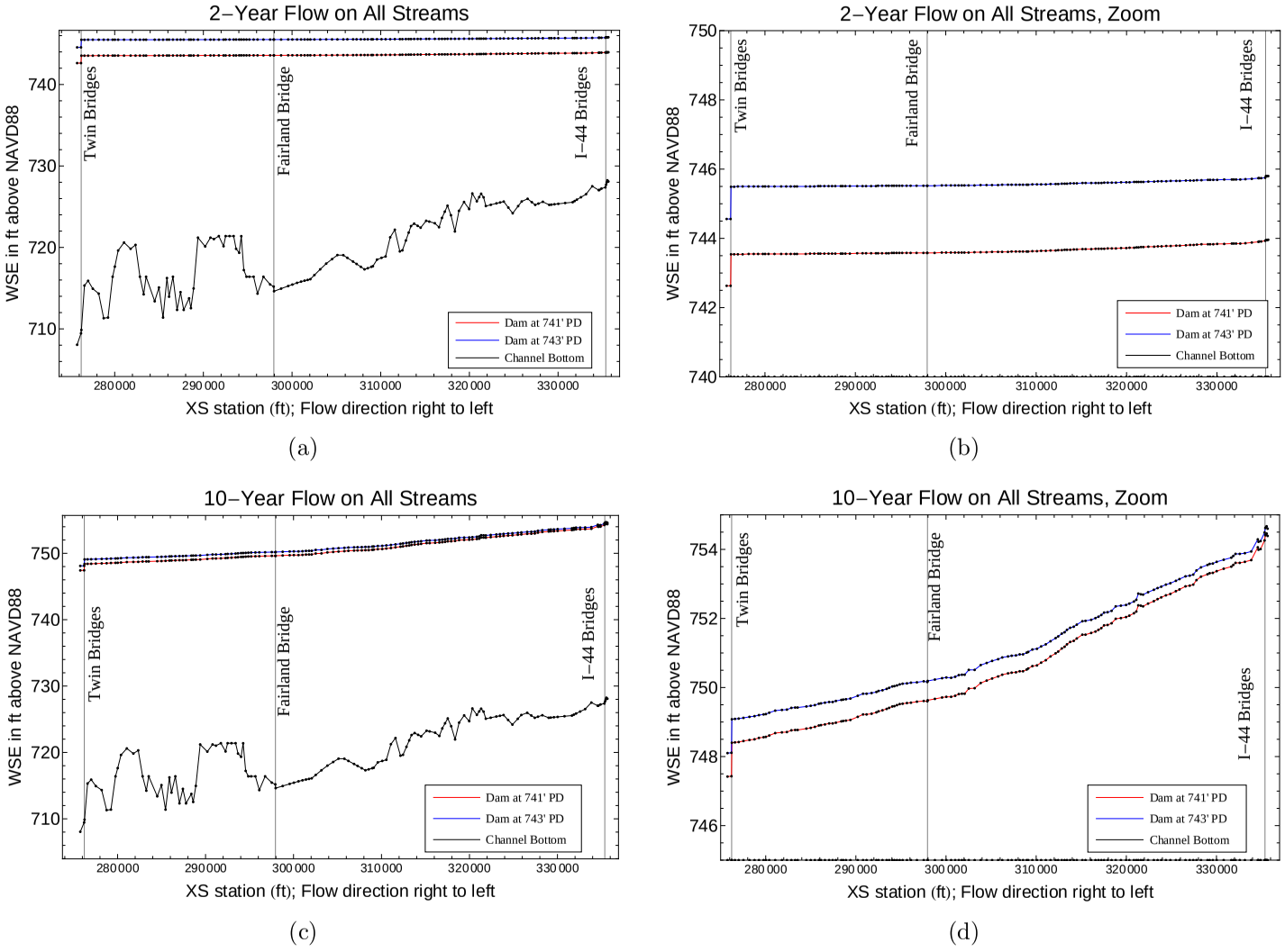

Figure 4.30. Physical changes in WSEs for priority 3 locations due to changing boundary condition at dam from 741 to 743 ft PD for 2- and 10-yr return periods. Figures on left are full vertical scale including channel bottom elevations, and figures on the right are zoomed in figures.

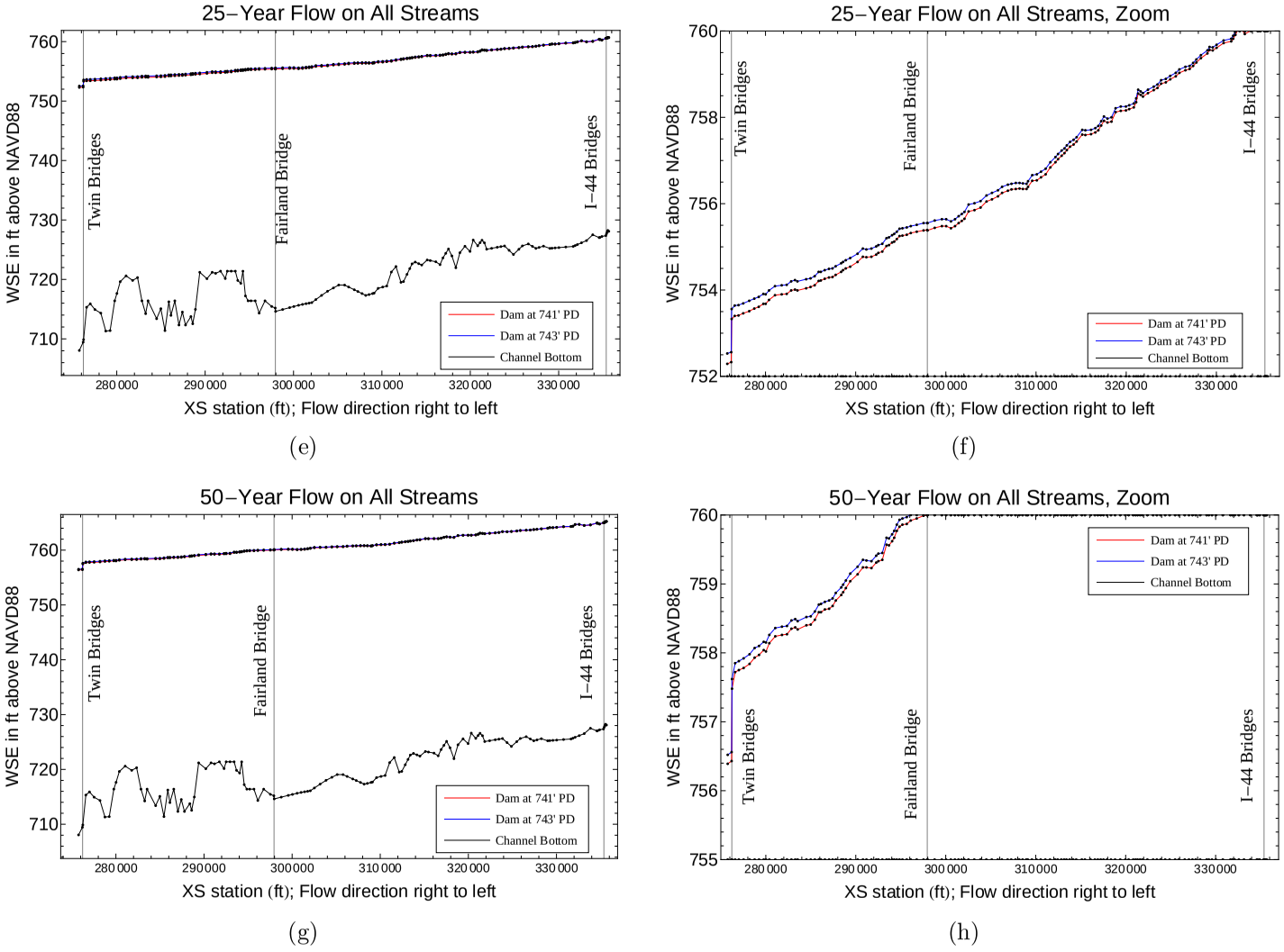

Figure 4.30. Physical changes in WSEs for priority 3 locations due to changing boundary condition at dam from 741 to 743 ft PD for 25- and 50-yr return periods. Figures on left are full vertical scale including channel bottom elevations, and figures on the right are zoomed in figures.

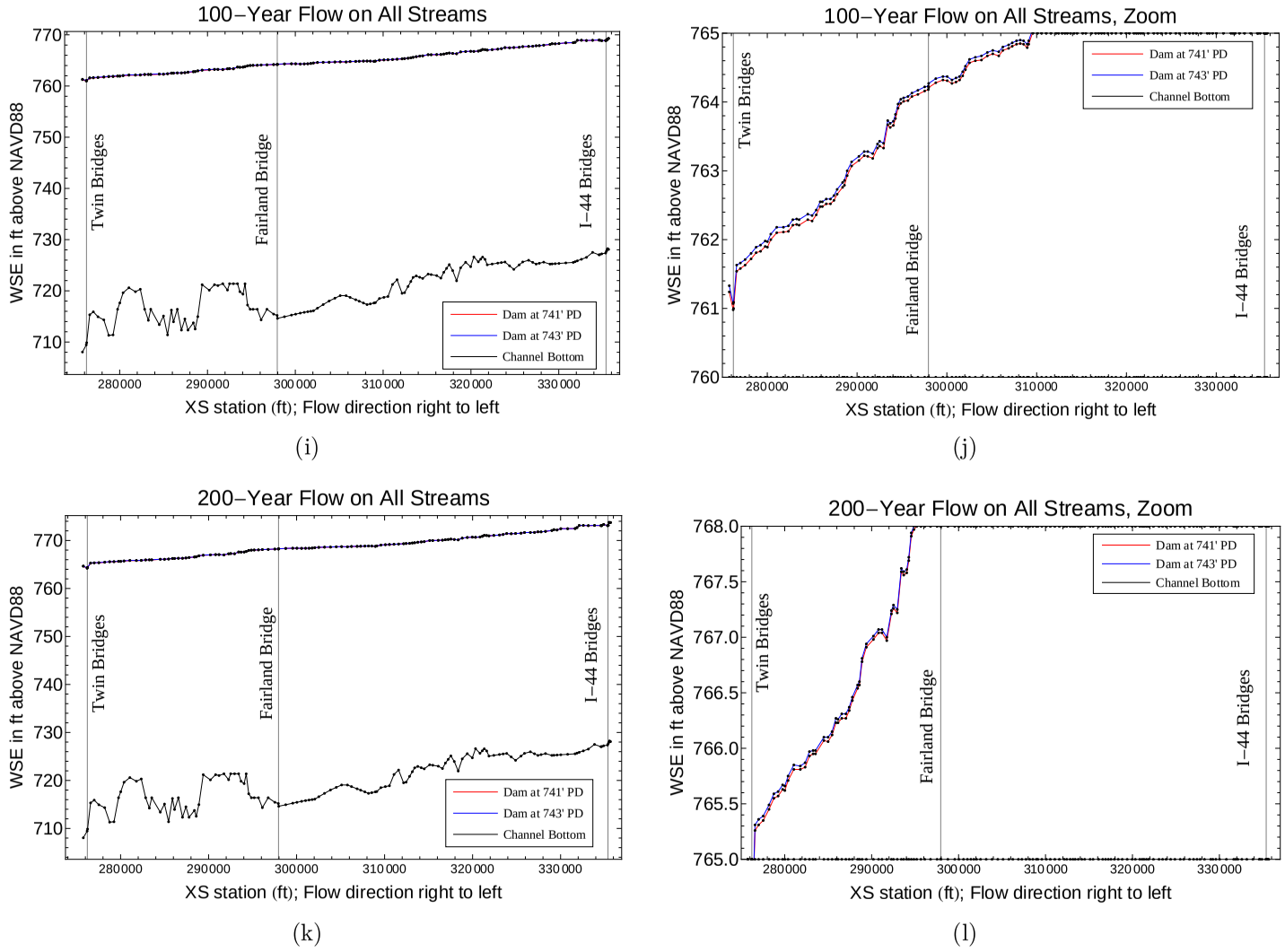

Figure 4.30. Physical changes in WSEs for priority 3 locations due to changing boundary condition at dam from 741 to 743 ft PD for 100- and 200-yr return periods. Figures on left are full vertical scale including channel bottom elevations, and figures on the right are zoomed in figures.

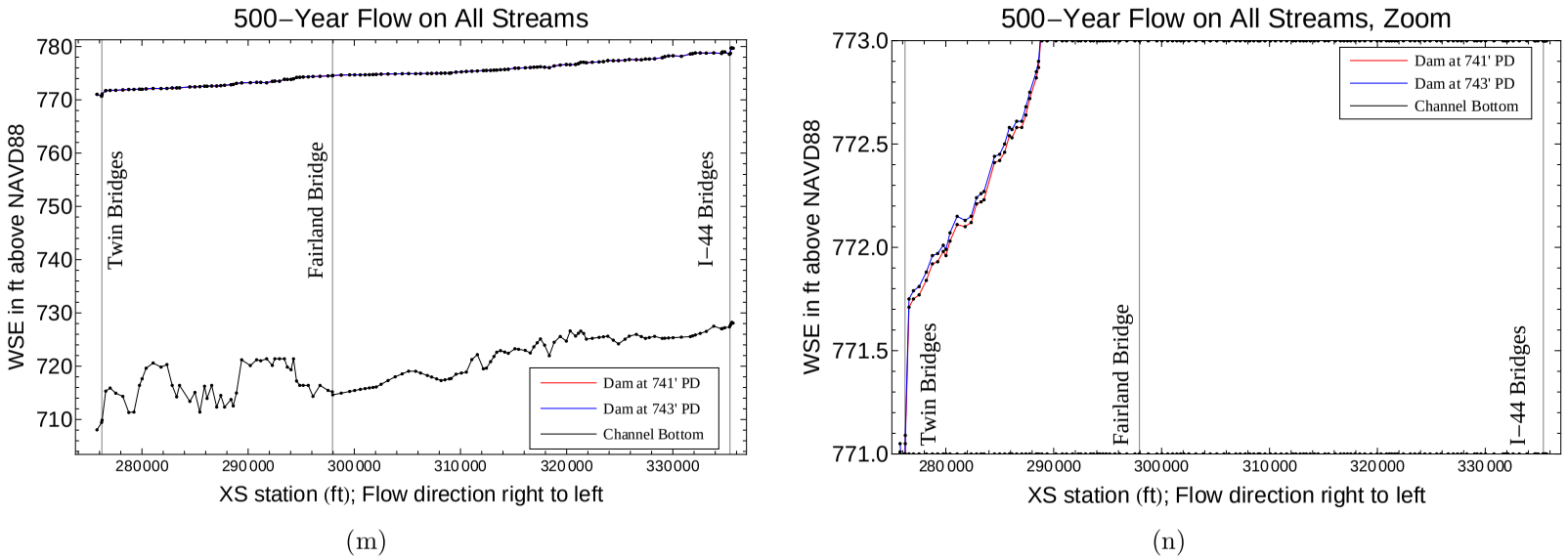

Figure 4.30. Physical changes in WSEs for priority 3 locations due to changing boundary condition at dam from 741 to 743 ft PD for 500-yr return period. Figure on left is full vertical scale including channel bottom elevations, and figure on the right is zoomed in figure.

The results shown in Figures 4.25, 4.29, and 4.30 reveal that the WSEs in all the priority locations are affected much more by the streamflow magnitude than the downstream dam WSE. This is evidenced by the fact that as the return period increases, the WSE elevation profiles representing each rule curve scenario move closer together. The WSE profiles, which represent the existing and proposed rule curve conditions, moving closer together represents a decreased effect of the proposed rule curve adjustment, as represented in Table 4.12. However, as the return period streamflow increases, the WSE profiles simultaneously rise to account for the increased streamflow volume, as shown in Table 4.11. This means that the downstream boundary condition at the dam has much less of an effect on WSEs in the priority locations than the streamflow magnitude.

There are several notable patterns in the figures shown in this section. For example, for several return period flows (c.f. Figures 4.25(l), 4.29(b), and 4.30(h)) the zoomed in figure cuts off the WSE profiles. This is due to the degree to which the figure is zoomed in, and the inability to capture the minuscule difference between the WSE profiles without cutting off some of the profile extent.

The effect of the bridges along the Neosho River constricting streamflow is particularly noticeable in Figure 4.25(j). This figure represents the 100-yr return period in the priority 1 section. At the locations of the bridges, there is a sharp dip in both WSE profiles. This phenomenon is due to a constriction of flow through the bridge embankments. This constriction is not noticeable on the 2- and 10-year flows because the flow remains in the river channel. Under the higher streamflow conditions of the more extreme return periods, the flow runs over the bank and backs up behind the bridge embankments. This causes a rise in WSEs upstream of the bridge, and as the flow accelerates through the bridge opening, the WSE dips to accommodate the increased velocity. This is the behavior expected from subcritical flow conditions, which

are the case for all the scenarios tested in this research, according to the hydraulic model results [Chow, 2009].

4.4 Model Verifications and Sensitivity Analyses Results

4.4.1 Hydraulic Model Verifications

Model Verification Part 1: Simplified model used to verify qualitative trend in backwater extent

Section 3.4.1 describes the reasoning behind defining the start of the backwater effect as 0.10 ft difference between the WSE under with-dam conditions and WSE under without-dam conditions. As an example of determining the backwater extent for the 100-year flow, the WSE for without-dam conditions at river station 2760+00 (approximate location of Twin Bridges in the simplified model) is 748.92 ft NAVD88, and the WSE for with-dam conditions is 750.89 ft NAVD88. The difference caused by backwater, therefore, is 750.89 - 748.92 = 1.97 ft. Moving upstream, at river station 3290+00 the WSE for no-dam conditions is 764.38 ft, and for with-dam conditions it is 764.48 ft, yielding a backwater effect of 0.10 ft. Therefore, because 0.10 ft is defined above as the upstream extent of the backwater effect for a given streamflow, river station 3290+00 is considered the approximate upstream extent of the backwater effect for the 100-year streamflow.

The simplified model of the Grand Lake region is represented by Figure 4.31. There are four user-defined cross sections at river stations 0+00, 1870+00, 2760+00, and 3980+00, as shown in Figure 4.31(a). Interpolated cross sections are created at 1000 ft spacing, as shown in Figure 4.31(b).

The results of this simplified approach to modeling the backwater effect are shown in Figure 4.32. For these models, the dam WSE was 743 ft, which is the high point of the proposed rule curve adjustment. The backwater effect from the dam extends

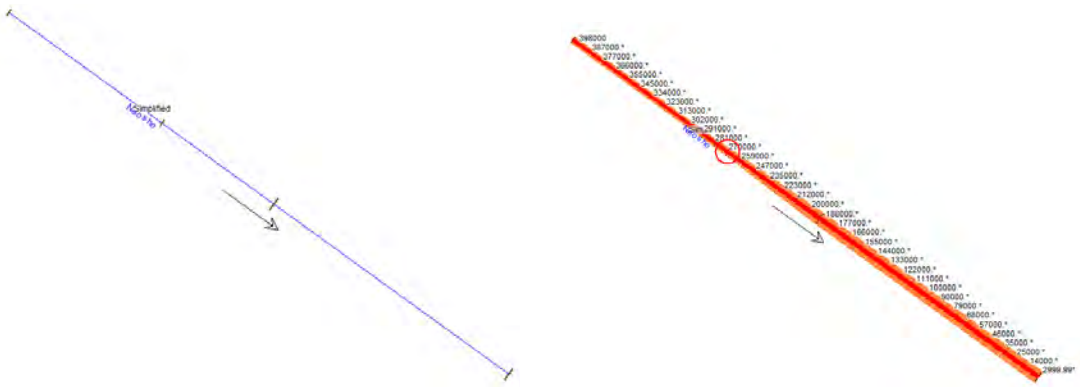

(a) (b)

Figure 4.31. HEC-RAS representation of simplified geometry used to verify qualitative results of backwater effect.

further upstream for the lower flow conditions (e.g., 2-year flow) than for the higher flow conditions (e.g., 500-year flow). This phenomenon seems counter-intuitive, but makes sense within an open-channel hydraulic system [Bedient et al., 2013]. As the streamflow magnitude increases, the WSE must rise to carry the flow. This rise in WSE intersects the lake, which is held at a consistent level-pool elevation of 743 ft PD. The water surface profile from upstream intersects with the level pool in an asymptotic transition phase. This transition phase moves downstream as the WSE levels upstream rise with the higher streamflow magnitudes. Therefore, at a location upstream of the level-pool, the WSE rises due to the increased streamflow and is affected less by the level-pool elevation during the higher streamflow condition.

The figures in Figure 4.32 show the backwater effect exceeding river station 2760+00 as the flow increases from the 2- to 100-year flows. With streamflows higher than 100-year, the extent of the backwater does not appear to move further upstream. When defining the backwater extent as the point upstream of the dam where the difference in WSEs is $\leq$0.1 ft, as defined in Section 4.4.3, the backwater extent for each flow frequency is shown in Table 4.13.

The results shown in Table 4.13 confirm the qualitative trend found with the complex model, in that the extent of the backwater effect is less extensive when the streamflow is more extreme. This simplified model also does not take into account the effect of bridge-embankement flow-constrictions and confluence areas of other streams as possible intermediate boundary conditions. The addition of these intermediate boundary conditions further reduces the backwater effect of the dam. Note that Riverview Park is located near river station 3436+00, which is just upstream of the extent of the backwater effect for the ≥100-yr flow under these idealized conditions. This verifies the conclusion that the backwater effect is minimal at the location of Miami when the WSE at the dam is 743 ft PD and high streamflow conditions exist on the Neosho River.

Table 4.13. Extent of backwater effect for each flow-frequency streamflow in simplified model.

Streamflow	Location of Backwater Effect ≤ 0.10ft	Difference in WSEs at upstream boundary (ft)
2-year	upstream of boundary	0.12
10-year	upstream of boundary	0.16
25-year	upstream of 3750+00	0.02
50-year	upstream of 3440+00	0.01
100-year	upstream of 3290+00	0.00
200-year	upstream of 3250+00	0.00
500-year	upstream of 3190+00	0.01

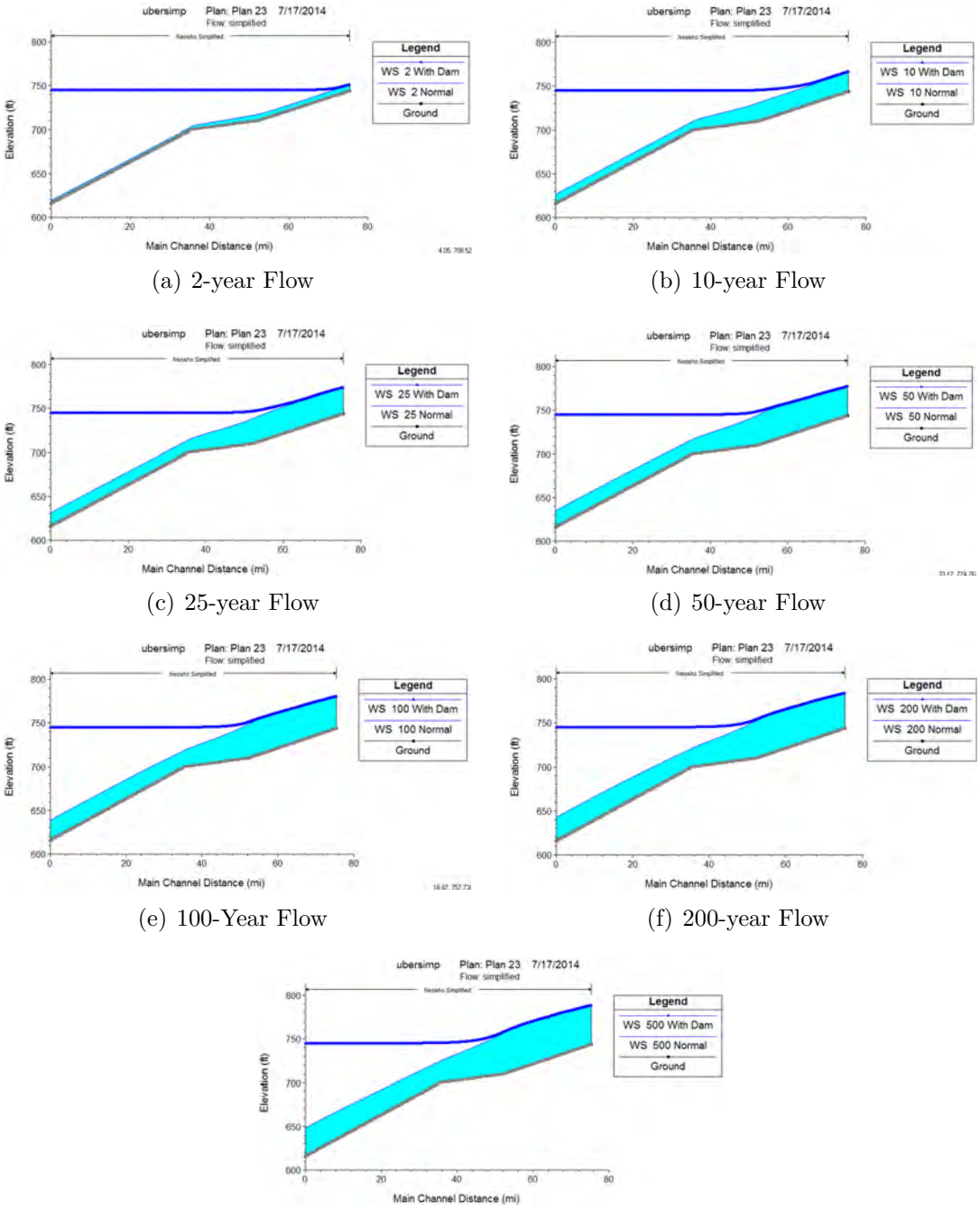

(a) 2-year Flow

(b) 10-year Flow

(c) 25-year Flow

(d) 50-year Flow

(e) 100-Year Flow

(f) 200-year Flow

(g) 500-year Flow

Figure 4.32. Backwater Extents for flood-frequency streamflows for a simplified model of the Grand Lake region.

Model Verification Part 2: Steady vs. Unsteady model comparison to verify conservativeness of steady-state model

As discussed in Section 4.4.3, the assumption that the steady-state computation method is more conservative for a given streamflow condition than the unsteady method was tested by comparing the two methods with the September 2009 flow scenario. The peak streamflow condition on the Neosho River occurred at 6:00AM on 9/12/2009, and the system boundary conditions at this time are represented in Table 4.14. These boundary conditions were used in a steady-state model in HEC-RAS in order to compare the WSEs from the steady state run to the WSEs at the 6:00AM time step of the unsteady run.

Table 4.14. Boundary conditions for use in steady-state comparison of September 2009 peak flow conditions: 9/12/2009 at 6:00 AM.

Boundary Name	Boundary Condition
Neosho River, Commerce gauge	44,600 cfs
Tar Creek, Miami gauge	63 cfs
Spring River, Quapaw gauge	2,250 cfs
Elk River, Tiff City gauge	431 cfs
Pensacola Dam	746.72 ft NAVD88

The results of this comparison are shown in Figure 4.33. These results represent the steady-state WSE minus the unsteady WSE. Therefore, a positive value represents a higher WSE in the steady-state model, and a negative value represents a higher WSE in the unsteady model.

The steady-state WSEs in the priority 1 section are generally 0.90 to 1.00 ft higher than those in the unsteady-flow simulation. This priority 1 section is most relevant because it is immediately downstream of the boundary condition at which the streamflow conditions are being introduced to the system. Because there are no negative values, this process confirms the assumption that for a given peak streamflow,

the steady-state WSE computation method of HEC-RAS is more conservative than the unsteady-state computation method.

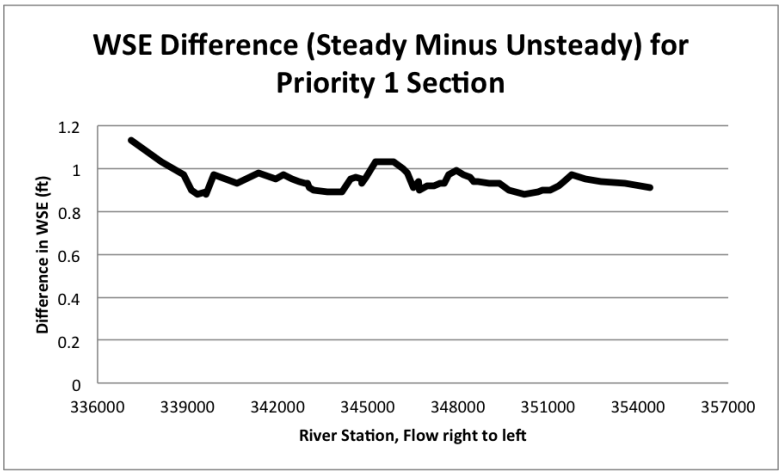

Figure 4.33. Comparison of steady vs. unsteady flow WSE computation techniques for peak September 2009 flow.

Model Verification Part 3: Comparison to Holly model to verify consistency with previous studies

This model verification compares the results included in Holly's (2004) report to results from the current hydraulic model for similar streamflow and downstream boundary conditions. These values are representative of the June 1995 storm WSEs, which were used by Holly in the 2004 report to compare the effect of two WSEs at Pensacola Dam. The difference in WSEs at the location of Miami, OK is included in the following figures. The location of Riverview Park (c.f. Section 4.3.3) in Miami is represented in Figures 4.34, and 4.35.

As discussed in Section 2.1.3, Holly used a pseudo-2D model called C1/C2 in order to calculate the WSEs for his report [Holly Jr., 2004]. Although this thesis research was conducted using a true 1D model, the results are very similar to Holly's results using the pseudo-2D model. This information helps to verify the validity of the 1D model, as opposed to a more complex model system, for this research context.

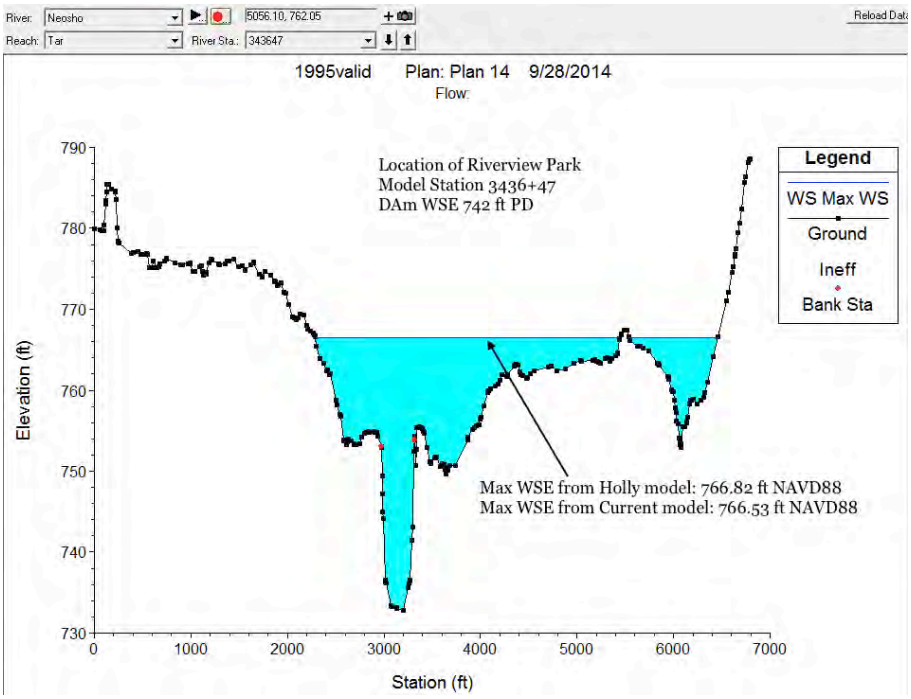

Figure 4.34. Comparison of Holly model WSE to Current model at location of RP in priority section 1. The WSE shown represents the max WSE calculated during the June 1995 flood with the dam WSE held at 742 ft PD.

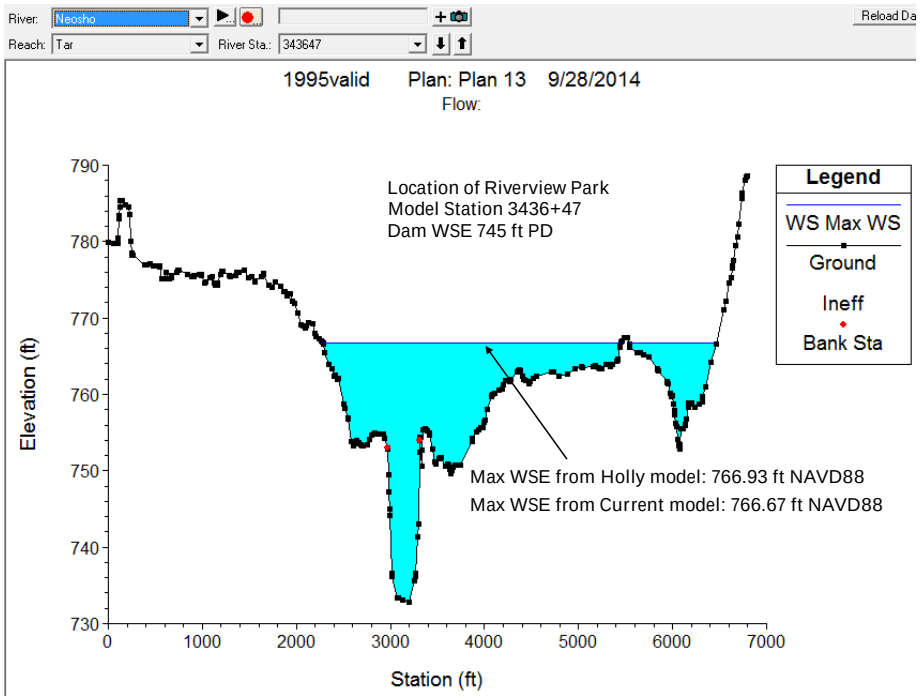

Figure 4.35. Comparison of Holly model WSE to Current model at location of RP in priority section 1. The WSE shown represents the max WSE calculated during the June 1995 flood with the dam WSE held at 745 ft PD.

4.4.2 Global Sensitivity Analysis

The RMSE values in Table 4.15 indicate the amount of influence each particular phenomenon has over the WSEs in each priority section. A few notable results from the global sensitivity analysis are discussed in the bulleted list below:

- Results in all three priority sections are most sensitive to the roughness coefficient (Manning's n) along the Neosho River channel, followed closely by the streamflow in the Neosho. These sensitivity rankings are somewhat subjective when comparing two completely different phenomena due to the fact that there are various degrees of extremes that may be used for each phenomenon. For example, the roughness coefficient is bound by the values explained in Section 3.4.2, while streamflow values are bound by upper and lower limits that are indicated by the probability of exceedance. These differences in extremes cause variation in what is represented by the RMSE value shown in the table, which is the sum of the effect of the analyzed range of each phenomenon.

- For the Priority 1 section, the WSEs are 5.5 times more sensitive to the streamflow on the Neosho River than the dam WSE. The WSEs in the Priority 2 section are about 2.4 times more sensitive to the Neosho River streamflow than the Tar Creek streamflow, although the section is along Tar Creek. This reveals that WSEs along Tar Creek near Miami are much more sensitive to high flows along the Neosho River (the downstream boundary condition of Tar Creek) than high flows along Tar Creek. The WSEs at each of the priority sections are also sensitive to the dam WSE, though not nearly so much as to the magnitude of the Neosho River streamflow. Note that the most conservative streamflow estimations were used for the model application portion of the research (c.f. Table 4.7 in Section 4.1.5). The B-17B procedure estimates a 100-yr streamflow

of 152,500 cfs while the best-fit, less-conservative procedure estimates a 100-yr streamflow of 65,000 cfs.

- Among the non-Manning's n phenomena, the streamflow magnitude, WSEs at the dam, and the bridges are the phenomena that create the largest effect on water levels near Miami.

- There are several phenomena included in the global sensitivity analysis that have no effect on WSEs in the priority sections. The phenomena that have a value of 0.000 in Table 4.15 in a specific priority section have no effect on the WSE in that priority section. The roughness coefficients on the Spring and Elk Rivers do not have an effect in any of the three priority sections.

Table 4.15. Global Sensitivity Analysis: Sensitivity of priority location WSEs to various model phenomena.

Phenomenon			*Degree of Sensitivity for Location*					
			Priority 1		Priority 2		Priority 3	
			Rank	RMSE	Rank	RMSE	Rank	RMSE
Streamflow		Neosho	2	5.362	2	2.950	2	3.492
		Spring	5	0.451	7	0.399	5	1.515
		Tar Creek	7	0.092	5	1.216	7	0.088
		Elk	8	0.003	10	0.003	8	0.006
Roughness Coefficient	Neosho	Channel	1	5.785	1	3.194	1	6.554
		Floodplain	3	2.298	4	1.281	3	2.836
	Tar Creek	Channel	-	0.000	3	1.576	-	0.000
		Floodplain	-	0.000	8	0.267	-	0.000
	Spring	Channel	-	0.000	-	0.000	-	0.000
		Floodplain	-	0.000	-	0.000	-	0.000
	Elk	Channel	-	0.000	-	0.000	-	0.000
		Floodplain	-	0.000	-	0.000	-	0.000
Dam WSE			4	0.965	6	0.828	4	2.087

4.4.3 Specific Sensitivity Analyses

Determining the sensitivity of results to changes in Manning's *n*

The Manning's n, being a lumped parameter for various physical phenomena in the system, is a user-defined parameter. The global sensitivity analysis determined that the model is significantly sensitive to this user-defined parameter along the Neosho River channel and floodplain. For this reason, a secondary sensitivity analysis is necessary to determine how sensitive the conclusions of the research are to changes in Manning's n.

This second phase of the sensitivity analysis involves varying the Manning's n in only the Priority 1 section, and then applying the research question to the modified scenarios in order to determine the sensitivity of the research conclusions to the changing parameters. The following tables represent the results of changing the Neosho River channel and floodplain Manning's n values across the typical ranges outlined in Chow (2009). Due to the fact that HEC-RAS outputs WSEs accurate to the hundredths decimal place, the values in the following tables have been rounded to the hundredths decimal place as well, in order to maintain consistency. The "Base" scenario in each table represents the final calibrated Manning's n values from Section 4.3.1.

Tables 4.16, 4.17, and 4.18 represent the research conclusions' sensitivity to the roughness value in the Neosho River *channel*. The Manning's n along the channel is varied (in quartiles) between 0.025 and 0.10, while the rest of the model remains the same as the base geometry. Table 4.16 represents the average difference between the WSEs calculated in the Priority 1 section when changing the boundary condition at the dam from a WSE of 741 to 743 ft PD. The values in Table 4.17 represent the maximum difference along the Priority 1 section for the same scenarios. Table 4.18 shows the maximum WSE calculated in the Priority 1 section when the boundary

condition at the dam is a WSE of 743 ft PD. This table is included to understand at what flow and roughness scenario the WSE begins to exceed flood stage (760.33 ft NAVD88) in the Miami area [NOAA, 2013]. In each table, the grey-colored cell values represent conditions at which the max WSE exceeds flood stage (i.e., the USACE easements).

Table 4.16. Sensitivity analysis of changes in Manning's n in Neosho River channel. Average change in WSE (ft) in Priority 1 section due to changing dam WSE from 741 to 743 ft PD shown. Shaded cells represent conditions for which the flooding easements are exceeded in Miami.

Roughness	Channel	Flood-Frequency (yrs)						
Scenario	Mannings n	2	10	25	50	100	200	500
Base	0.03	1.76	0.15	0.04	0.03	0.02	0.00	0.01
Holly	0.035	1.65	0.14	0.06	0.04	0.02	0.03	0.03
lowest	0.025	1.76	0.15	0.04	0.03	0.02	0.00	0.01
25%	0.04375	1.82	0.22	0.05	0.03	0.02	0.01	0.01
50%	0.0625	1.56	0.03	0.02	0.02	0.01	0.00	0.01
75%	0.08125	1.31	0.03	0.02	0.01	0.01	0.00	0.01
highest	0.10	0.90	0.02	0.01	0.01	0.01	0.00	0.01

Table 4.17. Sensitivity analysis of changes in Manning's n in Neosho River channel. Maximum change in WSE (ft) in Priority 1 section due to changing dam WSE from 741 to 743 ft PD shown. Shaded cells represent conditions for which the flooding easements are exceeded in Miami.

Roughness	Channel	Flood-Frequency (yrs)						
Scenario	Mannings n	2	10	25	50	100	200	500
Base	0.03	1.83	0.20	0.05	0.03	0.03	0.01	0.02
Holly	0.035	1.76	0.19	0.07	0.05	0.04	0.04	0.04
lowest	0.025	1.83	0.20	0.05	0.03	0.03	0.01	0.02
25%	0.04375	1.88	0.28	0.10	0.04	0.03	0.01	0.02
50%	0.0625	1.70	0.05	0.04	0.03	0.02	0.01	0.02
75%	0.08125	1.50	0.06	0.02	0.02	0.02	0.01	0.01
highest	0.10	1.10	0.03	0.02	0.01	0.01	0.01	0.01

Table 4.18. Sensitivity analysis of changes in Manning's n in Neosho River channel. Highest calculated WSE (ft NAVD88) in Priority 1 section due to dam WSE of 743 ft PD shown. Shaded cells represent conditions for which the flooding easements are exceeded in Miami.

Roughness Scenario	Flood-Frequency (yrs) 2	10	25	50	100	200	500
Base	746.24	757.26	763.27	767.79	772.30	776.00	781.18
Holly	746.55	758.84	765.94	771.23	776.40	781.50	788.62
lowest	746.24	757.26	763.27	767.79	772.30	776.00	781.18
25%	746.07	756.18	762.54	767.26	772.04	776.04	781.27
50%	746.80	759.16	764.70	768.85	773.01	776.24	781.33
75%	747.70	760.69	765.91	769.80	773.56	776.79	781.70
highest	749.57	762.28	767.18	770.83	774.30	777.67	782.54

Tables 4.19, 4.20, and 4.21 represent the research question's sensitivity to the roughness value in the Neosho River *floodplain*. The Manning's n along the floodplain is varied (in quartiles) between 0.025 and 0.20 while the rest of the model remains the same as the calibrated Manning's n values from Section 4.3.1. The tables are similar to, and follow the same order as, those listed above.

Table 4.19. Sensitivity analysis of changes in Manning's n in Neosho River floodplain. Average change in WSE (ft) in Priority 1 section due to changing dam WSE from 741 to 743 ft PD shown. Shaded cells represent conditions for which the flooding easements are exceeded in Miami.

Roughness Scenario	Floodplain Mannings n	Flood-Frequency (yrs) 2	10	25	50	100	200	500
Base	0.013-0.08	1.76	0.15	0.04	0.03	0.02	0.00	0.01
Holly	0.10	1.65	0.14	0.06	0.04	0.02	0.03	0.03
lowest	0.025	1.76	0.12	0.04	0.03	0.01	0.01	0.01
25%	0.06875	1.76	0.16	0.04	0.03	0.01	0.02	0.01
50%	0.1125	1.76	0.18	0.04	0.00	0.01	0.01	0.01
75%	0.15625	1.76	0.18	0.05	0.06	0.00	0.01	0.01
highest	0.20	1.76	0.18	0.05	0.03	0.01	0.01	0.01

This sensitivity analysis provides confidence in the results of the model application by demonstrating that within the entire range of plausible Manning's n values, the results of the proposed rule curve adjustment would not raise WSEs above flood stage more than 0.07 ft, as shown in the shaded cells in the tables. In model applications

Table 4.20. Sensitivity analysis of changes in Manning's n in Neosho River floodplain. Maximum change in WSE (ft) in Priority 1 section due to changing dam WSE from 741 to 743 ft PD shown. Shaded cells represent conditions for which the flooding easements are exceeded in Miami.

Roughness Scenario	Floodplain Mannings n	Flood-Frequency (yrs) 2	10	25	50	100	200	500
Base	0.013-0.08	1.83	0.20	0.05	0.03	0.03	0.01	0.02
Holly	0.10	1.76	0.19	0.07	0.05	0.04	0.04	0.04
lowest	0.025	1.83	0.17	0.05	0.04	0.01	0.02	0.02
25%	0.06875	1.83	0.21	0.06	0.03	0.02	0.03	0.02
50%	0.1125	1.83	0.23	0.06	0.01	0.02	0.01	0.01
75%	0.15625	1.83	0.23	0.06	0.07	0.00	0.01	0.01
highest	0.20	1.83	0.24	0.06	0.04	0.02	0.01	0.01

Table 4.21. Sensitivity analysis of changes in Manning's n in Neosho River floodplain. Highest calculated WSE (ft NAVD88) in Priority 1 section due to dam WSE of 743 ft PD shown. Shaded cells represent conditions for which the flooding easements are exceeded in Miami.

Roughness Scenario	Flood-Frequency (yrs) 2	10	25	50	100	200	500
Base	746.24	757.26	763.27	767.79	772.30	776.00	781.18
Holly	746.55	758.84	765.94	771.23	776.40	781.50	788.62
lowest	746.24	756.79	761.63	765.44	769.32	773.33	777.74
25%	746.24	757.37	763.92	768.97	774.10	778.18	784.29
50%	746.24	757.55	764.86	770.60	776.17	781.07	788.16
75%	746.24	757.64	765.36	771.53	777.31	783.00	790.45
highest	746.24	757.68	765.68	772.12	778.15	784.22	792.22

using lumped parameters such as Manning's n, there can be considerable debate over the "correct" value of Manning's n to use for a certain application, but this sensitivity study preempts such debate, because the flood elevations are relatively insulated from ranges of Manning's n found in practice.

Determining the sensitivity of results to WSEs at the dam exceeding 743 ft PD

Table 4.22 shows the results of the Riverware study completed by the USACE mentioned in Section 3.4.3 [Daylor, 2012]. The percentage of time in one year that a specific dam WSE is exceeded under each rule curve is shown in the table, along with

a conversion of that percentage into number of days. Note that the WSEs both above and below the target elevations are included, accounting for both flood and drought scenarios.

Table 4.22. Results of the USACE Riverware analysis [Daylor, 2012].

Percent of Time Lake Elevation is Equalled or Exceeded				
Elevation (ft PD)	Existing Rule Curve	Typical Year No. of Days	Proposed Rule Curve	Typical Year No. of Days
755.00	0.000%	<1	0.000%	<1
754.86	0.004%	<1	0.004%	<1
750.00	2.03%	7	2.05%	7
748.00	3.9%	14	3.9%	14
746.00	7.8%	29	7.9%	29
745.00	12.7%	46	13.0%	47
744.50	15.9%	58	16.3%	60
744.00	20.4%	75	20.8%	76
743.00	39.4%	144	41.3%	151
742.77	41.6%	152	50.0%	182.5
742.50	44.1%	161	53.0%	193
742.18	50.0%	182.5	60.1%	219
742.00	78.2%	285	96.3%	352
741.71	81.6%	298	100%	365
741.50	83.4%	304		
741.00	96.6%	353		
740.25	100%	365		

Table 4.23 shows the value of the difference (proposed minus existing) of the percent time the lake elevation is equaled or exceeded, along with the difference in the typical number of days per year the particular lake elevations is exceeded. This table helps to prioritize the dam WSE situations requiring further investigation for determining the effect of the proposed rule curve adjustment.

Steady-state high-dam analysis

In Table 4.23, it is apparent that dam WSEs 744, 744.5, and 745 require further investigation, because the proposed rule curve causes the dam WSE to be exceeded for at least one additional day per year. Dam WSEs of 746 and 750 are exceeded under

Table 4.23. Continued results of the USACE Riverware analysis.

Differences Between Existing and Proposed Rule Curves		
Elevation (ft PD)	Difference % Time Exceeded	Difference Typ. No. of Days
755.00	0.00%	0
754.86	0.00%	0
750.00	0.02%	0
748.00	0.00%	0
746.00	0.10%	0
745.00	0.30%	1
744.50	0.40%	2
744.00	0.40%	1
743.00	1.90%	7
742.77	8.40%	31
742.50	8.90%	32
742.18	10.10%	37
742.00	18.10%	67
741.71	18.40%	67
741.50	16.60%	61
741.00	3.40%	12
740.25	0.00%	0

the proposed rule curve 0.10% and 0.02% more often, respectively. These dam WSEs will be investigated using the 0.01%, 0.05%, and 0.02% probability streamflows (100-, 200-, and 500-yr flood-frequencies, respectively) in order to investigate the behavior of the system under extreme streamflows, which would feasibly cause the dam to rise to the 746 and 750 ft PD levels.

For each of these scenarios, the existing rule curve will be represented by a dam WSE 2 ft lower than the high-dam WSEs tested, because the existing rule curve is initially 2 ft below the proposed rule curve for the August 15 - September 15 time period. It would be impossible to predict the exact behavior of the stage vs. time hydrograph at the dam under the respective rule curves because the dam WSE is not controlled solely by meteorologic phenomenon, but by human intervention in the form of dam releases. The dam WSEs of 741 to 745 ft PD are controlled by GRDA, and WSEs of 745 to 755 ft PD are controlled by the USACE [GRDA, 2013]. However,

because of the geometry of Grand Lake, the stage vs. storage curve is of a shape that confirms a peak difference of 2 ft is conservative for maximizing the perceived effect of a raised rule curve. A proof that this assumption is physically reasonable may be found in Appendix D.

Table 4.24. Maximum WSE calculated in Priority 1 location for various high-dam conditions under the proposed rule curve conditions.

Dam WSE (ft PD)	Flood-Frequency (yrs) 2	10	25	50	100	200	500
744	747.13	757.34	763.29	767.81	772.31	776.01	781.19
744.5	747.58	757.38	763.30	767.82	772.32	776.01	781.19
745	748.03	757.43	763.32	767.83	772.32	776.01	781.20
746	748.97	757.54	763.36	767.86	772.34	776.02	781.21
750	752.86	758.26	763.66	768.03	772.47	776.07	781.26

Table 4.25. Maximum WSE difference between proposed and existing scenarios in Priority 1 location for various high-dam conditions. Note that existing rule curve WSEs are assumed to be exactly 2 ft lower in elevation at the dam.

Proposed Rule Curve Dam WSE (ft PD)	Flood-Frequency (yrs) 2	10	25	50	100	200	500
744	1.88	0.24	0.07	0.05	0.03	0.02	0.02
744.5	1.89	0.27	0.08	0.07	0.04	0.02	0.02
745	1.91	0.29	0.09	0.05	0.04	0.03	0.02
746	1.93	0.36	0.11	0.07	0.05	0.03	0.03
750	1.98	0.66	0.29	0.12	0.15	0.06	0.05

The results of the high-dam-WSE analysis, shown in Table 4.24, reveal that there is very little difference in upstream WSEs for the various dam conditions, particularly between dam WSEs 744 and 746 ft PD. In the event that the WSE at the dam rises a full 6 feet from the target WSE, the proposed rule curve adjustment causes a maximum of 0.15 ft difference for the 100-year flood in the Priority 1 section. An analysis of the 100-year flood reveals that the Abandoned Bridge in Miami is at overtopping stage for this streamflow condition, which likely contributes to the larger increase in backwater effect.

Table 4.26. Average WSE difference between proposed and existing scenarios in Priority 1 location for various high-dam conditions. Note that existing rule curve WSEs are assumed to be exactly 2 ft lower in elevation at the dam.

Proposed Rule Curve Dam WSE (ft PD)	Flood-Frequency (yrs)						
	2	10	25	50	100	200	500
744	1.82	0.18	0.05	0.04	0.02	0.01	0.01
744.5	1.84	0.20	0.06	0.05	0.03	0.01	0.02
745	1.86	0.23	0.07	0.04	0.03	0.02	0.02
746	1.89	0.27	0.09	0.06	0.03	0.01	0.02
750	1.98	0.53	0.24	0.10	0.10	0.04	0.04

Unsteady-flow high-dam analysis

A hypothetical unsteady-flow scenario was created in order to compare the results of the September 2009 flood used in the calibration process to the results of the same flood with WSEs at the dam 2 ft higher than the observed data. It is important to note that this hypothetical scenario is not meant to be a realistic representation of the expected conditions during the 2009 flood had the proposed rule curve been in effect at that time. However, this hypothetical scenario is used for the purpose of demonstrating that a two foot increase in WSE at the dam causes a similar effect in both unsteady and steady-state analyses.

According to the statistical analysis results, the September 2009 flood peak flow falls between the 10- and 25-year August 15 - September 15 flow magnitude. The peak observed WSE at the dam during this event was 746.84 ft PD, or 748.24 ft NAVD88. Therefore, under the hypothetical scenario, the peak WSE at the dam was 748.84 ft PD, or 750.24 ft NAVD88. The peak modeled WSE at the location of Riverview Park in Miami under the hypothetical scenario is 758.79 ft NAVD88, compared to the peak WSE in the calibrated model scenario of 758.55 ft NAVD88. This difference of 0.24 ft is consistent with the results found in the steady-state analysis shown in Table 4.26.

Fitting a polynomial to the daily-average data from Pensacola Dam

As mentioned in Section 3.4.3, a polynomial was fit to the daily-average dam WSE data for the September 2009 flood in order to determine whether the results of the model application are significantly different when using a finer time-increment at the dam location. The NSC efficiency value comparing the results from the model using the daily-average dam data to the 3 hr time-increment dam data is 0.99995 for the full 68-day time period, and 0.99998 for the peak event occurring between 9/8 - 9/16. These results show that using the finer time-increment dataset at the location of Pensacola dam has virtually no effect on the behavior of the WSE profile upstream, compared to the daily-average dataset. These conclusions suggest that using a stage vs. time hydrograph at a cross-section as the downstream boundary condition for the hydraulic model is a viable alternative to using an inline-structure approach to model time-varied effects at the dam.

Determining the sensitivity of results to the effect of structures constricting streamflow along the Neosho River

As discussed in Section 3.4.3, investigation of the structures constricting flow along the Neosho River is warranted by the Daylor (2012) study that hypothesized the structures cause an increase in WSEs near Miami. Furthermore, as discussed in Section 4.3.3, the simulations of this thesis show that the bridges constrict the flow at higher return periods.

Table 4.27 contains the results of the analysis of the effect of structures on WSEs in the priority 1 section. The maximum WSE and average WSE for each model scenario in the priority section are shown. The max WSE represents the highest calculated WSE in the priority section for the model scenario. The average WSE represents the mean of the WSEs calculated at each cross section.

The downstream dam WSE condition is 743 ft PD, and all return-period streamflows are shown. The structures that were taken out of the model were the Highway 10/69 bridge in Miami, the B&N Rail bridge in Miami, the Highway 125 bridge in Miami, the low-water dam at Riverview Park in Miami, the Abandoned bridge in Miami, the I-44 bridges in Miami, the Fairland County road bridge near Fairland, the Highway 60 bridge near Twin Bridges, the B&N rail bridge near Twin Bridges, and Sailboat Bridge near Monkey Island. The first six structures listed are in very close proximity to Miami, as shown in Figure 4.36.

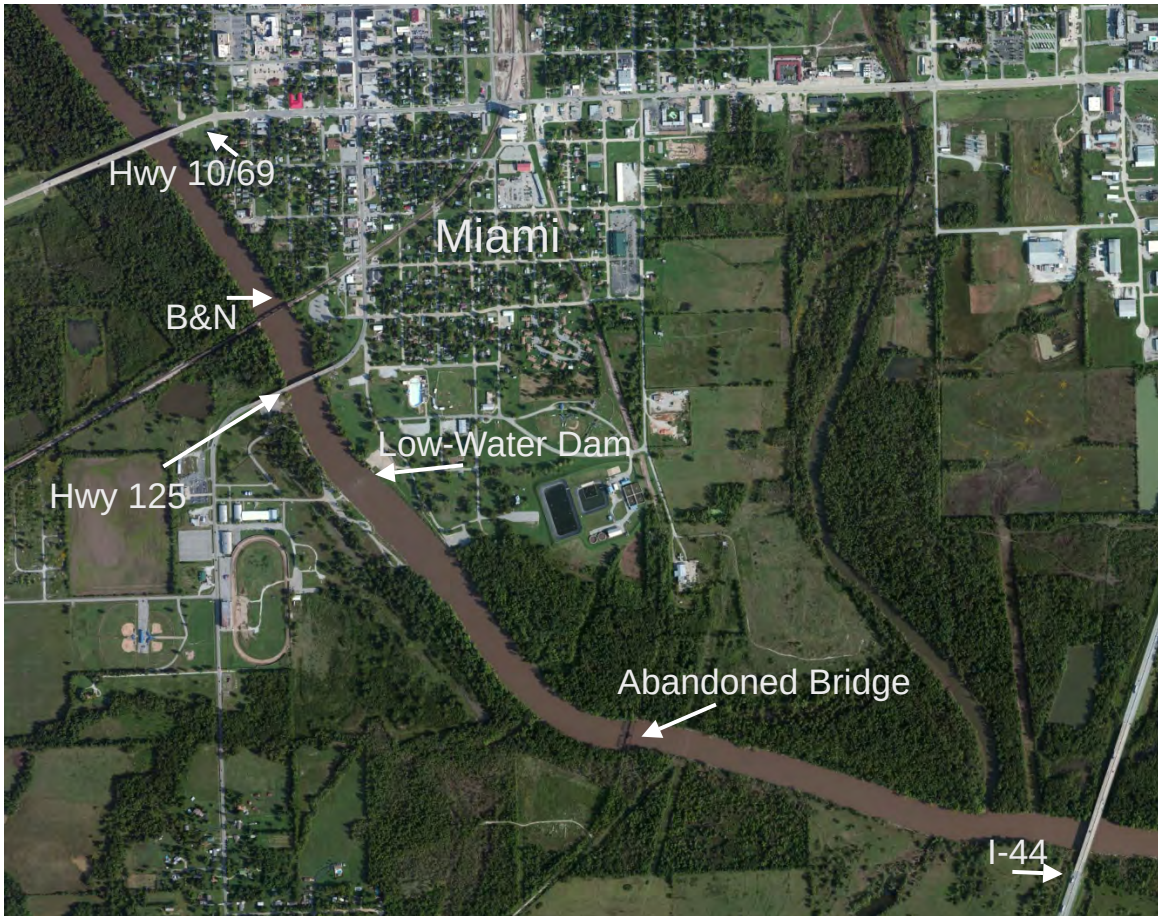

Figure 4.36. Structures over the Neosho River in close proximity to Miami, OK.

Interestingly, the effect of the bridges dips from the 2-year to the 10-year return period flows. This may be due to the higher sensitivity of the smaller streamflow

Table 4.27. Analysis of effect of bridges on upstream WSEs in the priority 1 section.

Scenario		Flood-Frequency (yrs) 2	10	25	50	100	200	500
With Bridges	Avg	746.03	756.07	762.08	766.69	771.22	775.12	780.59
	Max	746.24	757.26	763.27	767.79	772.30	776.00	781.18
No Bridges	Avg	745.03	755.67	761.59	765.77	769.80	773.70	779.14
	Max	745.26	756.85	762.72	766.76	770.59	774.33	779.56
Difference	Avg	1.00	0.40	0.49	0.92	1.42	1.42	1.45
	Max	0.98	0.41	0.55	1.03	1.71	1.67	1.62

magnitude to the bridge piers constricting flow in the channel. The 10-year flow, being more intense, but not overflowing the river banks, is affected by the bridge piers, is not as sensitive to the obstruction in the river channel. As the flow magnitude increases beyond the 10-year flow, however, the bridge embankments in the floodplain begin to influence the WSEs as well as the bridge piers in the river channel.

The results shown in Table 4.27 reveal that the bridges have a significantly greater effect on the WSEs in the priority 1 section than the proposed rule curve adjustment. These results would corroborate the findings that the proposed rule curve has a minimal effect on backwater WSEs. Because the structures create increased backwater effects at a location between the dam and the priority location, they are acting as an intermediate boundary condition, reducing the effect of the boundary condition at the dam [Bedient et al., 2013]. The results of this sensitivity analysis provide an explanation of the decreased effect of the proposed rule curve adjustment on WSEs near Miami.

The results confirm the bridges constrict the flow and create a greater difference in WSE than raising the water level at the dam 2 feet. For future research, a study should systematically remove one bridge at a time (while all the others remain) and rate the relative impact of the different bridges. Also for future research, a study should look at what flow each bridge constricts the flow enough that the upstream WSE is significantly changed.

CHAPTER 5

Conclusions and Future Research

5.1 Conclusions

A hydraulic model of the Grand Lake hydrologic system was developed for the purpose of analyzing the impact on upstream WSEs of a proposed rule curve adjustment at Pensacola Dam in Langley, Oklahoma. The model was developed with the HEC-RAS hydraulic model, and it was calibrated and validated using the unsteady flow routing capabilities of that program [Brunner, 2010]. The model geometry was developed in ArcGIS using the most advanced datasets for the region [ESRI, 2011; Gesch, 2007; OWRB, 2009]. The GIS model geometry was exported to HEC-RAS using the HEC-GeoRAS tool.

A statistical analysis was conducted of the historic August 15 to September 15 streamflow records for each of the four major tributaries. Annual maxima and partial duration data collection methods were compared. The annual maxima method was determined to be the most conservative method. The final statistical analysis was performed with annual maxima data according to the guidelines in Bulletin 17B of the U.S. Water Resources Council [USGS, 1982]. Return-period streamflows were calculated for each of the following streams: the Neosho River, Spring River, Elk River, and Tar Creek. These extreme streamflows were used as upstream boundary conditions for the hydraulic model. The USGS gauge locations at which the streamflow records were recorded were used as the upstream boundary locations on each tributary.

The downstream boundary condition for the steady-state hydraulic model was a known WSE representing the lake level at Pensacola Dam. In order to determine the upstream effect of the proposed rule curve adjustment, the downstream WSE was alternated between 742.4 ft NAVD88 (741 ft PD, the existing rule curve target WSE for the relevant time period) and 744.4 ft NAVD88 (743 ft PD, the proposed rule curve target WSE for the relevant time period).

According to the tests performed in this research, an increase in streamflow magnitude causes an increase in upstream WSEs, but the impact of the proposed rule curve adjustment on upstream WSEs decreases. The location of Riverview Park in Miami, OK is considered the first to flood by the National Weather Service [NOAA, 2013]. The impact of the proposed rule curve adjustment on this location is less than 0.20 ft for all of the scenarios investigated in this thesis research.

An investigation into effects of dam WSEs exceeding the target WSE due to the proposed rule curve was also conducted. The dam WSEs that are more likely to be exceeded due to the proposed rule curve were provided in a study from the USACE [Daylor, 2012]. These higher dam WSEs were investigated based on a difference in WSE at the dam of 2.0 ft between the proposed and existing rule curves. The proposed rule curve causes a maximum of 0.15 ft increase in WSEs in the Priority 1 location for the full range of flow scenarios and dam WSE scenarios tested. Thus, even with rarely seen WSEs at the dam, the two foot WSE difference at the dam causes much smaller changes at upstream priority locations.

A sensitivity analysis was performed to test the model sensitivity to changes in the hydraulic roughness parameter, Manning's n. The maximum increase in WSEs over flood-stage due to the proposed rule curve adjustment in the Priority 1 section, for all flow scenarios and Manning's n scenarios, was 0.07 ft. This sensitivity analysis provides confidence in the conclusion that the two foot WSE increase at the dam has minimal effect on the upstream WSEs in priority locations.

These results are consistent with conclusions of previous research by Holly (2004) that found that the raising the power pool from 741 to 745 ft PD causes less than a 0.20 ft increase on WSEs near Miami, OK. USACE (1998) also determined that the highest possible dam elevation of 755 ft PD has less than a 0.50 ft effect on depth in the locations named "Priority 1" in this research.

In conclusion, the effect of the proposed rule curve adjustment has been shown to have less than a 0.20 ft effect on WSEs in priority locations near Miami, OK.

5.2 Future Work

1. The hydraulic model developed for this thesis was created with the best available software and best available datasets at the time it was completed in 2014. More advanced data collection techniques will inevitably allow for improvement of the model geometry, and advances in computer modeling will inevitably lead to more accurate modeling capabilities in the future. Despite these advances, it is likely that the improved technology will serve to confirm the conclusions reached in this research as well as the prior research conducted by Holly (2004) and the USACE (1998).

2. Channel bathymetry datasets have significant room for improvement on the Neosho, Spring, and Elk Rivers. The most recent datasets were collected over 15 years ago using manual survey techniques. The level of sophistication of bathymetric surveying has improved dramatically since that time, as evidenced by the OWRB (2009) study included in this report. An updated bathymetric survey of these locations should be considered.

3. A two-dimensional unsteady hydraulic model may be more feasible with the release of HEC-RAS 5.0, a USACE software currently in "beta" form (i.e., not released for public use). This 2D capability may allow for more accurate

portrayals of the reservoir storage capacity for Grand Lake and upstream floodplains. An unsteady flow model depicting the reservoir and floodplains with a stage/storage relationship would be possible if this were the case. This type of model would allow for investigation of the lag time required to change the reservoir stage due to dam outflows and flood water inflows from upstream tributaries, and the effect that this lag time has on upstream water levels. A pseudo-2D unsteady flow model was used in the Holly (2004) research to portray the floodplain upstream of Miami, but this method has not been used to represent the Grand Lake reservoir. Future research could potentially use HEC-RAS 5.0 to include this approach to modeling the Grand Lake reservoir and floodplains along the tributaries.

4. There is a wide variety of data sources covering the Grand Lake region. These data should be organized, normalized, and confirmed. One example is the stage-storage relationship of the reservoir. The OWRB (2009) report concludes that the storage capacity of Grand Lake is 1,515,415 acre-ft when the dam WSE is 745 ft PD. The National Water Information System website for the Pensacola Dam gauge reports that the storage is 1,672,000 acre-ft at a dam WSE of 745 ft PD [USGS, 2012]. The true value of the stage-storage relationship should be determined so that stream inflow and dam outflow may be managed accurately. This report provides a large amount of organization and normalization of the Grand Lake data, and the TIN created for this research may be used with the HYPACK program that OWRB used to create the stage vs. storage curve in the 2009 report [OWRB, 2009]. The merged-TIN may be used in HYPACK to develop an updated stage vs. storage curve that extends all the way to the top of the flood pool (755 ft PD) at Pensacola Dam.

5. Future investigation of the effect of bridges in the Miami area is warranted by the results of this thesis, as mentioned in Section 4.4.3. The nine structures in the vicinity of Miami have been shown to have a significant effect on WSEs in the priority locations. Detailed investigations of the effect of particular bridges is a possibility for future research into the cause of higher WSEs in the priority locations.

6. An investigation into the effect of the reduced hydraulic roughness upstream of Miami due to agricultural development is another topic requiring future research. The wide floodplain of previously forested area upstream of Miami has been developed into agricultural land, likely reducing the ability of that area to detain floodwaters during an extreme-streamflow event. The global sensitivity analysis conducted for this research (Section 4.4.2) suggests that the floodplain hydraulic roughness value has an effect on WSEs in the priority locations. Research should be conducted investigating the effect of the agricultural development upstream of Miami on WSEs in Miami during extreme streamflow events occurring on the Neosho River.

7. The results contained in this thesis represent the effect of the current proposed rule curve modification, which affects the time period from August 15-September 15 in any given year. Therefore, the statistical return period streamflows contained herein represent the August 15-September 15 time frame. In the event that future rule curve modifications are proposed for other months of the year, more research will be required in order to determine return period streamflows for those portions of the year, and the model will require further calibration in order to represent roughness conditions for the new scenario.

References

Ackerman, C. T. *HEC-GeoRAS User's Manual*. U.S. Army Corps of Engineers, Davis, CA, September 2009.

Adamowski, K. Regional Analysis of Annual Maximum and Partial Duration Flood Data by Nonparametric and L-moment Methods. *Journal of Hydrology*, 229(3–4):219 – 231, 2000. ISSN 0022-1694. URL http://www.sciencedirect.com/science/article/pii/S0022169400001566.

Arcement Jr., G. and Schneider, V. Guide for Selecting Manning's Roughness Coefficient For Natural Channels and Flood Plains. *Hydraulics Engineering Publications*, 1984.

Ashkar, F. and Ouarda, T. On some methods of fitting the generalized Pareto distribution. *Journal of Hydrology*, 177(1):117–141, 03 1996.

Awawdeh, M. M. GIS-Based Evaluation of the Conservation Reserve Program in Texas County, Oklahoma. Master's thesis, Oklahoma State University, 05 2004.

Bedient, P. B., Huber, W. C., and Vieux, B. E. *Hydrology and Floodplain Analysis*. Pearson Education, Inc., 5 edition, 2013.

Brunner, G. *HEC-RAS River Analysis Systems User's Manual: Version 4.1*. USACE, January 2010.

Buckley, M. K. Memo on Policy for Use of HEC-RAS in the NFIP. Technical report, Federal Emergency Management Agency, Washington DC, April 2001.

Chow, T. *Open-Channel Hydraulics*. McGraw-Hill civil engineering series. Blackburn Press, 2009. ISBN 9781932846188. URL http://books.google.com.et/books?id=JG9_PwAACAAJ.

Cunnane, C. A Particular Comparison of Annual Maxima and Partial Duration Series Methods of Flood Frequency Prediction. *Journal of Hydrology*, 18(3–4):257 – 271, 1973. ISSN 0022-1694. URL http://www.sciencedirect.com/science/article/pii/0022169473900516.

Daylor, J. RiverWare Simulations for Proposed Change with Seasonal Pool Guide Curve. Technical report, USACE, 2012.

Efron, B. and Tibshirani, R. Bootstrap Methods for Standard Errors, Confidence Intervals, and Other Measures of Statistical Accuracy. *Statistical Science*, 1(1):pp. 54–75, 1986. ISSN 08834237. URL http://www.jstor.org/stable/2245500.

Ekanayake, S. and Cruise, J. Comparisons of Weibull- and exponential-based partial duration stochastic flood models. *Stochastic Hydrology and Hydraulics*, 7(4):283–297, 1993. ISSN 0931-1955. URL http://dx.doi.org/10.1007/BF01581616.

England Jr, J. F. and Cohn, T. A. Scientific and Practical Considerations Related to Revising Bulletin 17B: The case for improved treatment of historical information and low outliers. 2007.

ESRI. ArcGIS Desktop: Release 10, 2011.

Farmer, W. and Vogel, R. Performance-Weighted Methods for Estimating Monthly Streamflow at Ungauged Sites. *Journal of Hydrology*, 477(0):240 – 250, 2013. ISSN 0022-1694. URL http://www.sciencedirect.com/science/article/pii/S0022169412010116.

FEMA. Flood Zones: NFIP Policy Index. URL http://www.fema.gov/national-flood-insurance-program-2/flood-zones, 2012.

Flynn, K. M., Kirby, W. H., and Hummel, P. R. *User's Manual for Program PeakFQ, Annual Flood-Frequency Analysis Using Bulletin 17B Guidelines*. U.S. Geological Survey, 03 2014.

Gesch, D. The National Elevation Dataset: Digital Elevation Model Technologies and Applications: The DEM Users Manual, 2nd Edition. *American Society for Photogrammetry and Remote Sensing*, pages 99–118, 2007.

GLWAF. Grand Lake Watershed Plan: For improving water quality throughout the Grand Lake watershed. URL http://www.ok.gov/conservation/documents/Grand_Lake_%20WBP_DRAFT.pdf, November 2008.

GRDA. Pensacola Project: Shoreline Management Plan. URL http://www.grda.com/wpcontent/uploads/2010/09/SMP-FINAL-FERC-w-Maps.pdf, June 2008.

GRDA. Lake Management: Flood Control. URL http://www.grda.com/lake-management/flood-control/, 2013.

Haghizadeh, A., Shui, L. T., Mirzaei, M., and Memarian, H. Incorporation of GIS Based Program into Hydraulic Model for Water Level Modeling on River Basin. *Journal of Water Resource & Protection*, 4(1), 2012.

Hirsch, R. M. Probability plotting position formulas for flood records with historical information. *Journal of Hydrology*, 96(1–4):185 – 199, 1987. ISSN 0022-1694. URL http://www.sciencedirect.com/science/article/pii/0022169487901521. Analysis of Extraordinary Flood Events.

Holly Jr., F. M., editor. *Referee Report: Dalrymple, et al v. GRDA*, number Case CJ 94-444, February 1999. District Court of Ottawa County, Oklahoma.

Holly Jr., F. Analysis of Effect of Grand Lake Power-Pool Elevations on Neosho River Levels During a Major flood. Prepared for: Robert Sullivan, AGM of Risk Management and Regulatory Compliance, GRDA, 2004.

Holly Jr., F. and Benoit-Guyod, C. Programme CARIMA - Users Manual. Technical report, SOGREAH, Grenoble, France, 1977.

Holway, W. Dams on the Grand River. URL http://digital.library.okstate.edu/Chronicles/v026/v026p329.pdf, 1948.

Hosking, J. L-Moments: Analysis and Estimation of Distributions Using Linear Combinations of Order Statistics. *Journal of the Royal Statistical Society. Series B (Methodological)*, 52(1):pp. 105–124, 1990. ISSN 00359246. URL http://www.jstor.org/stable/2345653.

Hosking, J. *L-moments*, 2014. URL http://CRAN.R-project.org/package=lmom. R package, version 2.4.

Hosking, J. and Wallis, J. Parameter and Quantile Estimation for the Generalized Pareto Distribution. *Technometrics*, 29(3):pp. 339–349, 1987. ISSN 00401706. URL http://www.jstor.org/stable/1269343.

Ilorme, F. and Griffis, V. W. A novel procedure for delineation of hydrologically homogeneous regions and the classification of sites for design flood estimation. *Journal of Hydrology*, 492(0):151 – 162, 2013. ISSN 0022-1694. URL http://www.sciencedirect.com/science/article/pii/S0022169413002692.

Knebl, M., Yang, Z.-L., Hutchison, K., and Maidment, D. Regional scale flood modeling using NEXRAD rainfall, GIS, and HEC-HMS/RAS: a case study for the San Antonio River Basin Summer 2002 storm event. *Journal of environmental management*, 75(4):325–336, 2005.

Lim, Y. and Voeller, D. Regional Flood Estimations in Red River Using L -Moment-Based Index-Flood and Bulletin 17B Procedures. *Journal of Hydrologic Engineering*, 14(9):1002–1016, 2009. URL http://dx.doi.org/10.1061/(ASCE)HE.1943-5584.0000102.

Makkonen, L., Pajari, M., and Tikanmäki, M. Closure to "Problems in the extreme value analysis". *Structural Safety*, (0):65 – 67. ISSN 0167-4730.

Manders, G. Mapping of the July 2007 Miami, Oklahoma Flood. Research project, Emporia State University, May 2009.

Merwade, V. Dr. Merwade's Website, 2014 2014. URL https://web.ics.purdue.edu/~vmerwade/research.html.

Merwade, V., Cook, A., and Coonrod, J. GIS techniques for creating river terrain models for hydrodynamic modeling and flood inundation mapping. *Environmental Modelling & Software*, 23(10):1300–1311, 2008.

Moriasi, D. N., Arnold, J. G., Van Liew, M. W., Bingner, R. L., Harmel, R. D., and Veith, T. L. Model Evaluation Guidelines for Systematic Quantification of Accuracy in Watershed Simulations. *Transactions of the ASABE*, 50(3):885–900, 2007.

Mujere, N. Flood Frequency Analysis Using the Gumbel Distribution. *International Journal on Computer Science & Engineering*, 3(7), 2011.

Nash, J. and Sutcliffe, J. River Flow Forecasting through Conceptual Models Part I — A Discussion of Principles. *Journal of Hydrology*, 10(3):282 – 290, 1970. ISSN 0022-1694. URL http://www.sciencedirect.com/science/article/pii/0022169470902556.

NOAA. *Hydrologic Information on the Web: A Manual for Users*. National Oceanic and Atmospheric Administration, National Weather Service, U.S. Department of Commerce, 1.2 edition, 04 2013.

OWRB. *Hydrographic Survey of Grand Lake*. OWRB, Oklahoma City, OK, August 2009.

Pham, H., Shamseldin, A., and Melville, B. Statistical Properties of Partial Duration Series and its Implication on Regional Frequency Analysis. *Journal of Hydrologic Engineering*, 2013. URL http://dx.doi.org/10.1061/(ASCE)HE.1943-5584.0000916.

Price, C. V., Nakagaki, N., Hitt, K. J., and Clawges, R. M. Enhanced Historical Land-Use and Land-Cover Data Sets of the U.S. Geological Survey: polygon format files. Digital Data Set, 04 2007.

R Core Team. *R: A Language and Environment for Statistical Computing*. R Foundation for Statistical Computing, Vienna, Austria, 2013. URL http://www.R-project.org/.

Ritter, A. and Muñoz-Carpena, R. Performance evaluation of hydrological models: Statistical significance for reducing subjectivity in goodness-of-fit assessments. *Journal of Hydrology*, 480(0):33 – 45, 2013. ISSN 0022-1694. URL http://www.sciencedirect.com/science/article/pii/S0022169412010608.

Santhi, C., Arnold, J. G., Williams, J. R., Dugas, W. A., Srinivasan, R., and Hauck, L. M. Validation of the Swat Model on a Large River Basin with Point and Nonpoint Sources. *JAWRA Journal of the American Water Resources Association*, (37):1169–1188, 2001.

Singh, V. P. On Application of the Weibull Distribution in Hydrology. *Water Resources Management*, 1(1):33–43, 1987. ISSN 0920-4741. URL http://dx.doi.org/10.1007/BF00421796.

Smith, J. S. Email correspondence including cross sections for Neosho River floodplain. USGS, 08 2013.

Strong, S. Email correspondence including USGS gauge station cross-section elevation data. USGS Hydrologic Technician, 02 2014.

USACE. Hydraulic Analysis: Grand Lake Real Estate Adequacy Study. Technical report, USACE, 1998.

USGS. *Guidelines for determining flood flow frequency, Bulletin 17-B of the Hydrology Subcommittee*. U.S. Interagency Advisory Committee on Water Data: U.S. Geological Survey, Office of Water Data Coordination, Reston, Virginia, 1982.

USGS. National Water Information System. URL http://waterdata.usgs.gov/nwis/, 2012.

USGS. About Vertical Datums. URL http://ok.water.usgs.gov/projects/webmap/miami/datum.htm, 2014.

Vogel, R. and Wilson, I. Probability Distribution of Annual Maximum, Mean, and Minimum Streamflows in the United States. *Journal of Hydrologic Engineering*, 1(2):69–76, 1996. URL http://ascelibrary.org/doi/abs/10.1061/%28ASCE%291084-0699%281996%291%3A2%2869%29.

Weibull, W. *A Statistical Theory of the Strength of Materials*. Ingeniörsvetenskapsakademiens handlingar. Generalstabens litografiska anstalts förlag, 1939. URL http://books.google.com/books?id=otVRAQAAIAAJ.

Wilks, D. *Statistical Methods in the Atmospheric Sciences*. Academic Press, 3 edition, 2011.

Wolfram Research, I. *Mathematica*. Wolfram Research, Inc., Champaign, Illinois, version 8.0 edition, 2010.

Wyckoff, R. Email correspondence including channel bathymetry data for Neosho River. USACE, 01 2014.

Yang, J., Townsend, R. D., and Daneshfar, B. Applying the HEC-RAS model and GIS techniques in river network floodplain delineation. *Canadian Journal of Civil Engineering*, 33(1):19–28, 2006.

Appendices

Appendix A: Example Sensitivity Analysis

Table 1. Forcing Scenarios Used for Sensitivity Analysis of Spring River Streamflow (Streamflow units: cfs)

River	**Reach**	**Bench**	**2-yr**	**10-yr**	**20-yr**	**50-yr**	**200-yr**	**500-yr**
Spring	Tributary	76210	2428	15420	31270	49830	113000	183300
Neosho	Bound to Tar	110800	110800	110800	110800	110800	110800	110800
Neosho	Tar to Spring	124410	124410	124410	124410	124410	124410	124410
Neosho	Spring to Elk	200620	126838	139830	155680	174240	237410	307710
Neosho	Elk to Dam	219600	145818	158810	174660	193220	256390	326690
Elk	Tributary	18980	18980	18980	18980	18980	18980	18980
Tar Creek	Tributary	13610	13610	13610	13610	13610	13610	13610
Dam Elev.	NAVD88 (ft)	743.9	743.9	743.9	743.9	743.9	743.9	743.9

Appendix B: Normalization Procedures

General Normalization Procedures

Before downloading any data to a blank map in ArcMap 10.1, the Data Frame Projection was set using: "View → Data Frame Properties → Coordinate System." For this research, "NAD 1983 StatePlane Oklahoma North FIPS 3501 (Meters)" was used. Chapter 5.2.

NED Topography Dataset

1. The NED dataset was downloaded in multiple sections. A specific procedure was used for converting the very large raster datasets into data that was a manageable size and useful for the creation of a TIN for the entire Grand Lake area.

    - First, the raster .img files were projected into the appropriate map projection using the "Project Raster" tool in ArcMap 10.1. The raster was projected to the data frame projection.
    - The projected raster files were then converted to point data using the "Raster To Points" tool in ArcMap. This resulted in many millions of elevation data points at equal 3 m spacing (3m is the horizontal resolution of the LiDAR data).
    - A TIN was created from these data points using the "Create TIN" tool in ArcMap.
    - The "Decimate TIN" tool was used to remove TIN nodes which were within the declared vertical accuracy of the original data (10 cm).

- The "TIN Node" tool was used to extract the nodes out of the TIN. This results in much smaller point datasets than the datasets that were created in the first step.
- Because the NED data had "false" data points in the location of the Grand Lake reservoir, these data points were deleted using a "Select By Location" query in ArcMap. The OWRB study area boundary was used as the target location for selecting points to delete using the "Delete Features" tool.

2. Once the NED dataset was normalized and ready for use, the OWRB lake bathymetry data was addressed.
   - The lake bathymetry was downloaded in the form of 5 ft contour lines and a point dataset collected from the acoustic doppler technology. These point data, however, had elevations in Imperial units relative to the Pensacola Datum (PD).
   - The elevation attribute ("POINT_Z") of each point and contour line was added to the Attribute Table of its respective feature class using the "Add XY Coordinates" tool in ArcMap.
   - Using "Add Field" and "Field Calculator," the elevations were converted to SI units relative to the NAVD88 vertical datum.
   - Using the converted elevations in the point dataset as "mass points" and contour lines as "soft lines," a TIN was created for the lake bathymetry.
   - This TIN was decimated to remove redundant nodes which were outside of the 16 cm accuracy of the original dataset and the nodes were extracted from that TIN using the "TIN Node" tool.

3. With the topographic point datasets and the bathymetry point dataset normalized to SI units and the NAVD88 datum, they were able to be merged into a single dataset using the "Merge" tool in ArcMap.

4. The merged point data file along with the contour lines from the OWRB study were input into the "Create TIN" tool to create a TIN which represents the entire Grand Lake region, which will be referred to as the "Grand TIN".

5. The Grand TIN was decimated again in order to remove redundant points along the intersection of the raster data sections and the lake dataset.

6. The point elevation data was then converted to Imperial Units relative to the NAVD88 datum using the "Add XY Coordinates," "Add Field," and "Field Calculator" tools.

7. The converted point data and corresponding converted contour lines for the lake were then used as inputs to create a new Grand TIN with Imperial units.

Neosho River Bathymetry Cross Sections

The channel data from USACE were added to the map in the form of 3D polylines. The cross section locations were delivered as a shapefile from USACE, but this shapefile did not contain 3D polylines, only 2D locations. A complicated procedure was followed to draw 3D polylines with the correct elevations:

1. Using the "Create Feature Class" tool, a polyline feature class (henceforth referred to as XSProfiles) was created with "Z" and "M" enabled. Z being enable allows for the polyline to be 3D. M being enabled allows for the creation of "measures" along the length of the polyline.

2. Editing was enabled using the "Editor" toolbar and choosing "Start Editing $\rightarrow$ XSProfiles"

3. With the 2D cross section locations polyline visible on the map, "Create Features" was chosen on the editor toolbar and "XSProfiles" selected as the feature class within which to create features.

4. To create features within the XSProfiles feature class in the exact location of the existing 2D polyline locations, each line is right-clicked and "Replace Sketch" selected while creating features. One more right-click and "Finish Sketch" forms a 3D polyline within the XSProfiles feature class in the same location as the 2D lines downloaded from USACE.

5. With editing still enabled, but the normal "Editor" cursor engaged instead of the "Create Features" cursor, each polyline within the XSProfiles feature class was right-clicked, and "Edit Vertices" selected.

6. While editing vertices, the line was right-clicked again, and "Route Measure Editing→Set As Distance→Starting M: 0.00" chosen. This adds measures along the line starting at the LOB at zero, and continuing over the channel to the ROB.

7. In order to extract elevations for the XSProfiles from the Grand TIN, the "Interpolate Shape" tool was used with Grand TIN as the input surface and XSProfiles and the input feature class. Linear interpolation was used to extract the elevations.

8. Now that the XSProfiles contained measures and elevations, they could be matched with the corresponding cross section station/elevation coordinates for each cross section received in the form of a HEC-RAS geometry file from USACE.

9. After extracting the HEC-RAS cross section data to a spreadsheet, the station/elevation data for the XSProfiles was extracted to the same spreadsheet

using the "3D Analyst" toolbar in ArcMap. Using the "Select" tool, each XSProfile line was selected, then the "Profile Graph" button used to display a station/elevation graph. Right-clicking this graph and choosing "Export → Data → Save..." allowed for saving the station/elevation data to a .txt file, which was then extracted to the spreadsheet. The surveyed station/elevation data for the USACE cross sections was much more coarse than the LiDAR data extracted from the XSProfiles, but the general shape matched well for each cross section. The XSProfiles did not have bathymetry data for the channel, rather a horizontal plane representing the water surface at the time of the LiDAR data collection. The points within the channel needed to be added to the XSProfiles manually in ArcMap via the following procedure:

(a) First, the channel station/elevation coordinates were isolated using the spreadsheet.

(b) Each cross section was then selected in edit-mode, and edit vertices was initialized.

(c) Using the "Edit Sketch Properties" window, the (X,Y,Z,M) coordinates of each vertex was visualized, and the existing vertices within the river channel were deleted by right-clicking and selecting "Delete Vertex".

(d) Then, after right clicking on the line, "Route Measure Editing → Insert Vertex at M" was used to enter the station coordinates for the channel points from the USACE data.

(e) After entering each channel vertex, the Z-value of each vertex was updated based on the USACE data. This produced a 3D polyline with LiDAR topography and USACE bathymetry in place of the original 2D locations of the USACE cross section lines.

10. With the 3D XSProfiles polyline feature class, a GIS tool was used to interpolate between the cross sections along the channel, as explained in the next subsection.

Bathymetry Interpolation Tool For Neosho River

A Civil Engineering professor at Purdue University, Dr. Venkatesh Merwade, developed a tool for use in ArcGIS that allows for the interpolation of bathymetry between cross sections along a streamline. This tool was very useful for this research because it allowed for the drawing of more cross sections at finer resolution than the cross sections provided by USACE. In support of a finer resolution of cross sections, a preliminary run of HEC-RAS with only the cross sections provided by USACE raised many error notifications stating that there was a need for more cross sections because the flow was changing too much in between the existing cross sections during high flow scenarios. The process of using this tool is explained in detail in a tutorial at Dr. Merwade's webpage [Merwade, 2014].

Tar Creek Bathymetric Data Input

The data provided by GRDA containing channel bottom elevations for Tar Creek from its confluence with the Neosho to the Hwy 10 bridge location were sent as depths from the water surface. The following procedure was followed to convert the depths to elevations relative to the NAVD88 vertical datum.

1. The exact time of collection for each data point was included in the raw data file, and the water surface elevations recorded on the USGS gauge station in Miami, OK (07185080) for those times were downloaded from the USGS website.[1]

[1]The WSEs near Miami on the Neosho and lower Tar Creek for low flow conditions is primarily controlled by the WSE on Grand Lake. During the time period these depth measurements were taken, the gauge WSE varied between 742.56 and 742.60 ft PD, during which time the dam WSE varied between 742.29 and 742.32 ft PD. Therefore, the WSEs in this lower reach of Tar Creek can be reasonably assumed to be relatively equal to the WSE at the USGS gauge station.

2. The WSEs were converted from the gauge datum to NAVD88–Imperial units– and the depths were subtracted from the WSEs to yield channel bottom elevations.

3. The attribute table provided by GRDA containing the data point locations was then edited to include an elevation field, and the data was exported to a new shapefile as 3D points.

4. These point data were added to the Grand TIN using the "Edit TIN" tool.

Bathymetry Interpolation for Spring and Elk Rivers

The channel bottom elevations for the Spring and Elk Rivers were interpolated between the gauge station locations at Quapaw (Spring) and Tiff City (Elk) and the furthest extent of the OWRB bathymetry study. The channels were assumed to be trapezoidal and linearly interpolated along the length of the channel. 5.7 river miles of bathymetry were interpolated on the Elk River and 10.3 river miles were interpolated on the Spring River. This interpolation was completed manually in HEC-RAS after the cross-sections were extracted using HEC-GeoRAS.

TIN Cleanup for Use with HEC-GeoRAS

After using the bathymetry interpolation tool for the Neosho River and adding the Tar Creek channel bathymetry points the Grand TIN was messy, with the leftover "false" data points from the water surface causing small peaks all over the channels. These imperfections were corrected using the "TIN Editing" toolbar in ArcMap. The "Delete TIN Node," "Delete TIN Breakline," and "Connect TIN Nodes" tools were especially helpful during this process.

Appendix C: Bonus Model Application Graphs

The graphs included in this appendix represent the percent changes in flow depth and flow top-width due to the flood-frequency flows under the existing rule curve vs. the proposed rule curve.

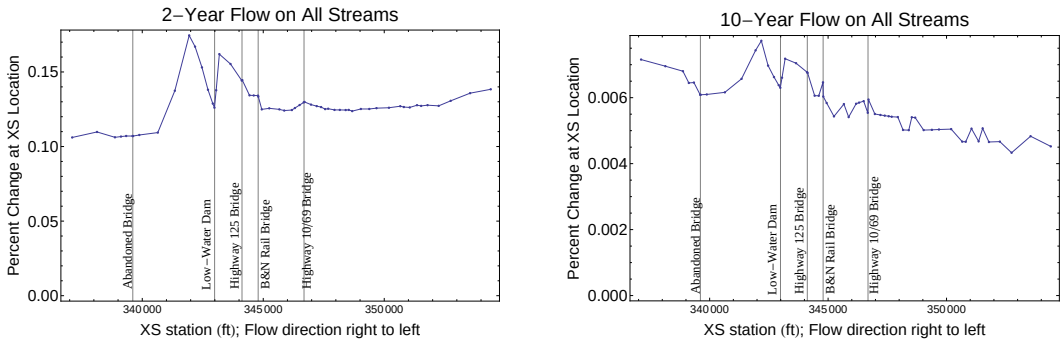

(a)

(b)

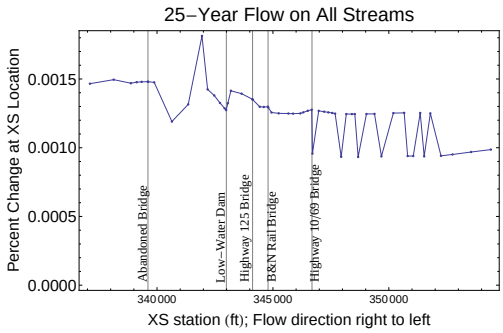

(c)

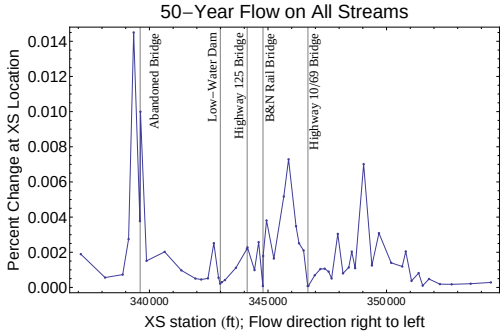

(d)

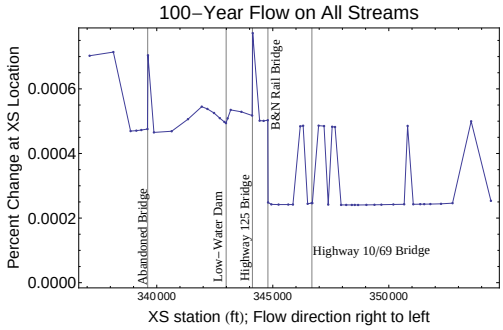

(e)

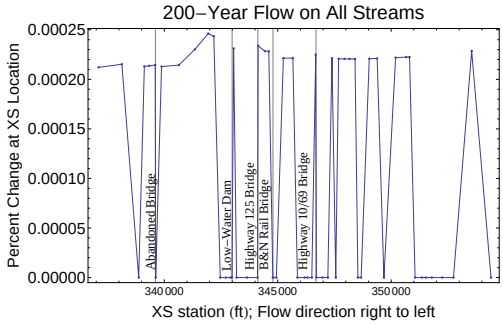

(f)

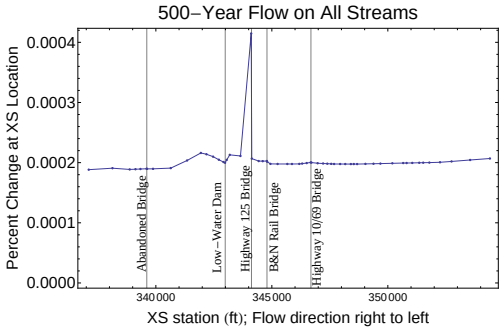

(g)

Figure 1. Percent changes in flow-depth for priority 1 location due to changing boundary condition at dam from 741 to 743 ft PD for various extreme flow scenarios. Note differences in scale on y-axis.

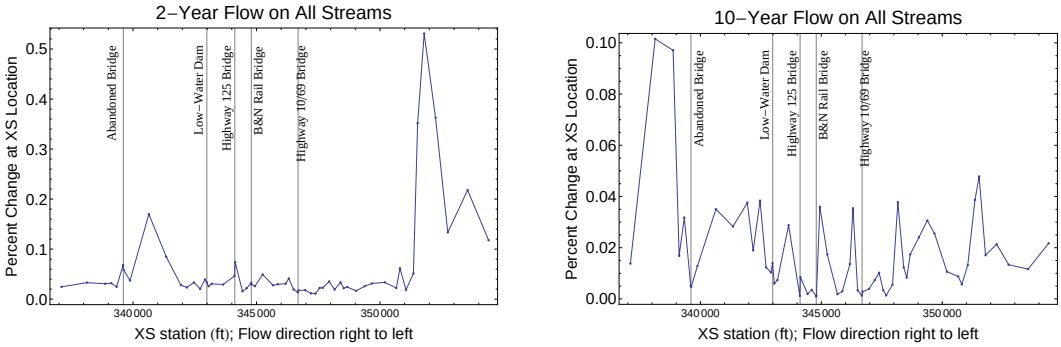

(a)

(b)

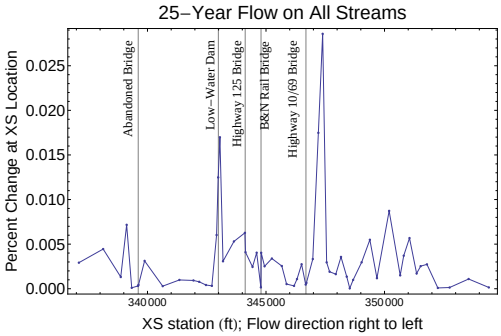

(c)

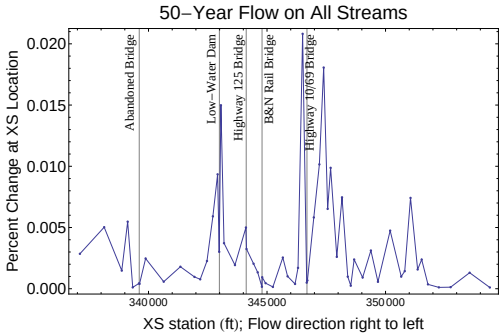

(d)

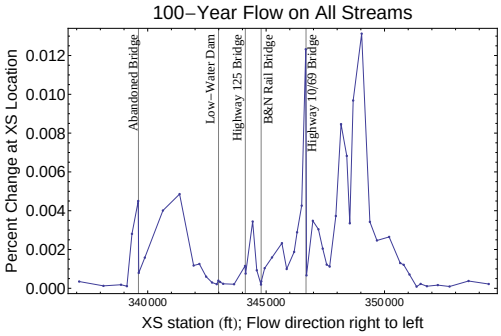

(e)

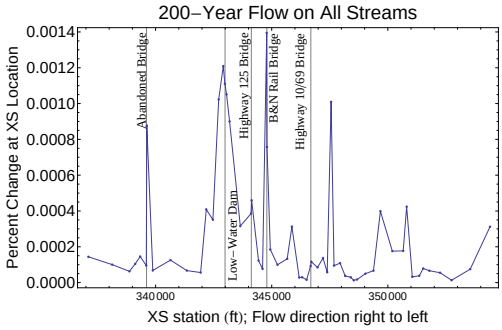

(f)

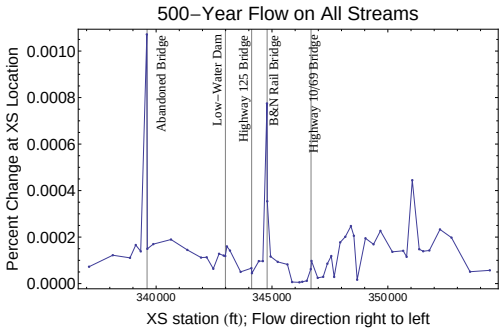

(g)

Figure 2. Percent changes in flow top-width for priority 1 location due to changing boundary condition at dam from 741 to 743 ft PD for various extreme flow scenarios. Note differences in scale on y-axis.

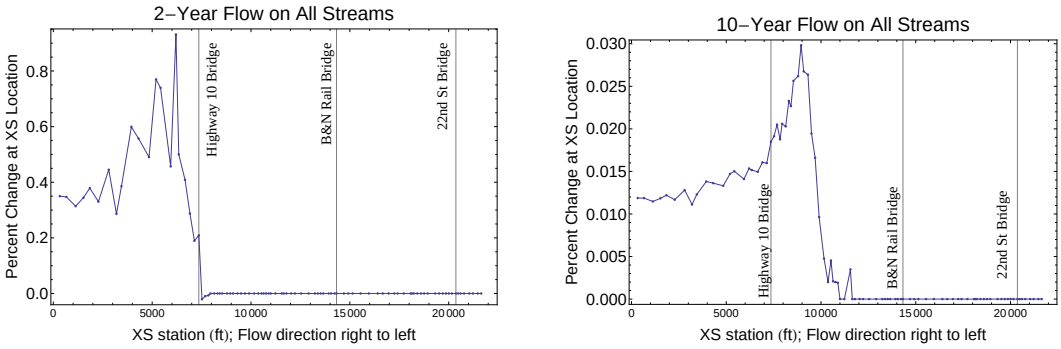

(a)

(b)

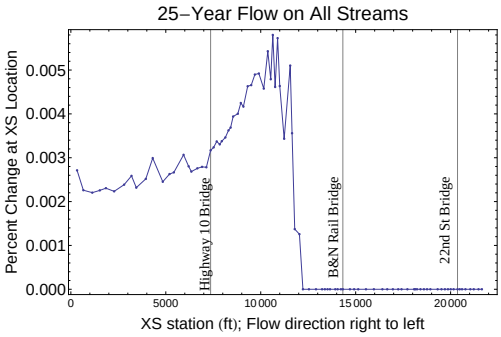

(c)

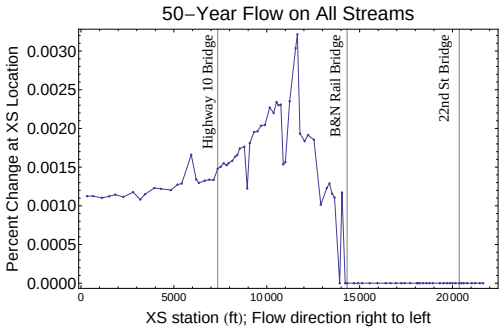

(d)

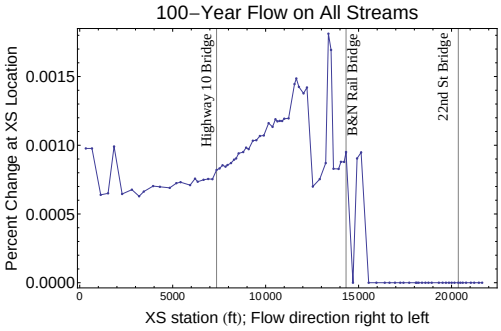

(e)

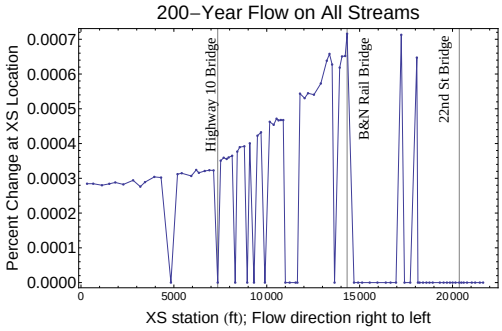

(f)

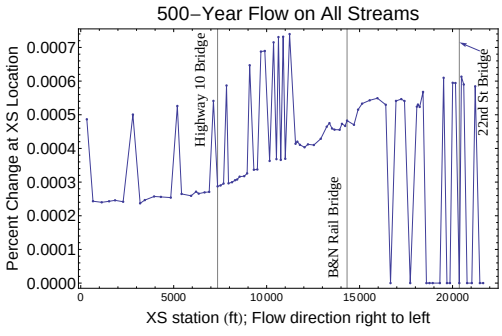

(g)

Figure 3. Percent changes in flow-depth for priority 2 location due to changing boundary condition at dam from 741 to 743 ft PD for various extreme flow scenarios. Note differences in scale on y-axis.

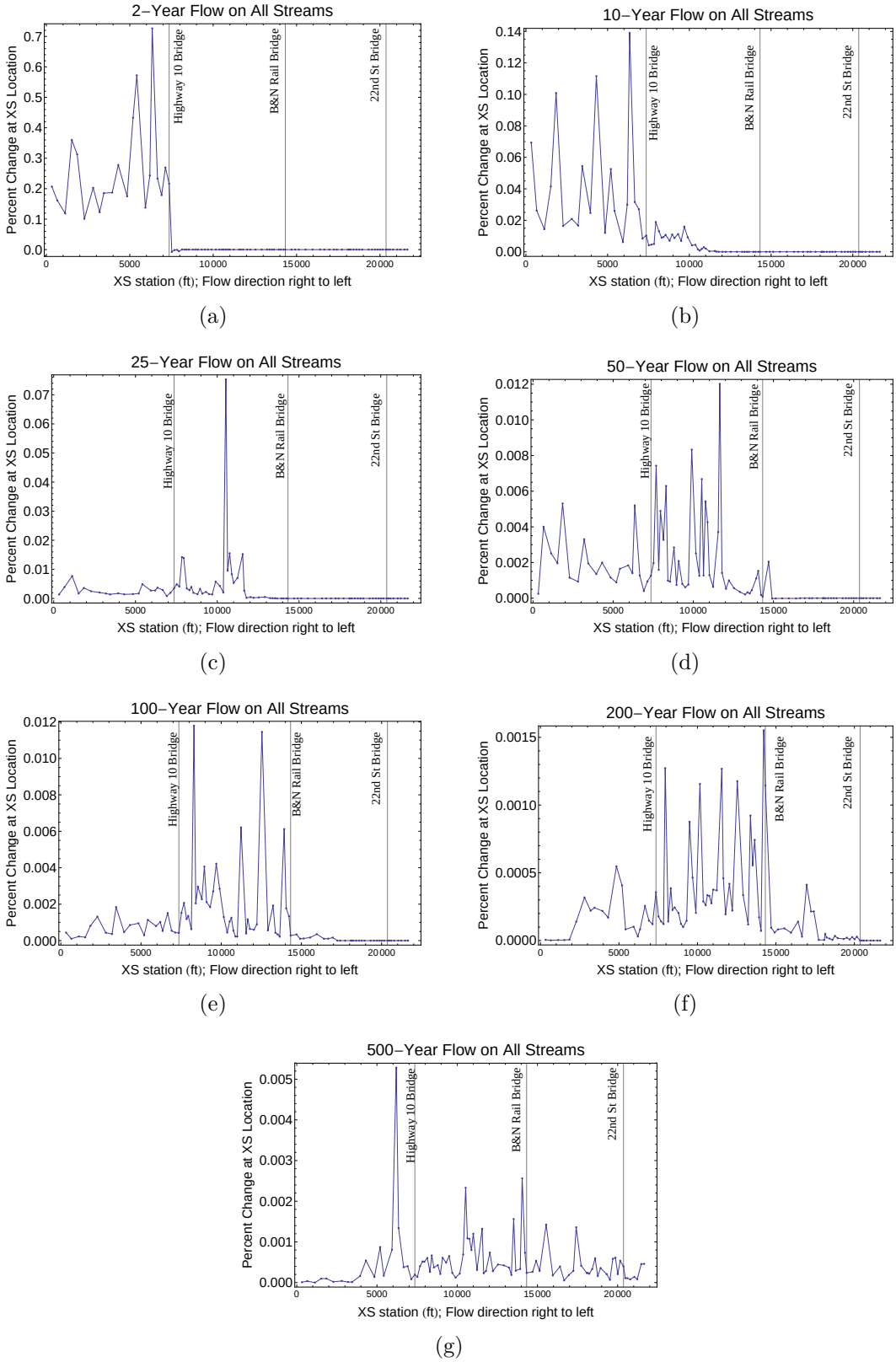

Figure 4. Percent changes in flow top-width for priority 2 location due to changing boundary condition at dam from 741 to 743 ft PD for various extreme flow scenarios. Note differences in scale on y-axis.

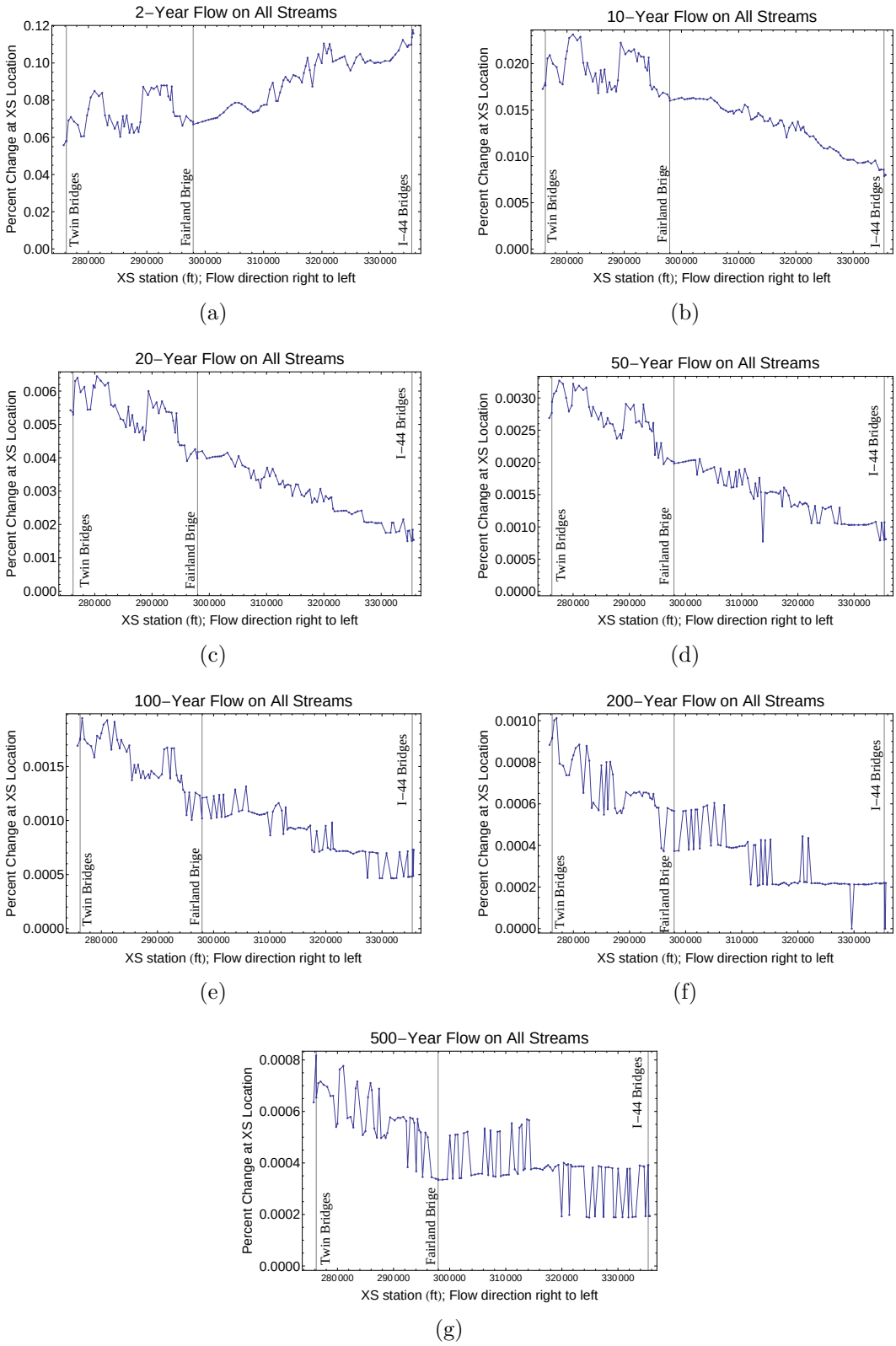

Figure 5. Percent changes in flow-depth for priority 3 location due to changing boundary condition at dam from 741 to 743 ft PD for various extreme flow scenarios. Note differences in scale on y-axis.

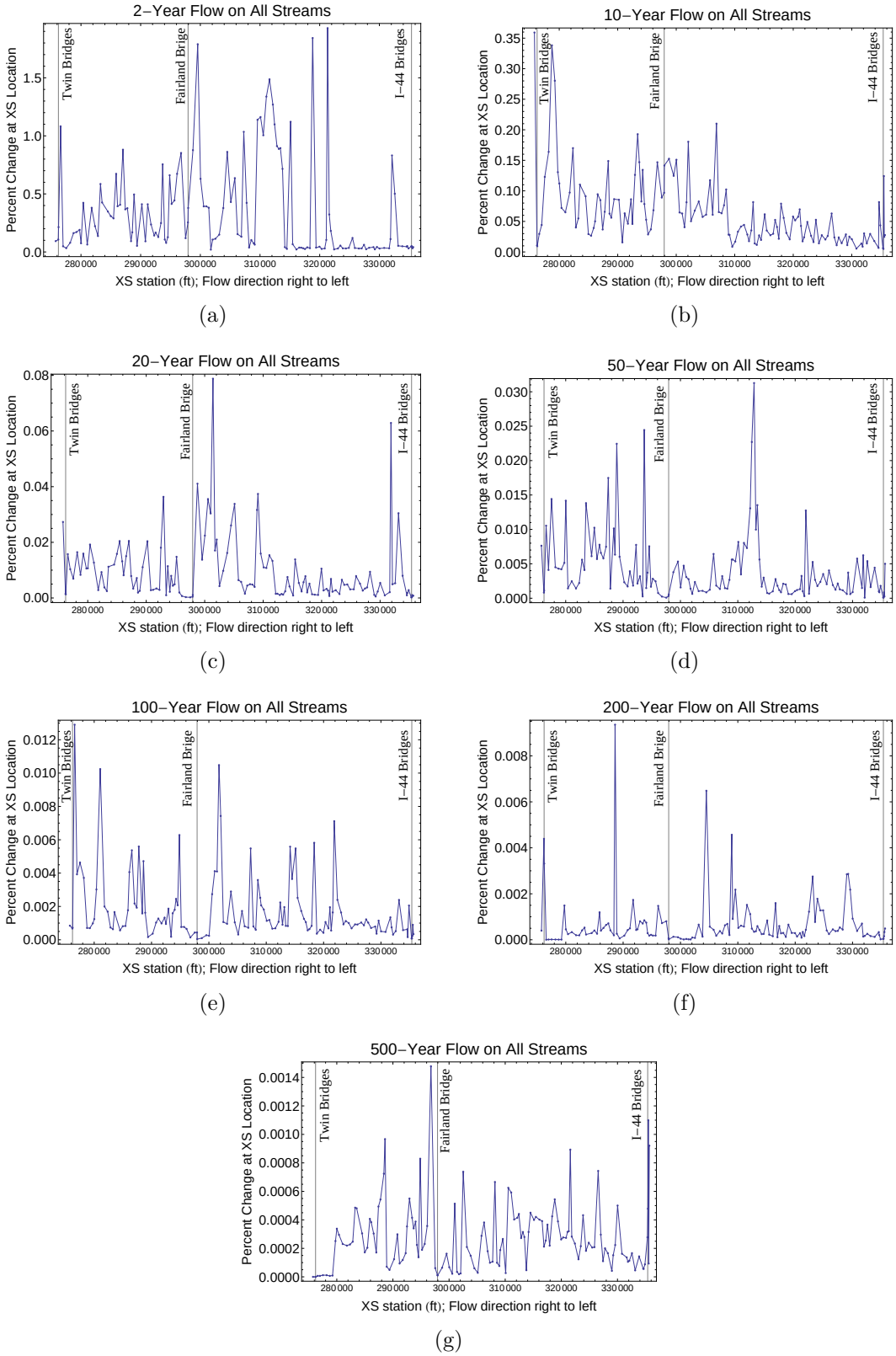

Figure 6. Percent changes in flow top-width for priority 3 location due to changing boundary condition at dam from 741 to 743 ft PD for various extreme flow scenarios. Note differences in scale on y-axis.

Appendix D: Proof of conservativeness of assumption that a rise in WSEs from the proposed rule curve target elevation would produce an equal rise in WSEs from the existing rule curve target elevation.

Problem Statement

The problem from which this question arises has to do with the question of how the dam stage elevation behaves apart from an intervention by human-controlled dam releases. Consider the following scenario: the Pensacola Dam WSE is maintained at 741 ft PD, as per the existing rule curve conditions. At this point, a high-volume streamflow event enters the system through all four boundary conditions, increasing the amount of water stored in the Grand Lake reservoir. The question investigated here is: "How would the reservoir behave under the existing rule curve, compared to how it would behave under the proposed rule curve, when a high-volume streamflow enters the system?" The OWRB [2009] study provides a stage vs. capacity curve for the Grand Lake reservoir. This curve suggests that as more water flows into Grand Lake, assuming no human interference by dam releases, the lake elevation ("stage") will rise based on the increased storage ("capacity") used by the lake to capture the high streamflows.

Solution

The stage vs. storage curve data provided in table form in OWRB [2009] is converted to graphical form in Figure 7. The OWRB [2009] data is extracted from the published

table for use in this research, and the same represented in Figure 7 is recreated in Figure 8. For this example, the curve is zoomed in to the 740 ft PD to 746 ft PD range in Figure 9. This zoomed-in portion of the stage vs. capacity curve will be used for illustrative purposes.

The y-axis values of 740.96, 742.96, and 744.96 ft PD are each marked with a horizontal line in Figure 9 in order to represent the closest data points to 741, 743, and 745 ft PD. These points correspond to capacities of 1,351,547, 1,431,403, and 1,513,746 acre-feet, respectively. Now, the question in Section 4.4.3 is, essentially, "To what level would the WSE at the dam rise had the WSE started at the existing rule curve target elevation, given that the WSE at the dam rises to a particular level when starting at the proposed rule curve target elevation instead?" In order to answer this question, the difference between the reservoir capacity at a high WSE (say, 745 ft PD) and the proposed rule curve target elevation (743 ft PD) may be considered the total volume caused by the high-volume streamflow event. This volume is added to the capacity of the reservoir at the existing rule curve target elevation, and the resulting capacity is compared to the data in the OWRB [2009] table to determine to what stage elevation the capacity corresponds.

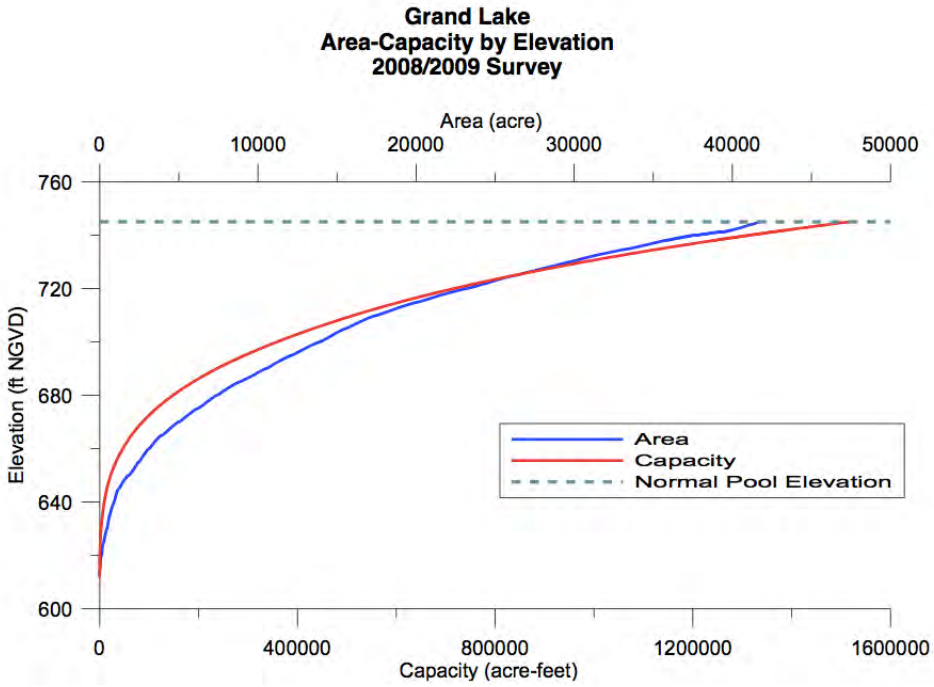

Figure 7. Stage vs. Capacity and Area curve taken directly from OWRB [2009] report.

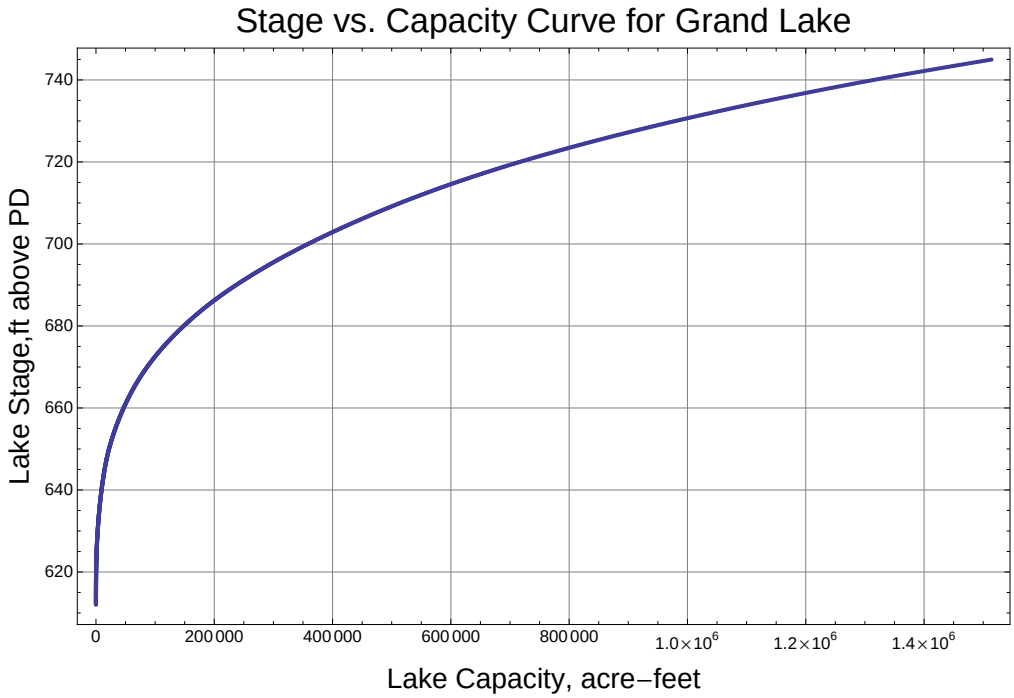

Figure 8. Full extent of recreated Stage vs. Capacity curve with data from OWRB [2009].

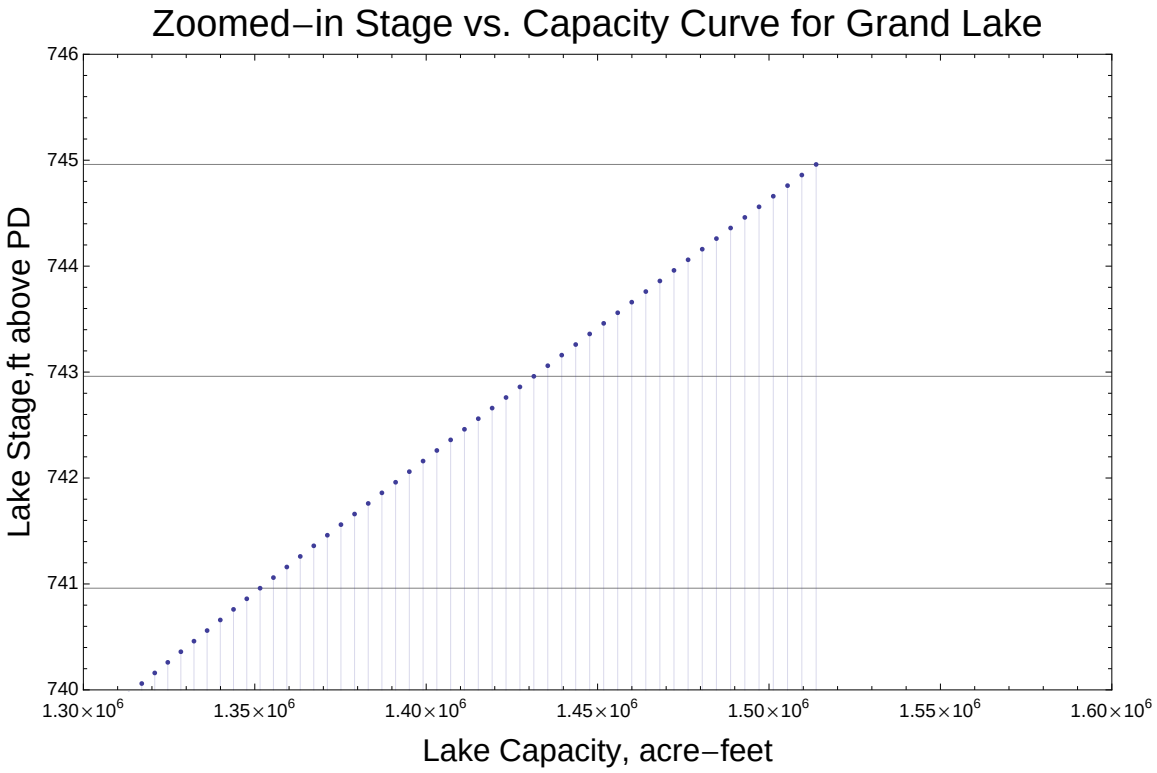

Figure 9. Stage vs. Capacity curve zoomed in to relevant stage elevations. Horizontal lines drawn through relevant data points, and vertical lines drawn from data to x-axis.

Results

The difference between the 745 and 743 ft PD corresponding capacities is 82,343 acre-feet. This volume is added to the 741 ft PD capacity, resulting in 1,433,890 acre-feet of capacity. This value is greater than the 743 ft capacity (1,431,403 ac-ft), meaning that the WSE rises to >743 when starting at 741 ft PD, for the same added volume as for the WSE rising to 745 from 743 ft PD. Therefore, an increase of 2 ft from the proposed rule curve target elevation will cause a >2 ft increase in WSE from the existing rule curve target elevation, and the resulting difference peak WSEs would be *less than* the original 2 ft difference in target WSEs. Therefore, using a WSE of 2 ft less than the final anticipated WSE from the proposed rule curve conditions to represent the final anticipated WSE from the existing rule curve conditions is *conservative* when desiring to maximize the difference between the two conditions.

Illustrative Example

An illustrative example of this phenomenon is a kitchen measuring cup. The bottom circumference is smaller than the brim circumference, similar to a lake. The distance between the 2-ounce measuring line and the 4-ounce measuring line will be greater than the distance between the 4-ounce measuring line and the 6-ounce measuring line, even though the volume required to move the water level between the lines is identical. In the same way, an identical increase of volume in a lake will create a greater increase in WSE if the WSE begins at a lower elevation, than if the WSE begins at a higher elevation.